Dynamic Positioning of Ships

A nonlinear control design study

Proefschrift

ter verkrijging van de graad van doctor
aan de Technische Universiteit Delft,
op gezag van de Rector Magnificus prof. ir. K.C.A.M Luyben,
voorzitter van het College voor Promoties,
in het openbaar te verdedigen op maandag 23 april 2012 om 12:30 uur

door

Shah MUHAMMAD,
Master of Science in Mathematics
Islamia University Bahawalpur, Pakistan

geboren te Dhurnal, Talagang, Pakistan.

Dit proefschrift is goedgekeurd door de promotor:
Prof. dr. ir. A.W. Heemink

Copromotor:
Dr. J.W. van der Woude

Samenstelling promotiecommissie:

Rector Magnificus	voorzitter
Prof. dr.ir. A.W. Heemink	Technische Universiteit Delft, promotor
Dr. J.W. van der Woude	Technische Universiteit Delft, copromotor
Prof. dr.ir. J.H. van Schuppen	Centrum Wiskunde & Informatica (CWI), Amsterdam
Prof. dr.ir. R.H.M. Huijsmans	Technische Universiteit Delft
Prof. dr.ir. B. De Schutter	Technische Universiteit Delft
Prof. dr.ir. R.L.M. Peeters	Maastricht University
Dr. A. Dòria-Cerezo	Univesitat Politècnica de Catalunya, Barcelona

This thesis has been completed in partial fulfillment of the requirements of Delft University of Technology, The Netherlands, for the award of the PhD degree. The research presented in this thesis was supported in part by two institutions: Delft University of Technology and HEC Pakistan. I thank them sincerely for their support.

Published and distributed by: Shah Muhammad
E-mail: abu.ash.hal@gmail.com

Keywords: Dynamic positioning, Nonlinear control design, State dependent algebraic Riccati equations, port-Hamiltonian systems.

ISBN # 978-94-6186-026-2

The cover design is done by Fay van leeuwen: designer@fayster.com
Printed in The Netherlands by Wöhmann Print Service

I want to dedicate this piece of work to my late father Dil Kabeer who realized the value of education for his kids and my beloved wife and kids, Hamael, Ashhal, Bazeed, and Ehab for their consistent love and endurance.

The fate of each man We have bound about his neck. On the Day of Resurrection We shall confront him with a book spread wide open, saying: ”Here is your book: read it. Enough for you this day that your own soul should call you to account.”

The Qurán (Verses 13 and 14 from the chapter The Children of Israel)

چاہتے تو سب ہیں کہ ہوں اوج ثریا پہ مقیم
پہلے ویسا کوئ پیدا تو کرے قلب سلیم
علامہ محمد اقبال

انشاء جی؛ یہ اور نگر ہے، اس دھرتی کی ریت یہی ہے
سب کی اپنی اپنی آنکھیں، سب کے اپنے اپنے چاند
شیر محمد خان ابن انشاء

Contents

Chapter 1

Introduction

THIS chapter explains the fundamental objective of this thesis and gives an overview of the related details. This study is about the control system design of a dynamic positioning (DP) vessel. A DP vessel is a vessel whose motion is controlled by a dynamic positioning system rather than by the conventional motion control techniques like mooring or anchoring.

1.1 What is a Dynamic Positioning (DP) System?

A DP system is a computer controlled system. The objective of this system is to keep the vessel within specified position and heading limits exclusively by using the propulsion system consisting of thrusters and propellers. Different types of thrusters, for instance, tunnel thrusters which produce thrust in sideway directions and azimuth thrusters which are fitted under the hull of vessel, are used to produce the desired effects. Azimuth thrusters can be rotated through 360 degrees and thus produce thrust in all directions in the horizontal plane. This is particularly useful because the environmental forces and moments change over time both in magnitude and direction.

A vessel in sea is subjected to various forces and moments due to waves, wind, sea currents, propulsion system, and unmodeled disturbances due to the environmental effects and the propulsion system. In practice, a floating vessel cannot maintain a completely static position at sea. Therefore, for practical reasons, position keeping means maintaining the desired position and heading within limits that reflect the environmental effects and the system capability. This limit may vary from centimeters to meters depending upon the nature of the operation. For instance, centimeter accuracy is desired for the operations like automatic berthing of ships and maneuvering in shallow and confined waters. An efficient DP system would be the one which achieves these goals with minimum fuel consumption and also tolerates transient errors or failures in the propulsion and measurement systems.

A complete DP system consists of three major parts: the vessel's power system, the thrusters system, and the DP control system. Figure 1.1 shows an overview of a

DP system, [77].

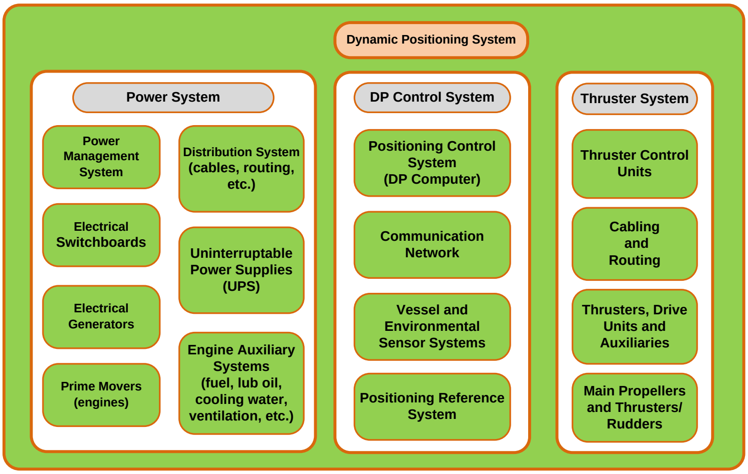

Figure 1.1: Major components of a DP system

1.1.1 Applications of DP Systems

DP vessels are used to achieve a variety of objectives in the offshore industry. The main vessel types used for various offshore operations include diving support vessels, drilling vessels (drill ships and semi-submersible drill ships), floating production storage and offloading (FPSO) units, landing platform docks, maritime research vessels, mine sweepers, pipe laying ships, platform supply vessels and anchor handling vessels, shuttle tankers, and survey ships. Figure 1.2 shows an FPSO unit, a naval vessel and a supply vessel.

Figure 1.2: A supply vessel, a naval ship and an FPSO vessel in sea (from left to right).

Dynamic positioning is vital in various offshore operations. From the operational aspects (for example in case of heavy lifts) it is important to maintain the vessel within precise navigational limits. For this, a very stable and accurate position keeping is required. There are situations in which a failure in position keeping, *i.e.*, failure in maintaining the position and heading angle, may result in serious safety and financial hazards. For instance, in case of diving vessels a failure in position keeping may result in the death or injury of the divers. In situations where the operation is being carried out very close to a fixed structure, then a position keeping failure may result in a collision. Consequently, damage to the structure or vessel, equipment, or a delay in the operation may occur. For instance, if a drilling vessel working in deep waters makes widely twitchy movements then it will cause damage to riser pipes or drilling pipes and subsequently the drilling operation will be abrupted.

The position keeping failure may occur because of multiple reasons; technical failure of the DP equipment, operator's error, extreme weather conditions not incorporated in the control design strategy, etc. In many ships and various operations, the overactuation feature is included to enhance the operational continuity by reducing the chances of failure of the propulsion and measurement systems. This feature gives rise to the problem of optimal allocation because in the presence of this feature there can be many possible combinations of actuators to yield a specific control action.

With the growing demand of the offshore industry, the development in the DP technologies is proliferating to meet the stringent safety, production and exploration demands. This has made the users and the manufacturers of the DP systems strive hard towards more refinements in the DP related equipments and expertise. Consequently, there have been developments in all the faculties of the DP technologies like navigation, control, propulsion and power units, and other subsidiary components.

DP systems have emerged as a popular replacement for the conventional position keeping techniques: anchoring and jack-up barge. While the conventional tools have no or limited maneuverability, DP systems have excellent maneuverability and can be easily moved from one place to another. No additional external equipment like the anchoring tugs are required for DP systems. The anchoring may take several hours but DP has very quick setup. The conventional techniques are limited by the sea obstructions and sea depth but DP systems do not have such limitations. For more information on the design, principles, and applications of dynamic positioning systems interested readers are referred to [23].

1.1.2 Focus of this Research

It is clear from the foregoing discussion that a DP system consists of several components. The focus of this thesis is the design and analysis of the positioning control system of the vessel, a sub-component of the DP control system. This component may well be considered as the heart of the DP system as it interacts with the rest of the components of the DP system. There can be different control design objectives depending upon the nature and demands of a DP operation. Some of these control objectives include position and heading regulation, path following, trajectory tracking, and wave-induced motion reduction. We focus on the position and heading regulation.

The basic element of a positioning control system is a mathematical model of the vessel which is an approximation of the reality. We consider a nonlinear vessel model from [24] and this model serves as a prototype for this study. The model will be introduced in Chapter 2. We study the design and analysis of the control laws to stabilize (or regulate) the model to a desired equilibrium point. From a physical point of view, we desire to maintain the position and heading of the vessel within desired limits. In control design, it is important to take into account the size and the dynamic response of the thrust devices which must be adequate to cope with various environmental conditions in different offshore operations. In practice, the maximum thrust forces and moments to maintain the position and heading in different environmental conditions are estimated and then the capability of the thrust devices to meet the demands is analyzed. This study is called a capability study.

The prototype vessel model is nonlinear due to the heading angle of the vessel. In [8], the state dependent coefficient (SDC) parametrization is introduced which is a strategy to transform the nonlinear system into a pseudo-linear form. The advantage of this approach is that it provides an opportunity to use concepts from linear system theory to study the nonlinear vessel model. We use the SDC framework throughout this thesis to study the control system design for the DP vessel.

The stability analysis is the an important feature of many control system designs. An unstable system may be potentially dangerous. Qualitatively, a dynamic system is called stable if starting from a position somewhere near its equilibrium or operating point implies that it will stay around the point ever after. Due to complex and exotic behavior of the nonlinear systems, more refined concepts of stability such as (local and global) asymptotic stability are required to describe the behavior of nonlinear systems. The asymptotic behavior implies that beside being stable, the system will converge to its equilibrium or operating position as time goes on.

Lyapunov stability theory is the most commonly used tool to study the stability properties of nonlinear systems. The prototype vessel model has a typical nonlinearity, when described in pseudo-linear form by using the SDC parametrization. We begin our study with the stability analysis of pseudo-linear systems similar to the prototype DP vessel system. The special form of the vessel model motivated us to combine the Lyapunov stability theory with linear matrix inequalities (LMIs) to come up with a new method to analyze the global asymptotic stability of the pseudo-linear systems of the form similar to the prototype vessel model.

PID controllers are commonly used in practice. We use the SDC framework to come up with the nonlinear version of the PID controller by using the state dependent algebraic Riccati equation (from now on we call it the SDARE) technique for the design of a stabilizing control law for the DP vessel. The computation of the controller and the observer gains require online computation of the solution of the SDARE. It can require large computation time, especially, for large systems. There are various off-the-shelf methods for the solution of the SDARE. We come up with a new method, the Fourier series interpolation (FSI) method, to solve the SDARE corresponding to the DP vessel model. The FSI method reduces the computation time for the SDARE in comparison with the Schur decomposition method.

The port-Hamiltonian formulation has also become a popular technique to study physical systems since a decade. We transform the DP vessel model into port-Hamiltonian form and then use the IDA-PBC design approach to come up with a family of control laws. These control laws may also be seen as the nonlinear version of the well-known PID controllers, in the port-Hamiltonian framework.

1.2 An Overview of this Thesis

Chapters 1 and 2 contain the basic introductory material about the main theme of this thesis. Our focus in this thesis is to address the control system design problem for dynamic positioning of a sea vessel. The first chapter of this thesis introduces the dynamic positioning problem. The DP system is illustrated and the importance of dynamic positioning is highlighted by describing its applications in various offshore and onshore operations. The second chapter introduces the details of the mathematical model we use in this thesis to describe the vessel motion. It highlights the necessary details of the vessel motion in mathematical form.

The main subject of the third chapter is the study of global asymptotic stability of a special type of nonlinear systems which are similar to the prototype vessel model. The SDC framework is used to express the nonlinear system in a pseudo-linear form and then the stability is analyzed based on the properties of the state dependent system matrix. Two counterexamples are presented in this chapter. The first counterexample shows that the conditions, that the system matrix in pseudo-linear form is continuous, Hurwitz, and exponentially bounded, as reported in the literature on this subject, are not sufficient for global asymptotic stability of the pseudo-linear system. In the second counterexample, in addition to the set of conditions mentioned in the first counterexample, additionally, we also assume that the system matrix is periodic. It is shown that the extended set too does not constitute the set of sufficient conditions for global asymptotic stability of the pseudo-linear system. Apart from this, we also propose in this chapter, a method for proving global asymptotic stability of the special pseudo-linear systems by combining the Lyapunov stability theory and the LMIs.

The fourth chapter addresses the control system design problem. The SDARE based control design and estimation technique is used to design an SDARE controller and an SDARE observer for dynamic positioning of the vessel. The fifth chapter is about the FSI method for the approximation of the solution of the SDARE. The FSI method reduces the online computations of the solution of the SDARE by performing the computationally expensive tasks offline. The sixth chapter is also about the control system design problem of the DP vessel. The main idea is to transform the vessel model in the port-Hamiltonian structure and then use the IDA-PBC design approach to address the control design problem. The thesis is concluded with the seventh chapter which briefly summarizes the thesis and provides some concluding remarks. The hindsight ideas for future research are also presented in this chapter.

1.3 Contributions of this Thesis

We study the stability analysis of nonlinear systems in the SDC framework. There had been some existing results on this subject. Our main contribution on this topic are two counterexamples. It is claimed in the literature that it is sufficient for global asymptotic stability of a pseudo-linear system that the system matrix in its SDC form is continuous, Hurwitz, and exponentially bounded. In a first counterexample, we show that this claim is not valid. Motivated by the special type of state dependence of the system matrix in DP vessel model, we assume additionally that the system matrix is periodic and show by means of another counterexample that an additional condition also does not guarantee the stability of the nonlinear system. Each of these counterexamples have separately been published, see [58] and [59].

The special form of the nonlinearity in the vessel model and the Lyapunov stability theory has lead us to propose a new approach to prove global asymptotic stability of the special type of pseudo-linear systems which resembles the prototype DP vessel model. This approach makes use of the LMIs to achieve global asymptotic stability. The approach is useful in particular for the vessel model and in general for the systems having similar structure as the vessel model.

Another contribution is the SDARE controller design for the DP vessel. The model based SDARE controller is a state feedback controller. The complete state of the DP vessel model is not available in practice. Therefore, a state observer is also required. We also used the SDARE observer to find the state estimate. It has been shown that the SDARE controller in combination with the SDARE observer gives the desired stability and performance of the DP vessel. Alongside the SDARE controller and observer, a numerical method for the approximation of the solution of the SDARE is proposed. We call this the Fourier series interpolation (FSI) method. This method is proved to be very handy in reducing the online computation time of the SDARE for controller and observer gains computations. The concept of the FSI method has been presented in a conference paper, see [57].

The final contribution of this thesis is the use of the port-Hamiltonian structure and the passivity theory for the first time for DP vessel control design. We propose a family of passivity based controllers for the DP vessel. Passivity idea is very attractive in a sense that it helps in assigning the physical meaning to various variables and quantities. The stability and performance of the family of the IDA-PBC designs are discussed. This idea was presented at a conference (see [55]) and it has recently been accepted in a journal (see [56]).

Chapter 2

Mathematical Model of a Sea Vessel

The details of a vessel model for DP considerations are presented in this chapter. The prototype vessel model described in this chapter will be used in the subsequent chapters for studying the control system design of the DP vessel.

2.1 Motion of a floating Vessel

In this section, we explain various terms associated with the motion of the vessel in the sea. Motion of a floating vessel can be described by six degrees of freedom (DOF), *i.e.*, a vessel can move in six different directions. We can categorize the six DOF in two categories:

1. The translational motion in the following three directions,

- *Surge*: motion in backward (aft/stern) and forward (bow/fore) directions
- *Sway*: motion along sideways (transversial directions): starboard (right side of the ship) and port (left side of the ship) directions
- *Heave*: motion in upward and downward directions

2. The rotational motion in the following three directions,

- *Roll*: rotation about the *surge* axis
- *Pitch*: rotation about the *sway* axis
- *Yaw*: rotation about the *heave* axis

Various modes of motion and the forces acting on the vessel are shown in Figure 2.1 and summarized in Table 2.1. A DP system is concerned primarily with control of

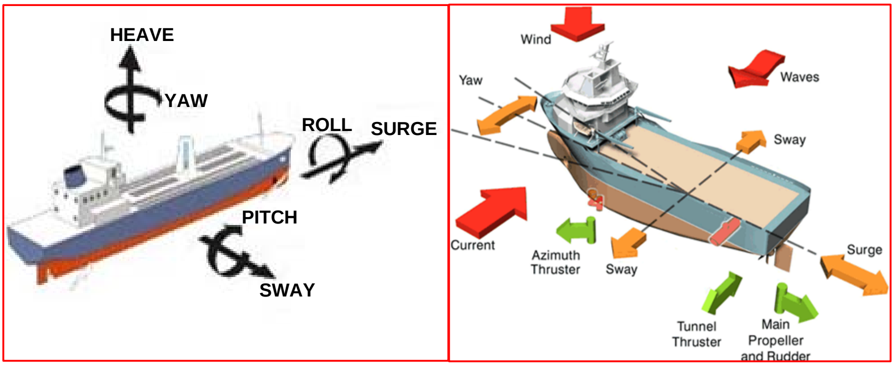

Figure 2.1: Six DOF of motion and forces acting on a floating vessel [Figure courtesy of www.km.kongsberg.com].

Table 2.1: Nomenclature of the vessel motion

axis	**x**	**y**	**z**
Translation	surge	sway	heave
position	x	y	z
velocity	u	v	w
force	X	Y	Z
+ direction	forward	starboard	downward
Rotation	roll	pitch	yaw
angle	ϕ	θ	ψ
rate	p	q	r
torque	K	M	N
+ direction	starboard	fore down	right turn

the vessel in the horizontal plane, *i.e.*, only the motions along *surge*, *sway* and *yaw* directions are considered for DP purposes.

In Table 2.1, X and Y represent the forces in the *surge* and *sway* directions and N denotes the turning effect because of the thrusters and environmental effects.

Dynamic positioning literature is very rich in terminology. For the convenience and interest of the reader, we briefly explain some important terms. A *superstructure* is an upward extension projected above the main deck of the vessel. The parallel lines marked on the hull of a vessel indicating the depth to which the vessel sinks under various loads, are called the *water lines*. The maximum legal load amount on a vessel is characterized by the top most water line. The distance from the top most water line to the edge of the lowest upper deck level is called the *freeboard*.

A vessel has got a volume which means that when it is placed on the surface of the water, it will displace water which is equal in volume to the volume of the part of the vessel immersed inside the surface of the water. The upward force on the vessel exerted by this displaced volume of water is called the force of *buoyancy*. The force of buoyancy depends on characteristics of water: it is low for fresh and warm water and it is high for cold and saline water which has more density. The center of mass of the water displaced by the vessel is called the *center of buoyancy*. The point at which the weight of the vessel is considered to act is called the *center of gravity*. The point of intersection of the vertical lines through the center of gravity and the center of buoyancy is called the *metacenter*.

The rear or aft part of the vessel is called the *stern*. Usually, during the night time, the stern of the vessel is indicated with a white navigation light on it. The foremost part of the vessel, opposite to the stern part, when the vessel is underway, is called the *bow*. The right hand side of the vessel as perceived by a person on board facing the bow is called the *starboard*. The opposite part of the vessel on the left hand side will then be called the *port*. All these terms are linked with the main deck of the vessel and has nothing to do with the location of the superstructure on the deck. Figure 2.2 illustrates all these terms.

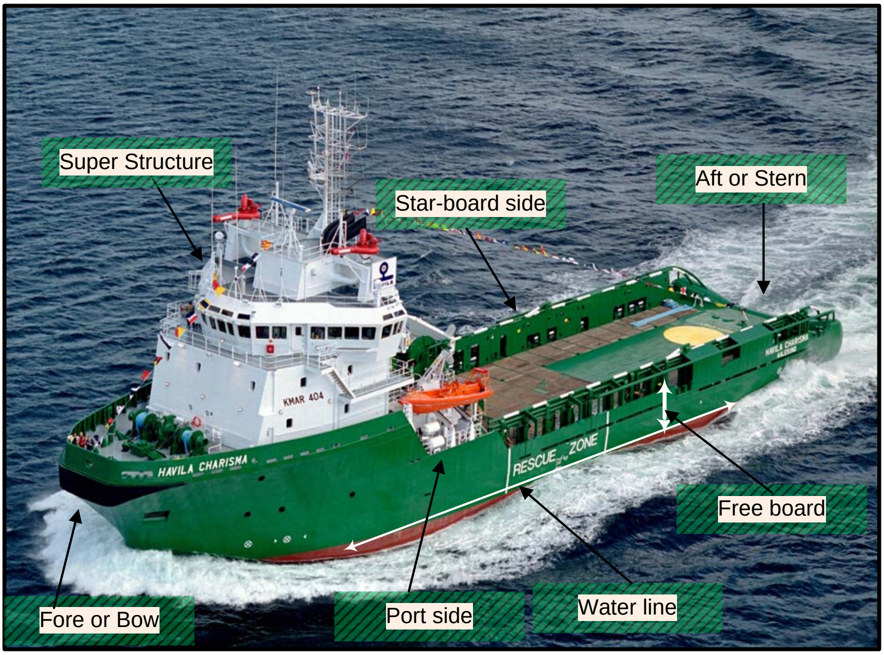

Figure 2.2: Commonly used terms in literature on dynamic positioning

2.2 Mathematical Model Describing the Dynamics of a floating Vessel

Modern DP control systems for ships use controllers based on a mathematical model of the ship. This mathematical model describes the hydrodynamic, damping, environmental and control forces and moments acting on the vessel. For rigorous details on the mathematical modeling of the dynamics of the floating vessel, interested readers are referred to [24] and for an up-to-date study we refer to [19] and [68]. The information from the measurement systems is transmitted to the controller and signals from the controller are sent to the propulsion systems consisting of the thrusters and propellers (planted at at least one of the aft, starboard, port and fore sides), propellers, and rudders to generate the desired activity to maintain the required position and heading of the vessel. Figure 2.3 shows an overview of the working of the DP system.

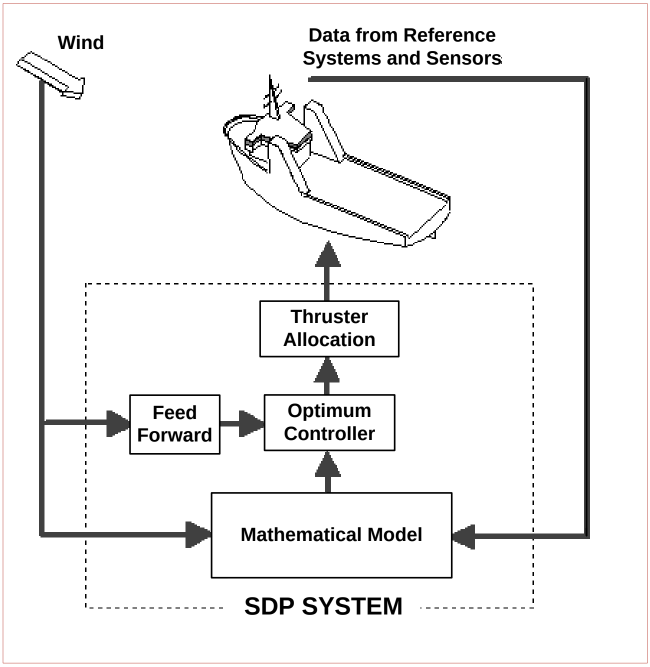

Figure 2.3: Flow chart of the DP control system (Figure courtesy of www.techteach.no).

The testbed vessel model used in this thesis is introduced in this chapter and the details describing the motion of a floating vessel are also explained. In the subsequent chapters, this model will be used for various design and analysis purposes. This section is divided into three major subsections. In the first one, dynamical equations of motion are explained. In the second subsection, we discuss how the perturbations or the environmental disturbances are incorporated into the mathematical model of the vessel dynamics. In the last subsection, the measurement model is explained.

2.2.1 The Dynamical Equations of Motion of the Vessel

The study of the dynamical equations of motion of a mechanical system can be divided into two parts: the kinematic equations of motion which deal with the geometrical aspects of the equations of motion, and the kinetic equations of motion which deal with the analysis of the forces causing the motion.

The Kinematic Equations of Motion

A floating vessel has six degrees of freedom. Two frames of reference are used to describe the motion: an Earth-fixed inertial frame of reference and a body-fixed relative frame of reference. Figure 2.4 explains the description of both frames of reference. For DP purposes, only the motion in the horizontal plane is considered. Let $\boldsymbol{\eta} = [x\ y\ \psi]^T$ describe the position (x, y) and heading ψ of the vessel in the inertial frame of reference and $\boldsymbol{\nu} = [u\ v\ r]^T$ describe the velocities of the vessel in the relative frame of reference. Then, the kinematic equations of motion in vectorial form are given by

$$\dot{\boldsymbol{\eta}} = J(\psi)\boldsymbol{\nu}. \tag{2.1}$$

where the transformation matrix is given by

$$J(\psi) = \begin{bmatrix} \cos\psi & -\sin\psi & 0 \\ \sin\psi & \cos\psi & 0 \\ 0 & 0 & 1 \end{bmatrix}. \tag{2.2}$$

The kinematic transformation (2.2) relates the body-fixed velocities to the derivative of the positions in the inertial frame of reference. Note that the transformation matrix is non-singular and orthogonal, *i.e.*, $J(\psi)J^T(\psi) = J^T(\psi)J(\psi) = I_3$, $\forall\psi \in \mathbb{R}$. This property is very important from the design and stability analysis perspective as we will see in the subsequent chapters. Also, we see that there is no uncertainty associated with (2.1) as it describes the well-known geometrical aspects of the model.

For conventional ships, it is an appropriate assumption that both the pitching and rolling motions are oscillatory with zero mean and limited amplitude. Also due to metacentric stability[1], there exist restoring moments in roll and pitch directions. Therefore, only the rotation matrix in *yaw* will be used to describe the kinematic equations of motion.

The Kinetic Equations of Motion

The nonlinear kinetic equations of motion can be formulated by using Newtonian or Lagrangian mechanics, for instance see [24] for a detailed study. In this work, the equations in the Newtonian formulation based on Newton's second law of motion are considered. The nonlinear kinetic equations of motion in vectorial form can be written as

$$\dot{\boldsymbol{\nu}} = -M^{-1}D\boldsymbol{\nu} + M^{-1}\boldsymbol{\tau} + M^{-1}J^T(\psi)\boldsymbol{b}, \tag{2.3}$$

$$\boldsymbol{\tau} = B_u\boldsymbol{u}. \tag{2.4}$$

[1]Metacentric stability is the tendency of the vessel to remain upright due to its center of gravity being below its center of buoyancy.

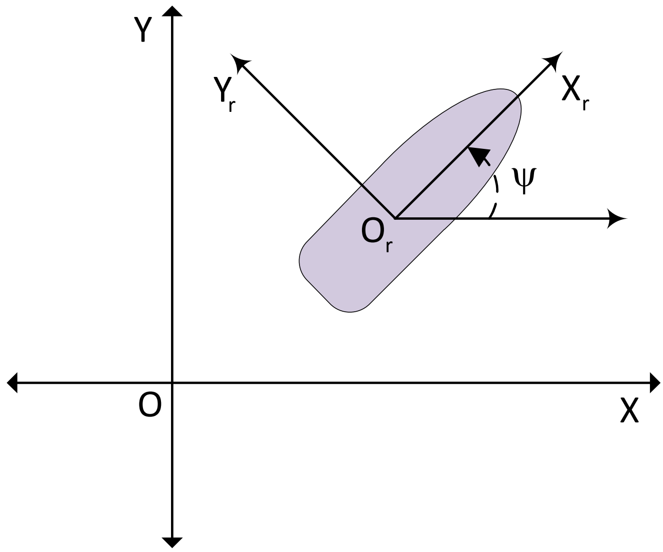

Figure 2.4: The Earth-fixed and the vessel-fixed frames of reference.

In (2.3) and (2.4), the vector $\boldsymbol{\tau} = [X, Y, N]^T \in \mathbb{R}^{3\times 1}$ represents the control forces and moment acting on the vessel in the body-fixed frame of reference, provided by the propulsion system of the ship consisting of propellers and thrusters. The vector $\boldsymbol{u} \in \mathbb{R}^{r\times 1}$ ($r \geq 1$) describes the control inputs and the matrix $B_u \in \mathbb{R}^{3\times r}$ is a constant matrix describing the actuator configurations. The vector $\boldsymbol{u}$ is the command to the actuators, which are assumed to have much faster dynamic response than the vessel; thus the coefficient B_u represents the mapping from the actuator command to the force generated by the actuators. In the following chapters, we assume a fully actuated vessel model and we will take $B_u = I_3$. In the forthcoming chapters, we therefore use the vectors $\boldsymbol{\tau}$ and $\boldsymbol{u}$ interchangeably, unless it is specified. The matrices M and D are 3×3 inertia and damping matrices, respectively. The vector $\boldsymbol{b} \in \mathbb{R}^{3\times 1}$ represents the slowly varying bias forces and moments in the Earth-fixed inertial frame of reference, due to the waves, wind, sea currents, and other environmental factors surrounding the vessel.

For DP consideration, the inertia matrix has the following form

$$M = \begin{bmatrix} m - X_{\dot{u}} & 0 & 0 \\ 0 & m - Y_{\dot{v}} & mx_G - Y_{\dot{r}} \\ 0 & mx_G - N_{\dot{v}} & I_z - N_{\dot{r}} \end{bmatrix} \in \mathbb{R}^{3\times 3}, \tag{2.5}$$

where m is the vessel mass, I_z is the moment of inertia about the vessel-fixed z-axis, and x_G denotes the longitudinal position of the center of gravity of the vessel with respect to the relative frame of reference. The added masses due to acceleration in the *surge*, *sway*, and *yaw* directions are defined as

$$X_{\dot{u}} \triangleq \frac{\partial X}{\partial \dot{u}}, \ Y_{\dot{v}} \triangleq \frac{\partial Y}{\partial \dot{v}}, \ N_{\dot{r}} \triangleq \frac{\partial N}{\partial \dot{r}}, \ Y_{\dot{r}} \triangleq \frac{\partial Y}{\partial \dot{r}}, \ N_{\dot{v}} \triangleq \frac{\partial N}{\partial \dot{v}}. \tag{2.6}$$

Note that the inertia along the *surge* direction is decoupled from the inertia effects along the *sway* and *yaw* directions. Due to small velocities and starboard-port symmetries of the vessel, the added mass in *sway* due to the angular acceleration in *yaw* is equal to the added mass in *yaw* due to *sway* acceleration, *i.e.*, $Y_{\dot{r}} = N_{\dot{v}}$. Hence, in DP applications, it is assumed that the matrix M is symmetric and strictly positive definite, *i.e.*, $M = M^T > 0$. This assumption is very useful for the purpose of analysis.

The vessel motion generates waves. This means energy is transferred from vessel to the fluid and this energy is modeled by the linear damping term. The linear damping matrix D for DP is taken as

$$D = \begin{bmatrix} -X_u & 0 & 0 \\ 0 & -Y_v & -Y_r \\ 0 & -N_v & -N_r \end{bmatrix} \in \mathbb{R}^{3\times 3}. \tag{2.7}$$

In most DP applications, the damping matrix is assumed to be real, non-symmetrical, and positive definite. However, for low speed applications where the damping matrix is reduced to (2.7), it can be assumed that $N_v = Y_r$. In such a case, we assume the damping matrix D to be real, symmetric, and positive definite. The damping components in *surge*, *sway*, and *yaw* directions are defined by

$$X_u \triangleq \frac{\partial X}{\partial u},\ Y_v \triangleq \frac{\partial Y}{\partial v},\ N_r \triangleq \frac{\partial N}{\partial r},\ Y_r \triangleq \frac{\partial Y}{\partial r},\ N_v \triangleq \frac{\partial N}{\partial v}. \tag{2.8}$$

Decoupling of the *surge* mode from the *sway* and *yaw* modes is beneficial for the convergence of parameter estimation algorithms, see [28]. An a priori estimate of the mass and damping parameters of the vessel can be obtained by using semi-empirical methods and hydrodynamic computations. See [22] for details about the identification and estimation of vessel model parameters. Often the estimates of mass and damping parameters are updated based on the data obtained from the practical experiments in calm waters.

2.2.2 The Disturbances Model

The forces acting on a sea vessel can be categorized in two main categories [37]: the internal and the external forces and moments. The internal forces and moments are formulated as functions of acceleration, velocities, propeller propulsions, and rudder excitations. These have partially been discussed in the previous subsection. Here we explain the external forces acting on the vessel. These forces are also termed as external disturbances. The external disturbances can be distinguished into 3 major categories [83]:

- Additive disturbances - These are the disturbances due to wind, waves, sea currents, etc. These forces act additively on the vessel. To model and analyze these forces, the model of the ship is extended by adding additional states.
- Multiplicative disturbances - A vessel in sea is also subject to the time varying parameters such as load conditions, water depth, trim, speed changes, etc. These disturbances are called multiplicative disturbances.

- Measurement disturbances - These are the disturbances due to the wrong functioning or noise in the measurement devices like DGPS and gyro compass.

The external disturbances due to unmodeled dynamics, waves, wind, and sea current acting on the vessel, are distinguished into two categories: second order[2] low frequency (LF) disturbances and first order[3] wave-induced wave frequency (WF) disturbances. See for instance, [26], [29], and [51]. Along this thesis, we call the motion of the vessel corresponding to these disturbances the LF motion and the WF motion, respectively. The total vessel motion is then defined to be the sum of the LF and WF motions. The effect of the WF disturbances is incorporated in the measurement model, described in the next section. Figure 2.5 illustrates the concept of the slowly varying LF and the oscillatory WF motions.

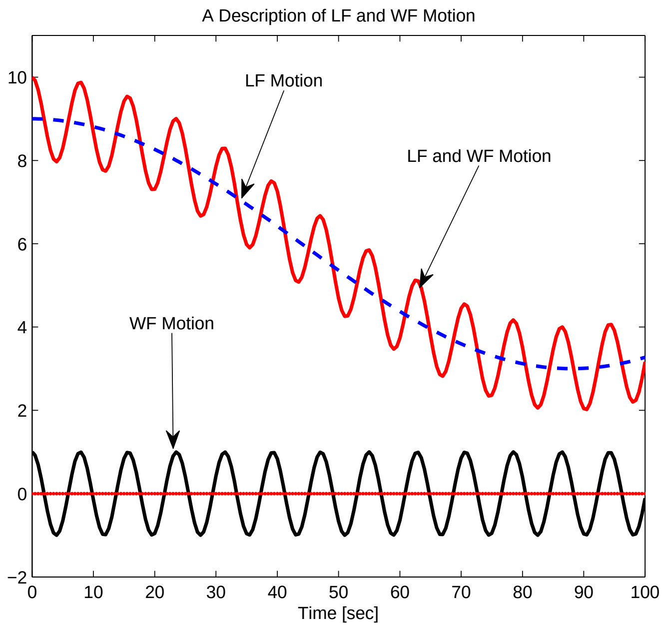

Figure 2.5: The LF and the WF motions

In what follows, both the LF and WF disturbances are characterized by respective dynamical models. In the following, some explanation of these dynamic models is given.

Second Order LF Disturbances

The LF disturbances are also sometimes termed as slowly varying bias forces and moment in *surge*, *sway*, and *yaw* directions. The low frequency motions are caused

[2]The order refers to the fact that the magnitude of these disturbances is proportional to the square of the wave amplitude

[3]The order refers to the fact that the magnitude of these disturbances is proportional to the wave amplitude

by the forces generated by the thrusters and propellers, wind forces, wave-induced forces, and hydrodynamic forces. In marine control applications, these forces and moment can be described, [24], by the first order Markov process given by

$$\dot{\boldsymbol{b}} = -T^{-1}\boldsymbol{b} + \Psi \boldsymbol{w}_b, \tag{2.9}$$

where $\boldsymbol{b} \in \mathbb{R}^{3\times1}$ is a vector of bias forces and moment, the vector $\boldsymbol{w}_b \in \mathbb{R}^{3\times1}$ represents the zero-mean Gaussian white noise process, *i.e.*, $\boldsymbol{w}_b \sim \mathcal{N}(0, Q_{c,b})$, $T \in \mathbb{R}^{3\times3}$ is a diagonal matrix of positive bias time constants and $\Psi \in \mathbb{R}^{3\times3}$ is a diagonal matrix scaling the amplitude of the noise vector $\boldsymbol{w}_b$. The matrix T is known as the *time constant*. In this context it will have relatively large values as sea states change very slowly. We can also interpret (2.9) as a low-pass filter.

In many applications, see for instance [27, 80], it is considered more appropriate from a physical point of view to use $\dot{\boldsymbol{b}} = \Psi \boldsymbol{w}_b$ to describe the bias model. This may be described as integration of the noise signal which in fact is a random walk phenomenon. Thus bias forces and moments are sometimes modeled as a random walk process. Another case could be that the bias forces and moment are constant. Then the bias model will be $\dot{\boldsymbol{b}} = 0$.

First Order Wave-Induced WF Disturbances

The fundamental assumption for the development of the WF motion model is that the sea state is known and can be described by a spectral density function. The first order wave-induced WF disturbances in *surge*, *sway*, and *yaw* directions are modeled as second order harmonic oscillations which are driven by Gaussian white noise process. It was Balchen who first modeled the WF motion in this way, [6]. For each of the three directions, the WF disturbances model in the frequency domain is given by

$$\xi_i(s) = \frac{\sigma_i s}{s^2 + 2\zeta_i \omega_{0i} s + \omega_{0i}^2} w_{\xi i}(s), \;\; i = 1, 2, 3 \tag{2.10}$$

where ω_{0i} is the dominating (sometimes also termed as undamped) wave frequency, ζ_i is the relative damping ratio, and σ_i is the wave intensity parameter. The input $w_{\xi i}$ represents the Gaussian white noise process, *i.e.*, $w_{\xi i} \sim \mathcal{N}(0, Q_{c,\xi i})$. The damping ratio ζ_i is a measure to describe how the oscillations in the system (2.10) decay when a disturbance is introduced. Normally, the damping ratio defines the level of damping (under-damped, over-damped, critically-damped, and undamped) of the system. The dominating wave frequency ω_{0i} is obtained by spectral analysis.

In state space representation, the WF disturbances model for each direction can be written as

$$\begin{aligned} \dot{\xi}_1^{(i)} &= \xi_2^{(i)} \\ \dot{\xi}_2^{(i)} &= -\omega_{0i}^2 \xi_1^{(i)} - 2\zeta_i \omega_{0i} \xi_2^{(i)} + \sigma_i w_i, \quad i = 1, 2, 3 \end{aligned} \tag{2.11}$$

A compact state space realization of the WF model is given by

$$\begin{bmatrix} \dot{\xi}_1 \\ \dot{\xi}_2 \end{bmatrix} = \begin{bmatrix} O_3 & I_3 \\ -\Omega^2 & -2Z\Omega \end{bmatrix} \begin{bmatrix} \xi_1 \\ \xi_2 \end{bmatrix} + \begin{bmatrix} O_3 \\ \Sigma \end{bmatrix} \boldsymbol{w}_\xi, \tag{2.12}$$

where $\boldsymbol{\xi}_1 = [\xi_1^{(1)}, \xi_1^{(2)}, \xi_1^{(3)}]^T$, $\boldsymbol{\xi}_2 = [\xi_2^{(1)}, \xi_2^{(2)}, \xi_2^{(3)}]^T$, $\Omega = \text{diag}\{\omega_{01}, \omega_{02}, \omega_{03}\}$, $Z = \text{diag}\{\zeta_1, \zeta_2, \zeta_3\}$, and $\Sigma = \text{diag}\{\sigma_1, \sigma_2, \sigma_3\}$. The matrix $O_3 \in \mathbb{R}^{3\times3}$ is a zero matrix. The WF motion parameters ω_0, ζ, and σ depend on the sea states, structure of the vessel and the direction of the incident waves. The vector $\boldsymbol{w}_\xi$ describes the Gaussian white noise process, *i.e.*, $\boldsymbol{w}_\xi \sim \mathcal{N}(0, Q_{c,\xi})$ The state vector may or may not have a physical interpretation depending on the particular state-space realization used.

For DP operations only the LF motion is required to be controlled. This is important to avoid unnecessary power consumption and possible wear and tear of the actuators. Therefore, the oscillatory WF motion is required to be filtered or separated from the LF motion. The WF response is required to be controlled in certain operations like ride control of a passenger vessel, where reducing pitch and role motion helps avoiding motion sickness. The stochastic nature of environmentally induced forces and moments has made the Kalman filter an essential part of the modern sea vessel motion control systems.

Filtering of the WF motion can be done either by using appropriate classical filtering techniques or it can be done by state estimation. Using filtering techniques, it is important to know the threshold frequency. Another problem with the filtering approach is possible phase lag due to delay of the signals. For an estimation approach, we need to know the parameters of the system. Even in the linearized case, parameters are required. It is also important to keep in mind that the linearized model may not be a good approximation of the actual model or system.

2.2.3 The Measurement Model

The position and heading of the vessel in the inertial frame of reference can be measured by using a differential global positioning system (DGPS) and a gyro-compass. For reliability, some vessels have multiple sensors. The measurement model can be described, using the superposition principle, by the following vector equation

$$\boldsymbol{y} = \boldsymbol{y}_b + \boldsymbol{y}_\xi + \boldsymbol{\upsilon}, \tag{2.13}$$

where $\boldsymbol{y}_b = \boldsymbol{\eta}$ and $\boldsymbol{y}_\xi = \boldsymbol{\xi}_1$ are, respectively, the position and heading measurements of the vessel corresponding to the LF and the WF motions and the vector $\boldsymbol{\nu} \in \mathbb{R}^{3\times1}$ is the Gaussian white noise process, *i.e.*, $\boldsymbol{\upsilon} \sim \mathcal{N}(0, R_c)$. The vector $\boldsymbol{\nu}$ describes the measurement noise.

2.2.4 Wave Filtering

In (2.13), the measured output is assumed to essentially contain the LF and WF motion components. The separation of the WF component from the LF component is termed as wave filtering. This action is also important to avoid thruster modulation, a phenomenon which gives rise to high frequency fluctuations in the thrust demand in the control loop. Knowledge of the sea states is required to determine the WF motion of the vessel. Sea states can be distinguished in 9 different forms (calm, smooth, rough, high, phenomenal, etc.) depending on the significant wave height [24].

Low-pass, notch, and deadband filters were the most commonly used wave filtering techniques in earlier DP systems, for instance see [82]. The main drawback of these techniques was the problem to meet the high gain control requirements due to a significant phase lag. In earlier DP systems, wave filtering was accomplished by using a proportional controller with a deadband non-linearity. This deadband produced a null control action until the control signal was inside the deadband. The length of this deadband could be increased by the operator with changing weather conditions. This change in length was termed as ‘weather’ as it was subject to the weather conditions [82].

2.3 Summary of the Mathematical Model

For more insight and a clear picture of the model of a dynamic positioning vessel, we summarize all the modeling details from the previous section of this chapter. The LF motion model is described by combining the equations (2.1), (2.3), and (2.9), and it is given by

$$\dot{\boldsymbol{\eta}} = J(\psi)\boldsymbol{\nu}, \tag{2.14}$$

$$\dot{\boldsymbol{\nu}} = -M^{-1}D\boldsymbol{\nu} + M^{-1}\boldsymbol{\tau} + J^T(\psi)\boldsymbol{b}, \tag{2.15}$$

$$\dot{\boldsymbol{b}} = -T^{-1}\boldsymbol{b} + \Psi \boldsymbol{w}_b. \tag{2.16}$$

In matrix form, we can write the LF motion model as

$$\begin{bmatrix} \dot{\boldsymbol{\eta}} \\ \dot{\boldsymbol{\nu}} \\ \dot{\boldsymbol{b}} \end{bmatrix} = \underbrace{\begin{bmatrix} O_3 & J(\psi) & O_3 \\ O_3 & -M^{-1}D & M^{-1}J^T(\psi) \\ O_3 & O_3 & -T^{-1} \end{bmatrix}}_{A_b(\psi)} \underbrace{\begin{bmatrix} \boldsymbol{\eta} \\ \boldsymbol{\nu} \\ \boldsymbol{b} \end{bmatrix}}_{\boldsymbol{x}_b} + \underbrace{\begin{bmatrix} O_3 \\ M^{-1} \\ O_3 \end{bmatrix}}_{B_b} \boldsymbol{\tau} + \underbrace{\begin{bmatrix} O_3 \\ O^3 \\ \Psi \end{bmatrix}}_{E_b} \boldsymbol{w}_b, \tag{2.17}$$

The output equation of the LF model is

$$\boldsymbol{y}_b = \underbrace{\begin{bmatrix} I_3 & O_3 & O_3 \end{bmatrix}}_{C_b} \begin{bmatrix} \boldsymbol{\eta} \\ \boldsymbol{\nu} \\ \boldsymbol{b} \end{bmatrix} + \boldsymbol{\upsilon}. \tag{2.18}$$

The dynamics of the WF motion model and its output are given by

$$\begin{bmatrix} \dot{\boldsymbol{\xi}}_1 \\ \dot{\boldsymbol{\xi}}_2 \end{bmatrix} = \underbrace{\begin{bmatrix} O_3 & I_3 \\ -\Omega^2 & -2Z\Omega \end{bmatrix}}_{A_\xi} \underbrace{\begin{bmatrix} \boldsymbol{\xi}_1 \\ \boldsymbol{\xi}_2 \end{bmatrix}}_{\boldsymbol{x}_\xi} + \underbrace{\begin{bmatrix} O_3 \\ \Sigma \end{bmatrix}}_{E_\xi} \boldsymbol{w}_\xi, \tag{2.19}$$

$$\boldsymbol{y}_\xi = \underbrace{\begin{bmatrix} I_3 & O_3 \end{bmatrix}}_{C_\xi} \begin{bmatrix} \boldsymbol{\xi}_1 \\ \boldsymbol{\xi}_2 \end{bmatrix}. \tag{2.20}$$

The complete model of motion of the vessel can be described by augmenting both the LF and WF models and it can be written in the following form.

$$\begin{bmatrix} \dot{\boldsymbol{\eta}} \\ \dot{\boldsymbol{\nu}} \\ \dot{\boldsymbol{b}} \\ \dot{\boldsymbol{\xi}}_1 \\ \dot{\boldsymbol{\xi}}_2 \end{bmatrix} = \underbrace{\begin{bmatrix} O_3 & J(\psi) & O_3 & O_3 & O_3 \\ O_3 & -M^{-1}D & M^{-1}J^T(\psi) & O_3 & O_3 \\ O_3 & O_3 & -T^{-1} & O_3 & O_3 \\ O_3 & O_3 & O_3 & O_3 & I_3 \\ O_3 & O_3 & O_3 & -\Omega^2 & -2Z\Omega \end{bmatrix}}_{A(\psi)} \underbrace{\begin{bmatrix} \boldsymbol{\eta} \\ \boldsymbol{\nu} \\ \boldsymbol{b} \\ \boldsymbol{\xi}_1 \\ \boldsymbol{\xi}_2 \end{bmatrix}}_{x} + \underbrace{\begin{bmatrix} O_3 \\ M^{-1} \\ O_3 \\ O_3 \\ O_3 \end{bmatrix}}_{B} \boldsymbol{\tau} + \underbrace{\begin{bmatrix} O_3 & O_3 \\ O_3 & O_3 \\ \Psi & O_3 \\ O_3 & O_3 \\ O_3 & \Sigma \end{bmatrix}}_{E} \underbrace{\begin{bmatrix} \boldsymbol{w}_b \\ \boldsymbol{w}_\xi \end{bmatrix}}_{w}. \tag{2.21}$$

The output of (2.21) can be obtained by using the superposition principle, see (2.13), and is written in matrix form as

$$\boldsymbol{y} = \underbrace{\begin{bmatrix} I_3 & O_3 & O_3 & I_3 & O_3 \end{bmatrix}}_{C} \begin{bmatrix} \boldsymbol{\eta} \\ \boldsymbol{\nu} \\ \boldsymbol{b} \\ \boldsymbol{\xi}_1 \\ \boldsymbol{\xi}_2 \end{bmatrix} + \boldsymbol{\upsilon}. \tag{2.22}$$

The complete model of the vessel in compact form is written as

$$\dot{\boldsymbol{x}} = A(\psi)\boldsymbol{x} + B\boldsymbol{\tau} + E\boldsymbol{w}, \tag{2.23}$$

$$\boldsymbol{y} = C\boldsymbol{x} + \boldsymbol{\upsilon}. \tag{2.24}$$

The vectors $\boldsymbol{w}$ and $\boldsymbol{\nu}$ represent the Gaussian white noise processes, *i.e.*, $\boldsymbol{w} \sim \mathcal{N}(0, Q_c)$ and $\boldsymbol{\upsilon} \sim \mathcal{N}(0, R_c)$, where $Q_c = \text{diag}\{Q_{c,b}, Q_{c,\xi}\}$. The system (2.23)-(2.24) is a pseudo-linear system because of dependency of the system matrix $A(\psi)$ on the heading angle. We call this pseudo-linear form the state dependent coefficient (SDC) parametrization of nonlinear system. Chapter 3 explains the concept of the SDC parametrization in more detail.

2.4 Properties of the Model

In this thesis, we deal with the control design and estimation problems of the DP vessel discussed in the previous sections. For this purpose, it is important to know certain properties of the vessel model which play a fundamental part in the control design and estimation techniques which we are going to use in the subsequent chapters. These properties include controllability, observability, stabilizability, and detectability. In the following, we recall some important results about these properties in the context of the pseudo-linear systems, presented in [7] .

Definition 2.4.1. (Controllability in terms of rank condition) *The pseudo-linear system of the form (2.23)-(2.24) with an n-dimensional state vector is pointwise controllable iff the rank of the controllability matrix*

$$\mathcal{C} = \begin{bmatrix} B & A(\psi)B & A^2(\psi)B & \cdots & A^{n-1}(\psi)B \end{bmatrix}, \tag{2.25}$$

is n, for each $\psi \in \mathbb{R}$. In other words, we also say the pair $(A(\psi), B)$ is pointwise controllable.

Definition 2.4.2. (Observability in terms of rank condition) *The pseudo-linear system of the form (2.23)-(2.24) with an n-dimensional state vector is pointwise observable iff the rank of the observability matrix*

$$O = \begin{bmatrix} C \\ CA(\psi) \\ CA^2(\psi) \\ \vdots \\ CA^{n-1}(\psi) \end{bmatrix}, \tag{2.26}$$

is n, for each $\psi \in \mathbb{R}$. In other words, we also say the pair $(C, A(\psi))$ is pointwise observable.

It can easily be checked that the controllability matrices corresponding to the systems (2.17) and (2.21) have rank 6 for all $\psi \in \mathbb{R}$, *i.e.*, only the position and the velocities can be controlled. This is not restrictive as the LF bias forces and the WF motions cannot be controlled. The observability matrices corresponding to both the systems have full column ranks for all $\psi \in \mathbb{R}$. So the systems are pointwise observable, *i.e.*, we can build the states of the system from the knowledge of the input and the output.

The stabilizability and detectability are weaker conditions than the controllability and observability, respectively. These properties are important from the point of view of the existence of the solution of the SDARE. In the following, we define a necessary and sufficient condition for the pointwise stabilizability and detectability of a pseudo-linear system, see [7] for more details.

Definition 2.4.3. (Pointwise Stabilizability) *The pseudo-linear system of the form of (2.23)-(2.24) with an n-dimensional state vector is pointwise stabilizable iff*

$$rank\begin{pmatrix} \lambda I - A(\psi) & B \end{pmatrix} = n, \tag{2.27}$$

for each eigenvalue λ of $A(\psi)$ which has a non-negative real part ($Re(\lambda \geq 0)$) and for all $\psi \in \mathbb{R}$. In other words, we also say the pair $(A(\psi), B)$ is stabilizable.

Definition 2.4.4. (Pointwise Detectability) *The pseudo-linear system of the form (2.23)-(2.24) with an n-dimensional state vector is pointwise detectable iff*

$$rank\begin{pmatrix} \lambda I - A(\psi) \\ C \end{pmatrix} = n, \tag{2.28}$$

for each eigenvalue λ of $A(\psi)$ which has a non-negative real part ($Re(\lambda \geq 0)$) and for all $\psi \in \mathbb{R}$. In other words, we also say the pair $(C, A(\psi))$ is detectable.

Due to the special structure of the system matrices $A_b(\psi)$ in (2.17) and $A(\psi)$ in (2.21), the eigenvalues of the system matrices do not change with the variable ψ. The only non-negative eigenvalue of both $A_b(\psi)$ and $A(\psi)$ is 0 with algebraic multiplicity 3. This makes it an easy task to compute the rank conditions (2.27) and (2.28). It can be checked that the rank is 9 for both stabilizability and detectability conditions corresponding to $A_b(\psi)$ and it is 15 for $A(\psi)$. Thus both the systems (2.17) and (2.21) are pointwise stabilizable and detectable.

Chapter 3

SDC Parametrization and Stability Analysis of Autonomous Nonlinear Systems[1]

The stability analysis of nonlinear systems has always been a challenging task. This is mainly because of phenomena like finite escape time and limit cycles, see for instance [32], [59], [79], [81], and [88]. Numerous techniques for stability analysis of nonlinear systems have been proposed over time, for further details see [43], [45], and [86]. One such approach is to first write the nonlinear system dynamics in linear-like form using a state dependent coefficient (SDC) parametrization and then analyze the possible extension of the results of linear systems theory for the stability analysis of nonlinear systems. The SDC representation provides a systematic way to analyze the extension of the results of linear systems theory for the stability analysis of nonlinear systems.

3.1 State Dependent Coefficient Parametrization

Let $\Omega \subseteq \mathbb{R}^n$ and $\boldsymbol{f}(\boldsymbol{x})$ be a vector function from Ω to $\mathbb{R}^n$. Consider the following nonlinear system

$$\dot{\boldsymbol{x}} = \boldsymbol{f}(\boldsymbol{x}), \quad \boldsymbol{x}_0 = \boldsymbol{x}(t_0), \tag{3.1}$$

where $\boldsymbol{x} \in \Omega$ is the state of the system. If the vector function $\boldsymbol{f} : \Omega \longrightarrow \mathbb{R}^n$, is continuously differentiable and $\boldsymbol{f}(0) = 0$[2], then it is always possible to write $\boldsymbol{f}(\boldsymbol{x}) = A(\boldsymbol{x})\boldsymbol{x}$, see [46]. Let us call the matrix $A(\boldsymbol{x})$ the state dependent coefficient (SDC)

[1] Section 3.4.1 and Section 3.5.1 of this chapter have been published in the form of two separate articles in the IMA Journal of Mathematical Control and Information, see [58] and [59].

[2] When it is clear from context (by the domain and codomain of the function) we write, e.g., $\boldsymbol{f}(0) = 0$ for $\boldsymbol{f}(\mathbf{0}) = \mathbf{0}$, and $A(0)$ for $A(\mathbf{0})$

parametrization of $\boldsymbol{f}(\boldsymbol{x})$. It is important to mention that the SDC parametrization is not unique unless $f(x)$ is a scalar function. For example, if $A_1(\boldsymbol{x})$ and $A_2(\boldsymbol{x})$ are two distinct parametrizations of $\boldsymbol{f}(\boldsymbol{x})$ then for $0 \leq \alpha \leq 1$,

$$\alpha A_1(\boldsymbol{x})\boldsymbol{x} + (1-\alpha)A_2(\boldsymbol{x})\boldsymbol{x} = \alpha \boldsymbol{f}(\boldsymbol{x}) + (1-\alpha)\boldsymbol{f}(\boldsymbol{x}) = \boldsymbol{f}(\boldsymbol{x}),$$

i.e.

$$\alpha A_1(\boldsymbol{x}) + (1-\alpha)A_2(\boldsymbol{x})$$

is also a parametrization of $\boldsymbol{f}(\boldsymbol{x})$. In fact infinitely many parametrizations are possible but one has to chose only those which are appropriate for the desired objectives. For more details on the SDC parametrization, interested readers are referred to [36] and to the references therein.

An important property of the SDC parametrization is that it preserves the linearization of nonlinear systems. If $A(\boldsymbol{x})$ is any parametrization of $\boldsymbol{f}(\boldsymbol{x})$ then $A(0) = \triangledown \boldsymbol{f}|_{\boldsymbol{x}=0}$. The following Lemma from [7] establishes this fact.

Lemma 3.1.1. *For any SDC parametrization $A(\boldsymbol{x})$ of $\boldsymbol{f}(\boldsymbol{x})$ with $\boldsymbol{f}(\boldsymbol{x})$ continuously differentiable and $\boldsymbol{f}(0) = 0$, $A(0)\boldsymbol{x}$ is the linearization of $\boldsymbol{f}(\boldsymbol{x})$ at the zero equilibrium.*

Proof. See [7]. □

From here onward, we will use the notions of the coefficient matrix $A(\boldsymbol{x})$ and the system matrix interchangeably. Consider the following pseudo-linear autonomous system

$$\dot{\boldsymbol{x}} = A(\boldsymbol{x})\boldsymbol{x}, \qquad \boldsymbol{x}_0 = \boldsymbol{x}(t_0). \tag{3.2}$$

In the remainder of this chapter, we analyze the stability properties of the pseudo-linear system (3.2). Our approach is based on the properties of the system matrix $A(\boldsymbol{x})$ in (3.2). In the following, we state four conditions on this matrix. To analyze the stability properties of (3.2), we will test all these conditions in the order in which they are stated.

C.1 The matrix function, $A : \Omega \longrightarrow \mathbb{R}^{n\times n}$ is a C^1 function[3]

C.2 $A(\boldsymbol{x})$ is pointwise asymptotically stable (Hurwitz) matrix, *i.e.*, all eigenvalues of $A(\boldsymbol{x})$ lie in the open left half plane for all $\boldsymbol{x} \in \Omega$. Consequently, we see that the origin $\bar{\boldsymbol{x}} = 0$ is the only equilibrium point of the system (3.2).

C.3 The system matrix, $A(\boldsymbol{x})$, is exponentially bounded *i.e.*, $\|e^{A(x)t}\| \leq M$ for some real $M > 0$ and $\forall \boldsymbol{x} \in \Omega$, $\forall t \in [0, \infty)$.

C.4 $A(\boldsymbol{x})$ is a periodic function with a period $\boldsymbol{\theta}$, *i.e.*, $A(\boldsymbol{x} + \boldsymbol{\theta}) = A(\boldsymbol{x})$, $\forall\, \boldsymbol{x} \in \Omega$.

In Chapter 2, we have introduced a mathematical model of a vessel. The system matrix of this model is a periodic function of the heading angle of the vessel. This fact is the motivation behind the fourth condition (**C.4**). The first two conditions imply that

[3] $C^1(\Omega \subseteq \mathbb{R}^n, \mathbb{R}^{n\times m}) := \{A : \Omega \longrightarrow \mathbb{R}^{n\times m}$ | A is continuous, $\partial_{x_i} A$ exists and are continuous for all $i = 1, 2, ..., n\}$.

there is only one isolated equilibrium point, $\bar{\boldsymbol{x}} = 0$, of (3.2). Therefore, the stability analysis of (3.2) will be with reference to this equilibrium point. The conditions C.1 and C.2 are sufficient to prove local asymptotic stability. The conditions C.3 and C.4 are imposed to analyze global asymptotic stability.

3.2 Local Asymptotic Stability Analysis

We start with the local asymptotic stability considerations. It can be defined as follows [73]:

Definition 3.2.1. *An equilibrium point $\bar{\boldsymbol{x}}$ of the nonlinear system (3.2) is (locally) asymptotically stable if it is stable, and if in addition there exists some $r > 0$ such that $\|\boldsymbol{x}(0)\| < r$ implies that $\boldsymbol{x}(t) \to \bar{\boldsymbol{x}}$ as $t \to \infty$.*

Since $A(\boldsymbol{x})$ is continuously differentiable, therefore, $\mathrm{col}\{A(\boldsymbol{x})\} \in C^1$. By $\mathrm{col}\{A(\boldsymbol{x})\}$, we mean the set of columns of $A(\boldsymbol{x})$. Applying the Mean Value Theorem [54] to $\mathrm{col}\{A(\boldsymbol{x})\}$, we can write

$$\mathrm{col}^j\{A(\boldsymbol{x})\} = \mathrm{col}^j\{A(0)\} + \frac{\partial \mathrm{col}^j\{A(\boldsymbol{z_j})\}}{\partial \boldsymbol{x}}\boldsymbol{x}, \qquad j = 1, 2, ..., n \tag{3.3}$$

where the vector $\boldsymbol{z_j}$ is a point, on the line connecting the origin and the point $\boldsymbol{x}$, which yields equality in the jth equation of (3.3). By $\mathrm{col}^j\{A(\boldsymbol{x})\}$, we mean the jth column of $A(\boldsymbol{x})$. Using (3.3) in (3.2), we can write

$$\begin{aligned}
\dot{\boldsymbol{x}} &= A(0)\boldsymbol{x} + \begin{bmatrix} \frac{\partial \mathrm{col}^1\{A(\boldsymbol{z_1})\}}{\partial \boldsymbol{x}}\boldsymbol{x} & \frac{\partial \mathrm{col}^2\{A(\boldsymbol{z_2})\}}{\partial \boldsymbol{x}}\boldsymbol{x} & \dots & \frac{\partial \mathrm{col}^n\{A(\boldsymbol{z_n})\}}{\partial \boldsymbol{x}}\boldsymbol{x} \end{bmatrix}\boldsymbol{x}, \\
&= A(0)\boldsymbol{x} + \sum_{j=1}^{n}\sum_{i=1}^{n} x_i x_j \frac{\partial \mathrm{col}^j\{A(\boldsymbol{z_j})\}}{\partial x_i}.
\end{aligned}$$

Multiplying and dividing the second term by $\|\boldsymbol{x}\|$ and defining

$$\psi(\boldsymbol{x}, \boldsymbol{z_1}, \boldsymbol{z_2}, ..., \boldsymbol{z_n}) \triangleq \sum_{j=1}^{n}\sum_{i=1}^{n} \frac{x_i x_j}{\|\boldsymbol{x}\|}\frac{\partial \mathrm{col}^j\{A(\boldsymbol{z_j})\}}{\partial x_i},$$

we get,

$$\dot{\boldsymbol{x}} = A(0)\boldsymbol{x} + \psi(\boldsymbol{x}, \boldsymbol{z_1}, \boldsymbol{z_2}, ..., \boldsymbol{z_n})\|\boldsymbol{x}\|. \tag{3.4}$$

Since

$$\lim_{\|\boldsymbol{x}\| \to 0} \psi(\boldsymbol{x}, \boldsymbol{z_1}, \boldsymbol{z_2}, ..., \boldsymbol{z_n}) = 0, \tag{3.5}$$

and $A(0)$ is Hurwitz, $\bar{\boldsymbol{x}}$ is a locally asymptotically stable equilibrium point of (3.4). This means, that the conditions C.1 and C.2 ensure that $\bar{\boldsymbol{x}}$ is a locally asymptotically stable equilibrium point of (3.2).

3.3 Global Asymptotic Stability Analysis

Now we proceed to the global asymptotic stability considerations. The requirements for global asymptotic stability of a nonlinear system of the form (3.2) are the following.

i. There is only one equilibrium point, $\bar{\boldsymbol{x}} \in \Omega$, of the system.

ii. The equilibrium point is locally asymptotically stable.

iii. $\lim_{t\to\infty} \boldsymbol{x}(t, \boldsymbol{x}_0) = \bar{\boldsymbol{x}}$, $\forall\, \boldsymbol{x}_0 \in \Omega$, *i.e.*, starting from any point $\boldsymbol{x}_0 \in \Omega$, the state of the system converges to the equilibrium point $\bar{\boldsymbol{x}}$ as time goes to infinity.

The conditions C.1 and C.2 are not sufficient to guarantee global asymptotic stability of (3.2). Global asymptotic stability of nonlinear systems in this form was first studied by Banks and Mhana [8]. They came up with the following result:

Proposition 3.3.1. *If $\bar{A}(\boldsymbol{x})$ is a continuous matrix-valued function which is asymptotically stable for each $\boldsymbol{x}$, then the equation*

$$\dot{\boldsymbol{x}} = \bar{A}(\boldsymbol{x})\boldsymbol{x}, \qquad \boldsymbol{x}(0) = \boldsymbol{x}_0, \tag{3.6}$$

is asymptotically stable for all $\boldsymbol{x}_0$.

This statement of Banks and Mhana is an optimistic extension of the eigenvalue based stability test for linear systems, to analyze the stability of the pseudo-linear systems (3.2). Ultimately, it was proved wrong, independently, in [47] and [81] by a simple counterexample. The counterexample is the following nonlinear system

$$\dot{\boldsymbol{x}} = \begin{bmatrix} -1 & x_1^2 \\ 0 & -1 \end{bmatrix} \boldsymbol{x}, \qquad \boldsymbol{x}_0 = \boldsymbol{x}(t_0). \tag{3.7}$$

This system satisfies Banks and Mhana's hypothesis: $A(x_1)$ is continuous and asymptotically stable. But if the initial condition is taken as $\boldsymbol{x}_0(0) = [2 \quad 2]^T$, then simple calculations yield the following solution of (3.7):

$$x_1(t) = \frac{2x_2(t)}{x_2^2(t) - 2} \quad \text{and} \quad x_2(t) = 2e^{-t}$$

for all $t \in [0, T_c)$ with $T_c = \ln \sqrt{2}$. It is obvious that as t tends to T_c then x_2 tends to $\sqrt{2}$ and consequently x_1 tends to ∞. Therefore, the system (3.7) is not asymptotically stable for all $\boldsymbol{x}_0$. Such a departure of a state variable to infinity at a finite time is called the finite escape time phenomenon. From this counterexample it is obvious that the pointwise asymptotic stability of the system matrix $A(\boldsymbol{x})$ does not help us to draw any conclusion about the stability of the nonlinear system (3.2).

In the following two sections, we continue with global asymptotic stability analysis. In Section 3.4, global asymptotic stability is analyzed with respect to the exponential boundedness of the system matrix. In Section 3.5, it is analyzed with respect to the periodicity assumption on the system matrix.

3.4 Exponential Boundedness and Global Asymptotic Stability

In this section, we continue with the findings of Langson and Alleyne and ultimately give a counterexample to show that global asymptotic stability is not guaranteed when the system matrix is exponentially bounded. Langson and Alleyne [47] studied this topic further and concluded the following:

Proposition 3.4.1. *Consider the system $\dot{\boldsymbol{x}} = A(\boldsymbol{x})\boldsymbol{x}$, where $A : \mathbb{R}^n \longrightarrow \mathbb{R}^{n\times n}$ is uniformly continuous in $\boldsymbol{x}$ and $A(\boldsymbol{x})$ is a stable matrix $\forall \boldsymbol{x} \in \mathbb{R}^n$. The origin of the given system is an asymptotically stable equilibrium point.*

Corollary 3.4.1. *If the hypothesis of Proposition 3.4.1 is satisfied with $\|e^{A(\boldsymbol{x})t}\| \leq M$ for some real $M > 0$ and $\forall \boldsymbol{x} \in \mathbb{R}^n$, $\forall t \in [0, \infty)$, then the system $\dot{\boldsymbol{x}} = A(\boldsymbol{x})\boldsymbol{x}$ is asymptotically stable for any arbitrary finite initial condition.*

In the following subsection, a counterexample [58] to these statements is presented. We construct a system where the hypotheses of Langson and Alleyne mentioned in Proposition 3.4.1 and Corollary 3.4.1 are satisfied, that is nonetheless not globally asymptotically stable.

3.4.1 A Counterexample Showing that the Exponential Boundedness of the System Matrix does not Guarantee Global Asymptotic Stability

Example 3.4.1. *We start with the following SDC formulation of a nonlinear system in a general setting*

$$\dot{\boldsymbol{x}} = \begin{bmatrix} a & b - c(\boldsymbol{x}) \\ -b - c(\boldsymbol{x}) & a \end{bmatrix} \boldsymbol{x}, \qquad \boldsymbol{x}_0 = \boldsymbol{x}(t_0), \tag{3.8}$$

where $a, b \in \mathbb{R}$ and $c(\boldsymbol{x})$ is a smooth function: $c : \mathbb{R}^2 \to \mathbb{R}$. We show that the coefficient matrix in (3.8) satisfies the hypothesis of Langson and Alleyne, for certain choices of the parameters a and b, and the scalar function $c(\boldsymbol{x})$: $a < 0$ and $b > |c(\boldsymbol{x})|$ for all $\boldsymbol{x} \in \mathbb{R}^2$.

1. *Continuity: From the description of the coefficient matrix in (3.8), it is obvious that the coefficient matrix is continuous: $A : \mathbb{R}^2 \to \mathbb{R}^{2\times 2}$ is a continuous function.*

2. *Asymptotic Stability: The general expression for the eigenvalues of the system matrix in (3.8) has the following form*

$$\lambda_{1,2} = a \pm \sqrt{c^2(\boldsymbol{x}) - b^2}. \tag{3.9}$$

Clearly, if $a < 0$ and $b^2 > c^2(\boldsymbol{x})$ for all $\boldsymbol{x} \in \mathbb{R}^2$, then $A(\boldsymbol{x})$ is Hurwitz (asymptotically stable).

3. *Exponential Boundedness: Under this subject, we derive a general expression for the upper bound of the matrix exponential of the coefficient matrix in (3.8). For the sake of convenience, in the sequel we write c instead of $c(\boldsymbol{x})$. We proceed as follows*

$$
\begin{aligned}
e^{\begin{bmatrix} a & b-c \\ -b-c & a \end{bmatrix} t} &= e^{\left(\begin{bmatrix} a & 0 \\ 0 & a \end{bmatrix} + \begin{bmatrix} 0 & b-c \\ -b-c & 0 \end{bmatrix}\right) t} \\
&= e^{\begin{bmatrix} a & 0 \\ 0 & a \end{bmatrix} t} e^{\begin{bmatrix} 0 & b-c \\ -b-c & 0 \end{bmatrix} t} \\
&= e^{at} e^{\begin{bmatrix} 0 & b-c \\ -b-c & 0 \end{bmatrix} t}.
\end{aligned} \tag{3.10}
$$

We use here the fact that if A_1 and A_2 commute then $e^{A_1+A_2} = e^{A_1}e^{A_2}$. Now consider the following transformation to make the anti-diagonal entries of the matrix in the second exponent of (3.10) the additive inverse of each other.

$$
\begin{bmatrix} 1 & 0 \\ 0 & \gamma^{-1} \end{bmatrix} \begin{bmatrix} 0 & b-c \\ -b-c & 0 \end{bmatrix} \begin{bmatrix} 1 & 0 \\ 0 & \gamma \end{bmatrix} = \begin{bmatrix} 0 & -k \\ k & 0 \end{bmatrix},
$$
$$
\begin{bmatrix} 0 & (b-c)\gamma \\ (-b-c)\gamma^{-1} & 0 \end{bmatrix} = \begin{bmatrix} 0 & -k \\ k & 0 \end{bmatrix}.
$$

Solving the pair of equations

$$
(b-c)\gamma = -k \quad \text{and} \quad \gamma^{-1}(-b-c) = k,
$$

for γ and k, we get

$$
\gamma = \pm\sqrt{\frac{b+c}{b-c}} \quad \text{and} \quad k = \pm\sqrt{b^2-c^2}.
$$

We know that

$$
e^{At} = Te^{(T^{-1}AT)t}T^{-1}. \tag{3.11}
$$

Therefore, by taking the positive value of γ, we have

$$
\begin{aligned}
& e^{\begin{bmatrix} 0 & b-c \\ -b-c & 0 \end{bmatrix} t} \\
&= \begin{bmatrix} 1 & 0 \\ 0 & \gamma \end{bmatrix} e^{\begin{bmatrix} 0 & \sqrt{b^2-c^2} \\ -\sqrt{b^2-c^2} & 0 \end{bmatrix} t} \begin{bmatrix} 1 & 0 \\ 0 & \gamma^{-1} \end{bmatrix}.
\end{aligned}
$$

Hence, we can write (3.10) as

$$
e^{\begin{bmatrix} a & b-c \\ -b-c & a \end{bmatrix}t}
= e^{at}\begin{bmatrix} 1 & 0 \\ 0 & \gamma \end{bmatrix} e^{\begin{bmatrix} 0 & \sqrt{b^2-c^2} \\ -\sqrt{b^2-c^2} & 0 \end{bmatrix}t} \begin{bmatrix} 1 & 0 \\ 0 & \gamma^{-1} \end{bmatrix}. \tag{3.12}
$$

We know that

$$
e^{\begin{bmatrix} 0 & x \\ -x & 0 \end{bmatrix}} = \begin{bmatrix} \cos x & \sin x \\ -\sin x & \cos x \end{bmatrix}. \tag{3.13}
$$

Taking the norm (we use the spectral norm) on both sides of (3.12) and using (3.13), we get

$$
\left\| e^{\begin{bmatrix} a & b-c \\ -b-c & a \end{bmatrix}t} \right\|
\le e^{at} \left\| \begin{bmatrix} 1 & 0 \\ 0 & \gamma \end{bmatrix} \right\| \cdot \left\| \begin{bmatrix} \cos\sqrt{b^2-c^2}t & \sin\sqrt{b^2-c^2}t \\ -\sin\sqrt{b^2-c^2}t & \cos\sqrt{b^2-c^2}t \end{bmatrix} \right\| \cdot \left\| \begin{bmatrix} 1 & 0 \\ 0 & \gamma^{-1} \end{bmatrix} \right\|. \tag{3.14}
$$

We have derived the general expressions for the eigenvalues, (3.9), and the upper bound of the matrix exponential, (3.14), for the system matrix in (3.8). Now, we show that the hypothesis of Langson and Alleyne, is satisfied if we take a suitable combination of the parameters a and b with scalar function $c(\boldsymbol{x})$. For example, we take $a = -0.1$, $b = 3$, and $c(\boldsymbol{x}) = -\frac{8}{\pi^2}\tan^{-1} x_1 \tan^{-1} x_2$. Then $e^{-0.1t} \le 1$, $\frac{1}{\sqrt{5}} < \gamma < \sqrt{5}$, and

$$
\left\| \begin{bmatrix} \cos\sqrt{b^2-c^2}t & \sin\sqrt{b^2-c^2}t \\ -\sin\sqrt{b^2-c^2}t & \cos\sqrt{b^2-c^2}t \end{bmatrix} \right\| = 1,
$$

$$
\left\| \begin{bmatrix} 1 & 0 \\ 0 & \gamma^{-1} \end{bmatrix} \right\| \le \sqrt{5} \quad \textit{and} \quad \left\| \begin{bmatrix} 1 & 0 \\ 0 & \gamma \end{bmatrix} \right\| \le \sqrt{5}.
$$

Therefore from (3.9) and (3.14), we have

$$
Re(\lambda_{max}) = -0.1 \quad \textit{and} \quad \left\| e^{\begin{bmatrix} -0.1 & 3-c(\boldsymbol{x}) \\ -3-c(\boldsymbol{x}) & -0.1 \end{bmatrix}t} \right\| \le 5,
$$

for all $\boldsymbol{x} \in \mathbb{R}^2$ and $t \in [0, \infty)$.

The system matrix has the following form

$$
A(\boldsymbol{x}) = \begin{bmatrix} -0.1 & 3 + \frac{8}{\pi^2}\tan^{-1} x_1 \tan^{-1} x_2 \\ -3 + \frac{8}{\pi^2}\tan^{-1} x_1 \tan^{-1} x_2 & -0.1 \end{bmatrix}. \tag{3.15}
$$

It is clear from the foregoing discussion that the system matrix in (3.15) is continuous, asymptotically stable (Hurwitz), and exponentially bounded. Thus the hypothesis of Langson and Alleyne is satisfied.

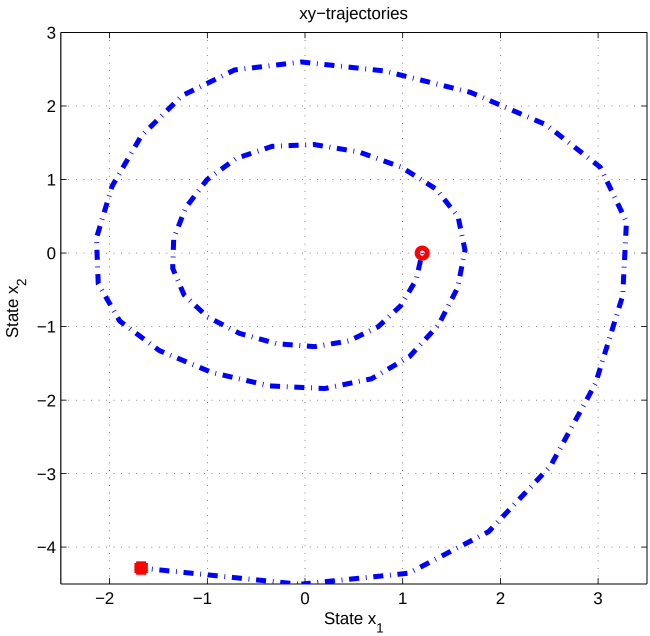

Figure 3.1: Phase-portrait of the system dynamics (3.8)

Fig. 3.1 shows the phase-portrait of the system dynamics in (3.8) using the system matrix (3.15) with an initial condition, $\boldsymbol{x}_0 = [1.2 \quad 0]^T$*. It indicates that the states of the system move away from the origin as time goes to infinity although the coefficient matrix satisfies the sufficient conditions (as claimed in [47]) for global asymptotic stability.* ▲

3.5 Periodicity and Global Asymptotic Stability

From the counterexample in the previous section, it is clear that the hypothesis of Langson and Alleyne is not sufficient to endorse global asymptotic stability of nonlinear systems of the form (3.2). At this point, a natural question is, what additional conditions would be required to establish global asymptotic stability of nonlinear systems of the form (3.2)? In addition to the smoothness conditions and exponential boundedness, we study the case that $A(\boldsymbol{x})$ is also a $\boldsymbol{\theta}$−periodic matrix, *i.e.*,

$$A(\boldsymbol{x}) = A(\boldsymbol{x} + \boldsymbol{\theta}) \text{ for all } \boldsymbol{x} \in \Omega \text{ and some } \boldsymbol{\theta} \in \mathbb{R}. \tag{3.16}$$

Condition C.4, that the system matrix $A(\boldsymbol{x})$ is periodic, ensures that the finite escape time phenomenon will not occur. If a function is continuous and periodic on Ω then it must be bounded. In the following proposition, we prove how the periodicity condition rules out the possibility of the finite escape time phenomenon.

Proposition 3.5.1. *Suppose that the system (3.2) satisfies the usual regularity (smoothness) conditions. If the system matrix in (3.2) is continuous, Hurwitz and periodic then the system has bounded solutions for all times* $t < \infty$.

Proof. The solution of (3.2) exists, because regularity conditions are assumed to be satisfied, and can be written as

$$\boldsymbol{x}(t) = \boldsymbol{x}_0 + \int_0^t A(\boldsymbol{x}(s))\boldsymbol{x}(s)ds. \tag{3.17}$$

Since the system matrix $A(\boldsymbol{x})$ is continuous, Hurwitz, and periodic for all $\boldsymbol{x} \in \Omega$, it must be bounded. Therefore, $\exists M > 0,\ s.t.\ \|A(\boldsymbol{x})\| < M,\ \forall \boldsymbol{x} \in \mathbb{R}^n$. Taking the norm on both sides of (3.17) and using the fact that $A(\boldsymbol{x})$ is bounded, it follows that

$$\|\boldsymbol{x}(t)\| \leq \|\boldsymbol{x}_0\| + \int_0^t M\|\boldsymbol{x}(s)\|ds.$$

Using Gronwall's Lemma [85, Chapter 1, page:5], we get

$$\|\boldsymbol{x}(t)\| \leq \|\boldsymbol{x}_0\|e^{Mt}.$$

This expression shows that the state of the system is bounded for all $t < \infty$, *i.e.*, the state does not blow up in finite time. This completes the proof. □

Further research on this topic results in yet another counterexample which leads us to the conclusion that adding the periodicity condition alone does not suffice to guarantee global asymptotic stability. The details are explained in the following subsection.

3.5.1 A Counterexample Showing that the Periodicity of the System Matrix does not Guarantee Global Asymptotic Stability

Example 3.5.1. *This example has two parts: first we analyze the system matrix and then analyze the corresponding system.*

Analysis of Coefficient Matrix

In order to present the counterexample, we first consider the matrix

$$A(x_1) = \begin{pmatrix} 2\alpha & -2 \\ 2 + 4\alpha^2 & -4\alpha \end{pmatrix}, \tag{3.18}$$

where $\alpha = \sin^2 x_1 + \varepsilon$, *with* $\varepsilon \in \mathbb{R}$ *such that* $0 < \varepsilon < 1$. *Hence,* α *is a real number such that* $0 < \alpha \leq 1 + \varepsilon < 2$ *for any* $x_1 \in \mathbb{R}$.

Note that the matrix $A(x_1)$ *is periodic with period* π, *i.e.,* $A(x_1) = A(x_1 + \pi)$ *for all* $x_1 \in \mathbb{R}$. *Further, note that* $A(x_1)$ *depends on* x_1 *in a continuous way.*

With ε *as above, the eigenvalues of* $A(x_1)$ *are given by*

$$\lambda_{1,2} = -\alpha \pm i\sqrt{4 - \alpha^2},$$

where "i" denotes the imaginary unit. Clearly, the eigenvalues of $A(x_1)$ *are complex, since* $4-\alpha^2>0$. *Furthermore, the eigenvalues of* $A(x_1)$ *are located in the open left half of the complex plane, since* $\alpha>0$. *Hence, for all* $x_1\in\mathbb{R}$, *the matrix* $A(x_1)$ *is a so-called Hurwitz matrix, i.e., all eigenvalues of* $A(x_1)$ *have a negative real part.*

An eigenvector for the eigenvalue $\lambda_1=-\alpha+i\sqrt{4-\alpha^2}$ *is given, for instance, by the nonzero complex-valued vector*

$$v_1=\begin{pmatrix}2\\3\alpha\end{pmatrix}+i\begin{pmatrix}0\\-\sqrt{4-\alpha^2}\end{pmatrix}.$$

It can indeed be verified that $A(x_1)v_1=\lambda_1v_1$. *Note that* $A(x_1)$ *is a real-valued matrix, but that* $A(x_1)v_1$ *and* λ_1v_1 *are complex-valued expressions. Then, equating the real and imaginary parts of* $A(x_1)v_1$ *and* λ_1v_1, *it follows that*

$$A(x_1)\begin{pmatrix}2\\3\alpha\end{pmatrix}=-\alpha\begin{pmatrix}2\\3\alpha\end{pmatrix}-\sqrt{4-\alpha^2}\begin{pmatrix}0\\-\sqrt{4-\alpha^2}\end{pmatrix}$$

and

$$A(x_1)\begin{pmatrix}0\\-\sqrt{4-\alpha^2}\end{pmatrix}=\sqrt{4-\alpha^2}\begin{pmatrix}2\\3\alpha\end{pmatrix}-\alpha\begin{pmatrix}0\\-\sqrt{4-\alpha^2}\end{pmatrix}.$$

Combining the expressions, it follows that

$$A(x_1)\begin{pmatrix}2&0\\3\alpha&-\sqrt{4-\alpha^2}\end{pmatrix}=\begin{pmatrix}2&0\\3\alpha&-\sqrt{4-\alpha^2}\end{pmatrix}\begin{pmatrix}-\alpha&\sqrt{4-\alpha^2}\\-\sqrt{4-\alpha^2}&-\alpha\end{pmatrix},$$

or

$$A(x_1)T=TD,$$

with

$$T=\begin{pmatrix}2&0\\3\alpha&-\sqrt{4-\alpha^2}\end{pmatrix},\quad D=\begin{pmatrix}-\alpha&\sqrt{4-\alpha^2}\\-\sqrt{4-\alpha^2}&-\alpha\end{pmatrix}.$$

By the restrictions on ε *and* α, *it is clear that matrix* T *is invertible. Hence, it follows that*

$$A(x_1)=TDT^{-1},$$

and, consequently, that

$$e^{A(x_1)t}=Te^{Dt}T^{-1}. \tag{3.19}$$

Because of the special form of the matrix D, *it follows (see any book on differential equations such as [10, page. 332]) that for all* $t\geq 0$,

$$e^{Dt}=e^{-\alpha t}\begin{pmatrix}\cos\sqrt{4-\alpha^2}t&\sin\sqrt{4-\alpha^2}t\\-\sin\sqrt{4-\alpha^2}t&\cos\sqrt{4-\alpha^2}t\end{pmatrix}.$$

The matrix on the right-hand side in the above equation has a finite norm. Indeed, considering the Frobenius norm, i.e., the square root of the sum of squared moduli of all matrix elements, see [33], it follows that the Frobenius norm of the real matrix

$$\begin{pmatrix}\cos\sqrt{4-\alpha^2}t&\sin\sqrt{4-\alpha^2}t\\-\sin\sqrt{4-\alpha^2}t&\cos\sqrt{4-\alpha^2}t\end{pmatrix},$$

is equal to $\sqrt{2}$. *The Frobenius norm of* e^{Dt} *is then given by* $\sqrt{2}e^{-\alpha t}$. *The Frobenius norms of the matrices* T *and* T^{-1} *are given by* $\sqrt{8+8\alpha^2}$ *and* $\sqrt{\frac{2+2\alpha^2}{4-\alpha^2}}$, *respectively.*

Let $\cdot\|_F$ denote the Frobenius norm. It is well-known (or easy to prove) that the Frobenius norm is sub-multiplicative, i.e., $\|UV\|_F \leq \|U\|_F\|V\|_F$ for any two square matrices U and V of the same size. Therefore, it follows from (3.19) that for all $t \geq 0$,

$$\left\|e^{A(x_1)t}\right\|_F \leq \|T\|_F \left\|e^{Dt}\right\|_F \left\|T^{-1}\right\|_F \leq \sqrt{8+8(1+\varepsilon)^2}\,\sqrt{2}e^{-\alpha t}\sqrt{\frac{2+2(1+\varepsilon)^2}{4-(1+\varepsilon)^2}}.$$

Since $\alpha > 0$, it follows that $0 \leq e^{-\alpha t} \leq 1$, for all $t \geq 0$. Hence, for all $t \geq 0$,

$$\left\|e^{A(x_1)t}\right\|_F \leq 2\sqrt{2}\frac{(2+2(1+\varepsilon)^2)}{\sqrt{4-(1+\varepsilon)^2}}.$$

So, there exists a number $M \in \mathbb{R}$, depending on ε, such that $\left\|e^{A(x_1)t}\right\|_F \leq M$, for all $t \geq 0$ and for all $x_1 \in \mathbb{R}$.

Recapitulating, the matrix $A(x_1)$ defined in (3.18), with $\alpha = \sin^2 x_1 + \varepsilon$ and with ε a fixed number such that $0 < \varepsilon < 1$, satisfies the following conditions:

- *$A(x_1)$ is Hurwitz for all $x_1 \in \mathbb{R}$, i.e., all eigenvalues of $A(x_1)$ have negative real part for all $x_1 \in \mathbb{R}$,*
- *$A(x_1)$ depends continuously on x_1,*
- *$e^{A(x_1)t}$ is "uniformly" bounded in $t \geq 0$ and $x_1 \in \mathbb{R}$, i.e., there exists an $M \in \mathbb{R}$ such that $\left\|e^{A(x_1)t}\right\|_F \leq M$, for all $t \geq 0$ and $x_1 \in \mathbb{R}$.*

In [47], it is claimed that the above conditions are sufficient for global asymptotic stability of the associated differential equation. In [58], we showed that this claim is not correct.

Here, in addition to the above properties, we also have that

- *$A(x_1)$ is periodic with period π, i.e., $A(x_1) = A(x_1 + \pi)$ for all $x_1 \in \mathbb{R}$.*

However, this additional property in general, does not offer anything extra as far as global asymptotic stability is concerned. This is shown in the following analysis of the differential equation.

Analysis of the Differential Equation

To show that the above conditions are generally not sufficient to guarantee global asymptotic stability, we consider the differential equation

$$\dot{\boldsymbol{x}} = A(x_1)\boldsymbol{x}, \qquad \textit{with} \quad \boldsymbol{x} = \begin{pmatrix} x_1 \\ x_2 \end{pmatrix}, \tag{3.20}$$

where $A(x_1)$ is as defined in (3.18), with $\alpha = \sin^2 x_1 + \varepsilon$, and with ε a fixed number such that $0 < \varepsilon < 1$.

Because $A(x_1)$ is Hurwitz for all $x_1 \in \mathbb{R}$, see the previous subsection, $A(x_1)$ is invertible for all $x_1 \in \mathbb{R}$. Therefore, differential equation (3.20) has only one equilibrium point, namely the origin. Moreover, since $A(x_1)$ is Hurwitz for $x_1 = 0$, it follows that the linearization of (3.20) around the origin, given by $\dot{\boldsymbol{x}} = A(0)\boldsymbol{x}$, is locally asymptotically stable. It is then well known, see for instance [85], that there exists a *neighborhood of the origin such that solutions of (3.20), starting in this neighborhood, converge to the origin for time going to infinity. However due to the non-linearity of (3.20), and often also in general, there are initial conditions for which this convergence does not take place. Indeed, as numerical simulations show, there are initial conditions such that the resulting solution does not converge.*

More specifically, for $\epsilon = 0.05$*, clearly satisfying* $0 < \epsilon < 1$*, starting from* $x_1(0) = 1, x_2(0) = 0$*, the solution of the differential equation spirals outwards. It further more follows from simulations that for* $x_1(0) = 1.5, x_0 = 0$*, the resulting solution spirals inwards, but does not converge to the origin. As a consequence, by a Poincaré-Bendixson kind of reasoning, see [85], both the solutions converge to a limit cycle that intersects the* x_1-*axis between 1 and 1.5. See also Figure 3.2, where the solutions are displayed starting from* $x_1(0) = 1,\ x_2(0) = 0$ *and* $x_1(0) = 1.5,\ x_2(0) = 0$*, respectively.*

In Figure 3.2, the limit cycle to which the two solutions converge is depicted by a dash-dotted red line. This limit cycle intersects the positive x_1-*axis around* $x_1 = 1.265$*. Figure 3.2 also contains a second smaller limit cycle, also depicted by a dash-dotted red line. This second limit cycle intersects the positive* x_1-*axis around* $x_1 = 0.460$*. It bounds the neighborhood around the origin in which solutions converge to the origin. Outside this neighborhood, the solutions converge towards the larger limit cycle.*

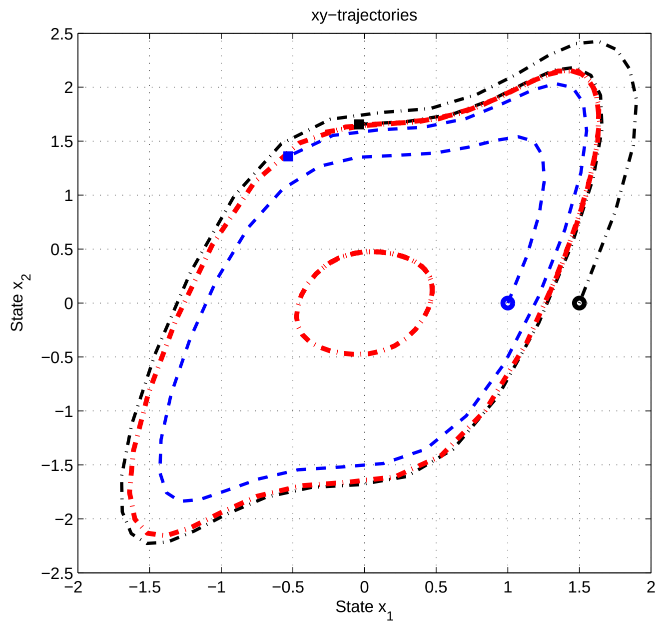

Figure 3.2: Phase portrait of the system dynamics (3.20).

Figure 3.2 indicates that the solution starting in certain initial states never reaches the only equilibrium state, as time goes to infinity, although the coefficient matrix satisfies the conditions in [47]. Hence, the origin, being the only equilibrium state, is not globally asymptotically stable. Also it is clear that the additional requirement of *periodic state dependency of the coefficient matrix does not help in attaining global asymptotic stability.*

Concluding Remarks

From the foregoing discussion, it is clear that the conditions C.1, C.2, and C.3 are not sufficient to guarantee global asymptotic stability of a non-linear system written as a pseudo-linear system in state dependent coefficient form (3.2), even with the periodicity condition as well, see [58]. ▲

3.6 An LMI Based Approach for Global Asymptotic Stability

In general, periodicity of the system matrix does not imply global asymptotic stability of (3.2). However, this assumption helps in analyzing its global asymptotic stability as we have seen in Example 3.5.1. For instance, we assume that the system matrix $A(\boldsymbol{x})$ is a function of a single state component and it is $\theta-$periodic as well. Then (3.16) becomes

$$A(x_1 + \theta) = A(x_1), \text{ for all } x_1 \in \mathbb{R} \text{ and } \theta \in \mathbb{R}, \tag{3.21}$$

where, without loss of generality, x_1 is the first component of the state vector.

The eigenvalue criterion is a well-known approach to analyze asymptotic stability of linear systems. It is stated as follows [15, Chapter 7, page:203].

Theorem 3.6.1. Eigenvalue Criterion for Stability. *The system*

$$\dot{\boldsymbol{x}} = A\boldsymbol{x}, \quad \boldsymbol{x}(0) = \boldsymbol{x}_0, \tag{3.22}$$

is asymptotically stable if and only if all the eigenvalues of the matrix A have negative real parts.

Before the advent of fast computing machines like modern age computers, computation of eigenvalues was a cumbersome task. In 1892, a Russian mathematician, A. M. Lyapunov (1857-1918) proposed a method to analyze asymptotic stability of linear systems. This method does not require eigenvalue computation. Lyapunov narrated his method as follows [15, Chapter 7, page:205].

Theorem 3.6.2. Lyapunov Stability Theorem. *The system (3.22) is asymptotically stable if and only if, for any symmetric positive definite matrix Q, there exists a unique symmetric positive definite matrix P satisfying the equation:*

$$PA + A^T P = -Q. \tag{3.23}$$

In (3.23), we can easily transform the matrix equation into a matrix inequality to get

$$PA + A^T P \prec 0, \ \because \ -Q \prec 0. \tag{3.24}$$

For a given $N \times N$ matrix P, the constraint $P(\succeq) \succ 0$ would denote that the matrix P is positive (semi-)definite and the constraint $P(\preceq) \prec 0$ would denote that the matrix P is negative (semi-)definite.

In this section, an LMI based approach is proposed and discussed to establish global asymptotic stability of the pseudo-linear systems of the form (3.2) when the system matrix has the form (3.21). The motivation for this approach comes from [71, Chapter 4] where asymptotic stability of linear systems is analyzed subject to parameter uncertainties. We see a similar situation in (3.21) where the system matrix depends on a single state component which varies periodically with period θ.

This approach has two steps. The first step is to formulate an LMI feasibility problem using the concept introduced in the Theorem 3.6.2. The solution of this LMI feasibility problem gives a constant symmetric positive definite matrix. In the second step, we use the solution matrix from the LMI feasibility problem (Step I) to prove the global asymptotic stability of the system under consideration by using a quadratic Lyapunov function. The details of this approach are as follows.

Step I- LMI Feasibility Problem Formulation

Inspired by the Lyapunov Stability Theorem, we propose an equivalent result for the pseudo-linear system (3.2). Before proceeding further, it is important to mention that the LMI solver SeDuMi which we use in the sequel, does not distinguish between $\succ$ and $\succeq$ (likewise between $\prec$ and $\preceq$). Therefore, we formulate the LMI feasibility problem with non-strict equality constraints. The system (3.2) is pointwise asymptotically stable if and only if for each $x_1 \in \mathbb{R}$, $\exists\, P(x_1) = P^T(x_1) \succeq 0$ s.t.

$$A^T(x_1)P(x_1) + P(x_1)A(x_1) + I_n \preceq 0. \tag{3.25}$$

It is important to mention that, without loss of generality, we take $Q = I_n$ as a constant identity matrix. The choice $Q = I_n$ helps us in stability analysis by ensuring strict inequalities, as we will see in the sequel. Intuitively, we are interested to investigate whether there exists a constant matrix $P = P^T \succeq 0$ for which the following holds

$$A^T(x_1)P + PA(x_1) + I_n \preceq 0, \quad \forall\, x_1 \in \mathbb{R}. \tag{3.26}$$

Therefore, if the LMI in (3.26) holds true for all x_1 in the principal interval $[-\frac{\theta}{2}, \frac{\theta}{2}]$ then it will hold for all $x_1 \in \mathbb{R}$.

To verify this we proceed as follows. We mark k (sufficiently large) number of points on $[-\frac{\theta}{2}, \frac{\theta}{2})$ and formulate an LMI feasibility problem as follows:
Does there exist a $P = P^T \succ 0$ which satisfies the LMI in (3.26) at k points, $x_{1_k} \in [-\frac{\theta}{2}, \frac{\theta}{2})$?
This gives rise to $k+1$ LMIs. The system matrix $A(x_1)$ is θ-periodic which means that it will be same at $x_1 = -\frac{\theta}{2}$ and $x_1 = \frac{\theta}{2}$. Hence, to ensure that all LMIs are distinct, we take $x_{1_k} \in [-\frac{\theta}{2}, \frac{\theta}{2})$. Mathematically, we formulate the LMI feasibility problem as follows:

Does there exist a symmetric matrix P which satisfies the following set of LMIs

$$\left.\begin{aligned} P - I_n &\geq 0 \\ A^T(x_{11})P + PA(x_{11}) + I_n &\leq 0 \\ A^T(x_{12})P + PA(x_{12}) + I_n &\leq 0 \\ &\vdots \\ A^T(x_{1k})P + PA(x_{1k}) + I_n &\leq 0 \end{aligned}\right\}? \tag{3.27}$$

We solve this LMI feasibility problem with YALMIP package (see [50] for more details) in *MATLAB*^{TM} using the solver SeDuMi (see [78] for more details).

Step II- Global Asymptotic Stability Analysis

Here we explain how we use the solution of the LMI feasibility problem to establish global asymptotic stability of the system under consideration. Before proceeding further, we recall the important Barbashin-Krasovskii theorem from [43, Chapter 4, page:124] which we use in the stability analysis.

Theorem 3.6.3. *Let $\bar{\boldsymbol{x}} = 0$ be an equilibrium point for (3.2). Let $V : \Omega \longrightarrow \mathbb{R}$ be a continuously differentiable function such that*

$$V(0) = 0 \quad \textit{and} \quad V(\boldsymbol{x}) > 0, \quad \forall \boldsymbol{x} \neq 0, \tag{3.28}$$

$$||\boldsymbol{x}|| \longrightarrow \infty \quad \Rightarrow \quad V(\boldsymbol{x}) \longrightarrow \infty, \tag{3.29}$$

$$\dot{V}(\boldsymbol{x}) < 0, \quad \forall \boldsymbol{x} \neq 0, \tag{3.30}$$

then $\bar{\boldsymbol{x}} = 0$ is globally asymptotically stable.

We define a quadratic Lyapunov function as:

$$V(\boldsymbol{x}) = \boldsymbol{x}^T P \boldsymbol{x}. \tag{3.31}$$

Here $P = P^T > 0$ is the solution of the LMI feasibility problem (3.27). Differentiating (3.31) w.r.t ‘t’

$$\dot{V}(\boldsymbol{x}) = \boldsymbol{x}^T[A^T(x_1)P + PA(x_1)]\boldsymbol{x}. \tag{3.32}$$

The function in (3.31) satisfies all requirements stated in Theorem 3.6.3 provided

$$A^T(x_1)P + PA(x_1) \leq -I_n < 0, \quad \forall x_1 \in \mathbb{R}.$$

Therefore, global asymptotic stability of the system (3.2) can immediately be established if the LMI feasibility problem, (3.27), has a feasible solution. We illustrate our approach by the following example.

Example 3.6.1. *We consider a fourth order nonlinear system of the form (3.2). We begin by defining a system matrix of the following form.*

$$\bar{A}(x_1) = A_0 + A_1 \cos x_1 + B_1 \sin x_1. \tag{3.33}$$

We generate the constant matrices A_0, A_1, and B_1 at random using the standard Gaussian distribution with mean 0 *and standard deviation* 1*. In particular, we randomly generate A_0 as a diagonal matrix and A_1 and B_1 as full matrices. Thus we form a system matrix which is continuous and periodic. To obtain a continuous, periodic, and Hurwitz matrix, we define,*

$$\beta \triangleq (1+\delta)\lambda_{max}(\bar{A}(x_1)), \qquad \forall x_1 \in [-\pi, \pi], \tag{3.34}$$

where $\delta > 0$ is a small number and λ_{max} denotes the maximum real part of the eigenvalues of $\bar{A}(x_1)$. Then the matrix

$$A(x_1) = \bar{A}(x_1) - \beta I, \tag{3.35}$$

where I is the identity matrix of the size of $\bar{A}(x_1)$, will be Hurwitz. Figure 3.3 shows the behavior of the state dynamics of a system of the form (3.2), having system matrix (3.35) and A_0, A_1, and B_1 are as given later in this example, with four different arbitrarily chosen initial conditions. We see that the states converge asymptotically to the origin. This indicates that the states of the system may converge asymptotically to the origin for all initial conditions $\boldsymbol{x}_0 = (x_1, x_2, x_3, x_4) \in \mathbb{R}^4$.

In retrospect of the theory discussed earlier, the first step is to formulate an LMI feasibility problem. We present three different results each with a different choice of the number of LMIs in the feasibility problem. The system matrix (3.35) is $2\pi-$ periodic. We mark $(k=)120, 300,$ and 440 points on the interval $[-\pi, \pi)$. In this way, we form a system of 121, 301, and 441 LMIs analogous to (3.27). As has been mentioned earlier, we generate the set of matrices A_0, A_1, and B_1 at random. We see in our experiments that for all such sets of matrices, the state dynamics of the nonlinear system, with arbitrarily chosen initial states, converge asymptotically to the origin. In a particular set, we have the following matrices

$$A_0 = \begin{bmatrix} 0.3146 & 0 & 0 & 0 \\ 0 & 0.8596 & 0 & 0 \\ 0 & 0 & 0.1287 & 0 \\ 0 & 0 & 0 & 0.0166 \end{bmatrix},$$

$$A_1 = \begin{bmatrix} -0.0728 & 0.9884 & 0.6450 & 0.2224 \\ -0.9943 & -0.5990 & -1.3099 & 1.8713 \\ -0.7474 & 1.4766 & -0.8674 & 0.1100 \\ -0.0308 & -0.8138 & -0.4742 & -0.4113 \end{bmatrix},$$

$$B_1 = \begin{bmatrix} 0.5112 & -0.2958 & 1.6777 & 0.3630 \\ -1.1991 & -0.1680 & 1.9969 & -0.5670 \\ -0.0964 & 0.1795 & 0.6970 & -1.0442 \\ 0.4458 & 0.4211 & -1.3664 & 0.6971 \end{bmatrix}.$$

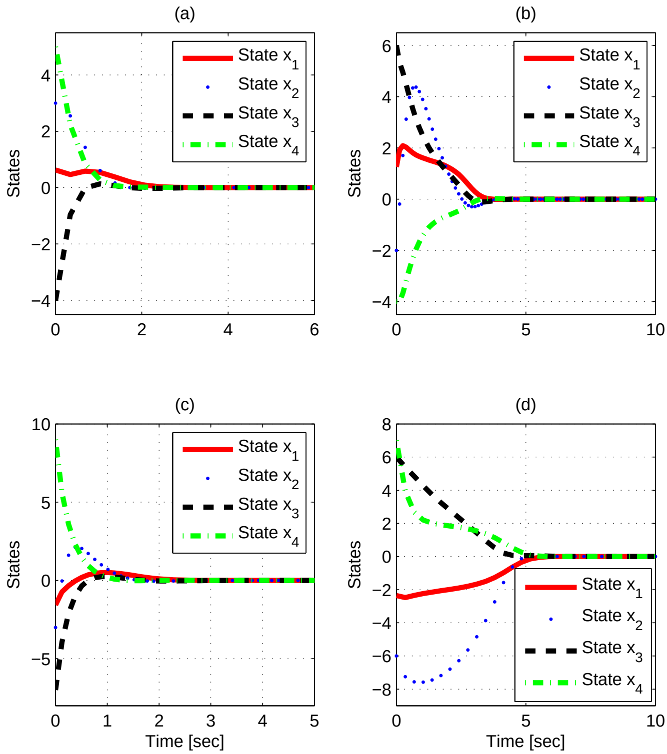

Figure 3.3: Behavior of the state dynamics of the system (3.2)-(3.35) with four arbitrary initial conditions (a).$(\frac{\pi}{5}, 3, -4, 5)$, (b).$(\frac{2\pi}{5}, -2, 6, -4)$, (c).$(-\frac{\pi}{2}, -3, -7, 9)$, (d).$(-\frac{3\pi}{4}, -6, 6, 7)$.

We solve the three LMI feasibility problems consisting of 121, 301, and 441 LMIs and we get the following feasible solutions, respectively. For $k = 120$, in 9 iterations, SeDuMi yields

$$P_1 = \begin{bmatrix} 3.4727 & -0.0050 & -0.5492 & 0.0835 \\ -0.0050 & 2.8798 & -0.4821 & -0.0967 \\ -0.5492 & -0.4821 & 4.1219 & 0.1140 \\ 0.0835 & -0.0967 & 0.1140 & 3.7498 \end{bmatrix}.$$

The eigenvalues of the matrix P_1 are 2.6626, 3.2274, 3.7827, and 4.5515. Since all eigenvalues are positive, P_1 is a symmetric positive definite (SPD) matrix. For $k = 300$, in 7 iterations, SeDuMi yields

$$P_2 = \begin{bmatrix} 4.3305 & -0.0830 & -0.6174 & 0.1847 \\ -0.0830 & 3.5683 & -0.4611 & -0.0278 \\ -0.6174 & -0.4611 & 5.0721 & -0.0345 \\ 0.01847 & -0.0278 & -0.0345 & 4.6450 \end{bmatrix}.$$

The eigenvalues of the matrix P_2 are 3.3606, 4.0759, 4.6743, and 5.5051. Since all eigenvalues are positive, P_2 is an SPD matrix. For $k = 440$, in 7 iterations, SeDuMi yields

$$P_3 = \begin{bmatrix} 8.8841 & -0.2495 & -1.1634 & 0.4852 \\ -0.2495 & 7.3402 & -0.8016 & 0.0303 \\ -1.1634 & -0.8016 & 10.3775 & -0.2747 \\ 0.4852 & 0.0303 & -0.2747 & 9.5379 \end{bmatrix}.$$

The eigenvalues of the matrix P_3 are 6.9676, 8.4366, 9.5000, and 11.2355. Since all eigenvalues are positive, P_3 is an SPD matrix.

Now, a quadratic Lyapunov function $V(\boldsymbol{x}) = \boldsymbol{x}^T P_{i'} \boldsymbol{x}$, $i' = 1, 2, 3$ satisfies all the conditions for global asymptotic stability stated in Theorem 3.6.3. Therefore, this fourth order nonlinear autonomous system is globally asymptotically stable. ▲

Figure 3.4 shows the maximum eigenvalue profiles of $A^T(x_{1_i})P_{i'} + P_{i'}A(x_{1_i})$ for all $x_{1_i} \in [-\pi, \pi)$, $i = 1, 2, ..., k$ vs x_1 corresponding to LMI systems consisting of 121, 301 and 441 constraints. We see that the curves lie below the horizontal axis. This implies that the symmetric matrices $A^T(x_{1_i})P_{i'} + P_{i'}A(x_{1_i})$, $\forall\, x_{1_i} \in [-\pi, \pi]$, are negative definite and the pattern of the eigenvalues profiles shows that they become more negative-definite as the size of the system of LMIs grows.

The above described LMI based Lyapunov method to prove global asymptotic stability of the systems of the form (3.2), depends on the solution of the LMI feasibility problem. If the LMI feasibility problem does not have a feasible solution then we cannot directly deduce global asymptotic stability with this method. Nevertheless, this method may still be useful with a naive modification in the LMI constraints. The following subsection explains this situation.

3.6.1 Infeasibility of the LMI Feasibility Problem

Example 3.6.2. *Consider the following autonomous nonlinear system*

$$\begin{bmatrix} \dot{\boldsymbol{\eta}} \\ \dot{\boldsymbol{\nu}} \end{bmatrix} = \begin{bmatrix} O_3 & J(\psi) \\ O_3 & -M^{-1}D \end{bmatrix} \begin{bmatrix} \boldsymbol{\eta} \\ \boldsymbol{\nu} \end{bmatrix} + \begin{bmatrix} O_3 \\ M^{-1} \end{bmatrix} \boldsymbol{\tau}. \tag{3.36}$$

This model has been introduced in Chapter 2 where more details about the model can be found.

We see that the system matrix in (3.36) is not Hurwitz. But by verifying the rank condition of (2.27), we find that it is a stabilizable system. We use the following stabilizing state feedback control law

$$\boldsymbol{\tau} = \begin{bmatrix} -MJ^T(\psi) & D - 2M \end{bmatrix} \begin{bmatrix} \boldsymbol{\eta} \\ \boldsymbol{\nu} \end{bmatrix}. \tag{3.37}$$

This results in a continuous, Hurwitz, and 2π–periodic feedback system matrix given by

$$A_c(\psi) = \begin{bmatrix} O_3 & J(\psi) \\ -J^T(\psi) & -2I_3 \end{bmatrix}. \tag{3.38}$$

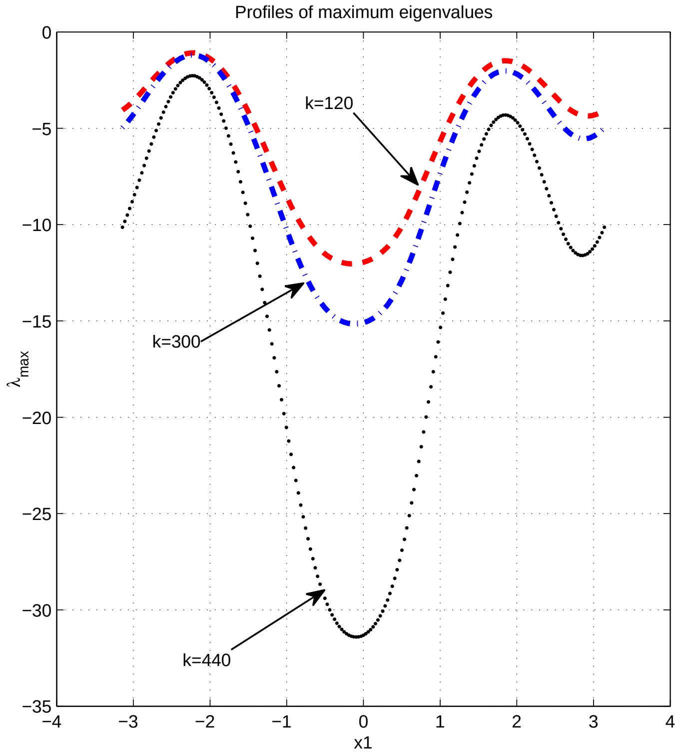

Figure 3.4: Profiles of the maximum eigenvalues of the symmetric matrices $A^T(x_{1i})P_{i'} + P_{i'}A(x_{1i})$, $\forall\, x_{1_i} \in [-\pi, \pi]$, $i = 1, 2, ..., k$ and $i' = 1, 2, 3$ vs state component x_1.

Figure 3.5 shows the state dynamics of the closed loop system (3.36)-(3.37) with four different arbitrarily chosen initial conditions. Clearly, the states converge asymptotically to the origin.

We formulate an LMI feasibility problem as described in (3.27) by using the closed loop system matrix (3.38). The outcome from the LMI solver SeDuMi is: the LMI feasibility problem is infeasible. This means, the LMI based Lyapunov stability approach is not working in this case. ▲

Remark 3.6.1. *Consider a naive modification in the inequality constraints (3.27) which results the following form*

$$A_c^T(\psi)P + PA_c(\psi) + \begin{bmatrix} O_3 & O_3 \\ O_3 & I_3 \end{bmatrix} \leq 0. \tag{3.39}$$

We get a feasible solution for this LMI feasibility problem from SeDuMi. But we cannot use Theorem 3.6.3 because $\dot{V}(\boldsymbol{x})$ is only positive semidefinite in this case. We require LaSalle's Principle for stability analysis in such situations.

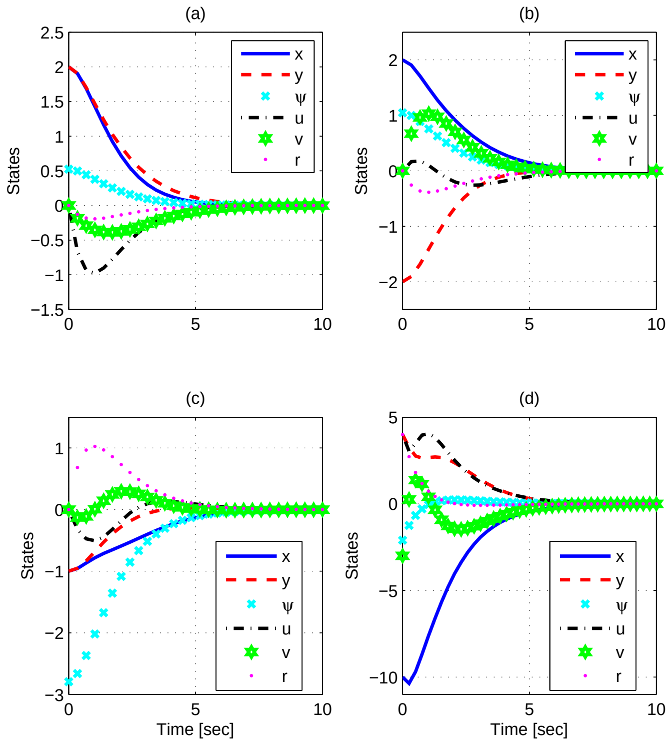

Figure 3.5: Behavior of the state dynamics of the system in Example 3.6.1 with four arbitrary initial conditions (a).$(2, 2, \frac{\pi}{6}, 0, 0, 0)$, (b).$(2, -2, \frac{\pi}{3}, 0, 0, 0)$, (c).$(-1, -1, -\frac{8\pi}{9}, 0, 0, 0)$, (d).$(-10, 4, -\frac{2\pi}{3}, 4, -3, 4)$.

Remark 3.6.2. *A more practical and useful form of (3.37) can be*

$$\tau = \begin{bmatrix} -MJ^T(\psi) & \mathcal{R} - 2M \end{bmatrix} \begin{bmatrix} \boldsymbol{\eta} \\ \boldsymbol{\nu} \end{bmatrix}, \tag{3.40}$$

where $\mathcal{R}$ denotes the additional damping effect introduced via controller action.

To investigate the infeasibility issue in more detail, an analytic approach to the LMI feasibility problem associated with the system in Example 3.6.2, is presented in the following subsection.

Analytic approach to the LMI problem

For the closed loop system matrix (3.38), we would like to find an SPD matrix P s.t.

$$A_c^T(\psi)P + PA_c(\psi) \prec 0, \;\; \forall \psi \in [-\pi, \pi].$$

Suppose that P has the following form

$$P = \begin{bmatrix} P_a & P_b^T \\ P_b & P_c \end{bmatrix}.$$

For the sake of convenience, from here onward in this subsection, we omit the argument ψ from $J(\psi)$. Now consider,

$$A_c^T P + PA_c \prec 0,$$

$$\iff \begin{bmatrix} O_3 & -J \\ J^T & -2I_3 \end{bmatrix}\begin{bmatrix} P_a & P_b^T \\ P_b & P_c \end{bmatrix} + \begin{bmatrix} P_a & P_b^T \\ P_b & P_c \end{bmatrix}\begin{bmatrix} O_3 & J \\ -J^T & -2I_3 \end{bmatrix} \prec 0,$$

$$\iff \begin{bmatrix} -JP_b - (JP_b)^T & P_aJ - 2P_b^T - JP_c \\ (P_aJ - 2P_b^T - JP_c)^T & (P_bJ)^T + P_bJ - 4P_c \end{bmatrix} \prec 0. \tag{3.41}$$

Or equivalently,

$$\iff -\begin{bmatrix} -JP_b - (JP_b)^T & P_aJ - 2P_b^T - JP_c \\ (P_aJ - 2P_b^T - JP_c)^T & (P_bJ)^T + P_bJ - 4P_c \end{bmatrix} \succ 0. \tag{3.42}$$

It is a well-known fact that a symmetric matrix is positive definite if and only if all the leading principal minors of the matrix are positive, see [43]. Therefore, we focus on the leading principal block diagonal entry

$$-JP_b - (JP_b)^T.$$

The inequality 3.42 holds true only if

$$JP_b + (JP_b)^T \succ 0, \ \forall \psi \in [-\pi, \pi]. \tag{3.43}$$

In the sequel, we show that the necessary condition (3.43) for (3.42) to hold true, does not hold.

Consider P_b in the following form

$$P_b = \begin{bmatrix} P_{b_{11}} & * \\ * & * \end{bmatrix},$$

where $P_{b_{11}}$ is a 2×2 block entry while the entries of P_b which are not relevant for the analysis are marked by asterisks. Since (3.43) must be true for all $\psi \in [-\pi, \pi]$, we take the following two cases:

Case 1. $\psi = 0$,

$$JP_b + (JP_b)^T = \begin{bmatrix} P_{b_{11}} + P_{b_{11}}^T & * \\ * & * \end{bmatrix}.$$

Case 2. $\psi = \pi$,

$$JP_b + (JP_b)^T = \begin{bmatrix} -P_{b_{11}} - P_{b_{11}}^T & * \\ * & * \end{bmatrix}.$$

Now the inequality (3.43) holds only if the following holds

$$P_{b_{11}} + P_{b_{11}}^T \succ 0 \quad \text{and} \quad -P_{b_{11}} - P_{b_{11}}^T \succ 0.$$

This is an improbable scenario. Therefore, about the LMI feasibility problem of Example 3.6.2, we conclude the following

"$\nexists \quad P = P^T > 0 \quad s.t. \quad A_c^T(\psi)P + PA_c(\psi) < 0$, holds true for all $\psi \in [-\pi, \pi]$."

In the foregoing discussion, we have proved analytically that the LMI problem corresponding to the system (3.36) has no solution. In the following, we continue with global stability analysis of the system (3.36) by using Lyapunov stability theory and LaSalle's invariance theorem.

3.6.2 Further Analysis for Global Asymptotic Stability

Before proceeding further, we recall an important result from stability theory which was first formulated by J. P. LaSalle, see Appendix B for more details. It is stated as follows [43, Chapter 4, page:128]:

Theorem 3.6.4. The LaSalle's Invariance Theorem (Principle). *Let $\Omega_0 \subset \Omega$ be a compact set that is positively invariant with respect to a nonlinear system: $\dot{\boldsymbol{x}} = \boldsymbol{f}(\boldsymbol{x})$, $\boldsymbol{x}_0 = \boldsymbol{x}(t_0)$. Let $V : \Omega \longrightarrow \mathbb{R}$ be a continuously differentiable function such that $\dot{V}(\boldsymbol{x}) \leq 0$ in Ω_0. Let E be the set of all points in Ω_0 where $\dot{V}(\boldsymbol{x}) = 0$. Let M be the largest invariant set in E. Then every solution starting in Ω_0 approaches M as $t \to \infty$.*

An invariant set is defined as:

Definition 3.6.1. (Invariant Set) *A set M is an invariant set for a dynamic system if every system trajectory which starts from a point in M remains in M for all future time.*

The system matrix (3.38) has a special structure with a skew symmetric part. We try to use this structure to analyze global asymptotic stability of the system. Let us consider a Lyapunov function of the form

$$V(\boldsymbol{x}) = \boldsymbol{x}^T \boldsymbol{x}. \tag{3.44}$$

Differentiating the Lyapunov function, we get

$$\begin{aligned} & \dot{V}(\boldsymbol{x}) = \boldsymbol{x}^T \begin{bmatrix} O_3 & J(\psi) \\ -J^T(\psi) & -2I_3 \end{bmatrix} \boldsymbol{x}, \\ \Rightarrow \quad & \dot{V}(\boldsymbol{x}) = -4\boldsymbol{\nu}^T \boldsymbol{\nu}, \\ \Rightarrow \quad & \dot{V}(\boldsymbol{x}) \leq 0, \ \forall\, \boldsymbol{x} \neq 0. \end{aligned}$$

Now,

$$\dot{V}(\boldsymbol{x}) = 0, \qquad \Rightarrow \qquad \boldsymbol{\nu} = 0, \ \text{and } \boldsymbol{\eta} \text{ is arbitrary.}$$

Therefore,

$$\begin{aligned} E_l &= \{\boldsymbol{x} : \dot{V}(\boldsymbol{x}) = 0\} \\ &= \{\boldsymbol{\nu} = 0, \ \boldsymbol{\eta} \text{ is free}\}. \end{aligned}$$

The next step is to find the largest invariant subset of E_l. Suppose $\boldsymbol{\eta}(t)$ and $\boldsymbol{\nu}(t)$ is a solution pair of closed loop system (3.36) and (3.37) that belongs identically to E_l. Then

$$\begin{aligned} \boldsymbol{\nu}(t) \equiv 0, \;\; &\Rightarrow \;\; \dot{\boldsymbol{\nu}}(t) \equiv 0, \\ &\Rightarrow \;\; -J^T(\psi)\boldsymbol{\eta}(t) \equiv 0, \\ &\Rightarrow \;\; \boldsymbol{\eta}(t) \equiv 0. \end{aligned} \tag{3.45}$$

Therefore, from (3.45), we conclude that the only solution of the closed loop system (3.36) and (3.37) which stays identically in E_l, is the trivial solution. Hence $(\boldsymbol{\eta}, \boldsymbol{\nu}) = (0, 0)$ is a globally asymptotically stable equilibrium point of the the closed loop system (3.36) and (3.37) .

3.7 Summary and Conclusions

This chapter focuses on the stability analysis of a special type of nonlinear systems. They can be transformed to pseudo-linear form by using the SDC framework. The system matrix in the new representation depends on a single state variable. Local asymptotic stability is easy to analyze but the major topic of interest in this chapter is global asymptotic stability analysis. We start with a brief review of the past results on this topic. The main contributions are two counterexamples. Example 3.4.1 shows that the exponential boundedness of the system matrix together with the continuity and Hurwitzness conditions does not imply global asymptotic stability of the nonlinear dynamical system (3.2). Example 3.5.1 shows that, in addition, even if the periodicity of the system matrix is assumed, it does not ensure global asymptotic stability of (3.2).

However, as a consequence of the periodicity of the system matrix, we introduce another method to prove the global asymptotic stability of the pseudo-linear system (3.2). This method combines the concepts of the Lyapunov stability theory and the LMIs. This approach is motivated from the idea of LPV approach introduced in [71] to the pseudo-linear systems of the form (3.2). We use the periodicity of the system matrix together with the Lyapunov stability theory and the LMIs to formulate an LMI feasibility problem. This LMI feasibility problem is solved by using the YALMIP interface under MATLAB. YALMIP uses SeDuMi (an LMI solver) which transforms the LMI feasibility problem into a convex optimization problem. The positive (semi-)definite solution of the LMI feasibility problem is then used to get a quadratic Lyapunov function. Global asymptotic stability is then followed by Lyapunov stability theory.

We first explained this method by using an academic example of a fourth order pseudo-linear system. Afterwards, we proceed to prove global asymptotic stability of the nominal vessel model (3.36) subject to a naive state feedback controller (3.37). It turns out that the LMI feasibility problem associated with the closed loop system matrix (3.38) does not have a feasible solution. This outcome is then proved analytically. More investigation to this bottleneck revealed that a small modification in the LMI feasibility problem, see (3.39), resolves this problem. The consequence of this modification is that the derivative of the Lyapunov function will be positive semidefinite in this situation. In this case, the LaSalle's invariance principal is used to establish global asymptotic stability of the pseudo-linear system.

Chapter 4

State Dependent Riccati Equation Based Control Design[1]

The use of DP systems for the positioning control of ships started in the early sixties. The first DP control system used the conventional PID type control law together with a notch filter, to control each of the *surge*, *sway*, and *yaw* motions. The purpose of the notch filter was to filter out the effects of the WF motions from the feedback loop. There were two main disadvantages of this approach: the integral action of the PID controller is very low due to the coupling between the *surge*, *sway*, and *yaw* motions and there is a phase lag in the control loop due to the notch filter.

The disadvantages of the PID control law motivated a Norwegian company, Kongsberg, to initiate efforts to invent new DP control systems using the concepts of optimal control theory and Kalman filtering from the modern control theory. These efforts made way for the modern concepts for wave filtering like state estimators or observers. Observers are more useful than the classical filtering techniques because they also give estimates of the unknown states of the system.

Observer based wave filtering techniques have been reported by many researchers, for instance see [1], [29], and [51]. One such approach is reported in [74] and it is based on the state dependent algebraic Riccati equation, also known as SDARE. An SDARE observer is proposed to estimate the states of a DP vessel model. This observer was then separately used in combination with a backstepping controller [74] and a PID controller [75].

In this chapter, we extend the ideas of LQR theory to address the nonlinear control design and estimation problems for the DP vessel. The nonlinear model of the vessel motion described in Chapter 2 can be assumed as a pseudo-linear system by considering the SDC parametrization which is discussed in Chapter 3. Our aim is to study the SDARE controller and observer design techniques in connection with the control design problem of a DP vessel. The state dependent algebraic Riccati equation plays

[1] Part of this work has been published in the proceedings of the UKACC International Conference on Control (CONTROL 2010), see [57].

a fundamental role in this theory. We will see that the SDARE controller is a state feedback or an output feedback controller.

4.1 Optimal Control Problem and the SDARE

We mimick the LQR problem for the linear systems to address the control design problem of the pseudo-linear vessel system. Let us start by defining the optimal control (OC) or linear quadratic regulation (LQR) problem for the pseudo-linear system describing the sea vessel motion. We adapt the definition of the LQR problem from [15] to customize it according to the pseudo-linear model under consideration.

Definition 4.1.1. (LQR/OC problem for pseudo-linear system of vessel model) *Given matrices Q and R, find a control signal $\boldsymbol{u}(t)$ such that the quadratic cost function*

$$J(\boldsymbol{x}_0, \boldsymbol{u}(t)) = \frac{1}{2}\int_{t_0}^{\infty} \left(\boldsymbol{x}^T(t)Q\boldsymbol{x}(t) + \boldsymbol{u}^T(t)R\boldsymbol{u}(t)\right) dt, \tag{4.1}$$

is minimized, subject to

$$\dot{\boldsymbol{x}} = A(\psi)\boldsymbol{x}(t) + B\boldsymbol{u}(t),\ \ \boldsymbol{x}(t_0) = \boldsymbol{x}_0. \tag{4.2}$$

In (4.1) and (4.2), the n-dimensional vector $\boldsymbol{x} \in \mathbb{R}^n$ describes the state of the system, $Q = H^T H \in \mathbb{R}^{n\times n}$ ($H^T \in \mathbb{R}^{n\times p}$) is a symmetric positive semidefinite (SPSD) matrix, $\boldsymbol{u} \in \mathbb{R}^m$ is the control input vector, $R \in \mathbb{R}^{m\times m}$ is an SPD matrix, $A(\psi) \in \mathbb{R}^{n\times n}$ is the system matrix, and the matrix $B \in \mathbb{R}^{n\times m}$ describes the controller configuration.

The matrices Q and R in (4.1) are called weighting or penalty matrices. These are also called the tuning parameters of the SDARE controller as the performance of the SDARE controller can be manipulated by playing around with these matrices. Although we assume Q and R to be constant matrices, they can be state dependent as well. Physically, the expression $\boldsymbol{x}^T(t)Q\boldsymbol{x}(t)$ describes the deviation of the state vector from the origin (equilibrium state) and the expression $\boldsymbol{u}^T(t)R\boldsymbol{u}(t)$ describes the control cost.

In [7], it has been proved that the problem defined in Definition 4.1.1 has a suboptimal solution. The following theorem states this result.

Theorem 4.1.1. (The SDARE controller) *Consider a nonlinear system in the SDC form*

$$\dot{\boldsymbol{x}} = A(\boldsymbol{x})\boldsymbol{x} + B(\boldsymbol{x})\boldsymbol{u}. \tag{4.3}$$

The SDC form implies that the matrices $A(\boldsymbol{x})$ and $B(\boldsymbol{x})$ are continuous in $\boldsymbol{x}$ for all $\|\boldsymbol{x}\| \leq \hat{r},\ \hat{r} > 0$, see Section 3.1. Assume further that the matrices $A(\boldsymbol{x})$, $B(\boldsymbol{x})$, and Q are such that the pair $(H, A(\boldsymbol{x}))$ is detectable and the pair $(A(\boldsymbol{x}), B(\boldsymbol{x}))$ is stabilizable for all $\boldsymbol{x} \in \Omega \subseteq \mathcal{B}_{\hat{r}}(0)$[2], where Ω is a nonempty neighborhood of the origin.

Then the system (4.3) with control

$$\boldsymbol{u}(\boldsymbol{x}) = -K_c(\boldsymbol{x})\boldsymbol{x}, \tag{4.4}$$

[2] $\mathcal{B}_{\hat{r}}(0) = \{\boldsymbol{x} \in \mathbb{R}^n : \|\boldsymbol{x}\| < \hat{r}\}$

where the controller gain is

$$K_c(\boldsymbol{x}) = R^{-1}B^T(\boldsymbol{x})\Pi_c(\boldsymbol{x}), \tag{4.5}$$

is locally asymptotically stable. In (4.5), $\Pi_c(\boldsymbol{x})$ *is the solution of the SDARE associated with (4.1) and (4.3), which is given by*

$$\Pi_c(\boldsymbol{x})A(\boldsymbol{x}) + A^T(\boldsymbol{x})\Pi_c(\boldsymbol{x}) + Q - \Pi_c(\boldsymbol{x})B(\boldsymbol{x})R^{-1}B^T(\boldsymbol{x})\Pi_c(\boldsymbol{x}) = 0. \tag{4.6}$$

Proof. See [7]. □

4.2 Control System Design for the DP Vessel

In this section, we illustrate the SDARE-based controller and observer design technique for the control system design of the DP vessel. A DP vessel model is given in Chapter 2. The SDARE (4.6) in context of the vessel model becomes

$$\Pi_c(\psi)A(\psi) + A^T(\psi)\Pi_c(\psi) + Q - \Pi_c(\psi)BR^{-1}B^T\Pi_c(\psi) = 0. \tag{4.7}$$

This is a special SDARE in the sense that only the system matrix depends on state and this state dependence too is only on a single state component in a periodic way. Many solutions of (4.7) could be possible, but the one which is positive (semi-)definite is desired for most of the applications. The sufficient conditions for the pointwise existence of the solution of the SDARE (4.7) as given in [54], are: the pairs $(A(\psi), B)$ and $(H, A(\psi))$ are, respectively, pointwise stabilizable and detectable for all $\psi \in \mathbb{R}$.

We divide our study into two steps. First, we assume that there is no WF motion in the measured output and only the LF motion is to be regulated. Later on, we assume that the WF motion component is also present in the measured output.

4.2.1 Nonlinear Regulation Problem for the LF Model

The LF motion as described in Chapter 2 is given by

$$\dot{\boldsymbol{\eta}} = J(\psi)\boldsymbol{\eta}, \tag{4.8}$$

$$\dot{\boldsymbol{\nu}} = -M^{-1}D\boldsymbol{\nu} + M^{-1}J^T(\psi)\boldsymbol{b} + M^{-1}\boldsymbol{\tau}, \tag{4.9}$$

$$\dot{\boldsymbol{b}} = -T^{-1}\boldsymbol{b} + \Psi\boldsymbol{w}_b, \tag{4.10}$$

$$\boldsymbol{y}_b = C_b\boldsymbol{\eta} + \boldsymbol{\upsilon}, \tag{4.11}$$

where $\boldsymbol{\eta} = [x, y, \psi]^T$ is position coordinate vector, $\boldsymbol{\nu} = [u, v, r]^T$ is velocity coordinate vector, $\boldsymbol{b} \in \mathbb{R}^3$ describes the environmental disturbances, and $\boldsymbol{\tau}$ represents the control forces and torque. The vectors $\boldsymbol{w}_b$ and $\boldsymbol{\upsilon}$ represent the process and measurement noise, respectively. They are described by the zero-mean Gaussian white noise processes, *i.e.*, $\boldsymbol{w}_b \sim \mathcal{N}(0, Q_{c,b})$ and $\boldsymbol{\upsilon} \sim \mathcal{N}(0, R_c)$. We study the LF motion regulation problem by dividing it in two parts. In the first part, we assume that the bias forces are completely given or their estimate is available. In the second part, we assume that slowly varying bias forces and moments are unknown and hence should be estimated.

I. Disturbance vector $\boldsymbol{b}$ is known

We assume that the disturbance vector $\boldsymbol{b}$ is known or its estimate $\hat{\boldsymbol{b}}$ is available and there is no measurement noise. The LF model in the SDC form may then be written as

$$\begin{bmatrix} \dot{\boldsymbol{\eta}} \\ \dot{\boldsymbol{\nu}} \end{bmatrix} = \begin{bmatrix} O_3 & J(\psi) \\ O_3 & -M^{-1}D \end{bmatrix} \begin{bmatrix} \boldsymbol{\eta} \\ \boldsymbol{\nu} \end{bmatrix} + \begin{bmatrix} O_3 \\ M^{-1} \end{bmatrix} \boldsymbol{u} + \begin{bmatrix} O_3 \\ M^{-1}J^T(\psi) \end{bmatrix} \boldsymbol{b}, \tag{4.12}$$

$$\boldsymbol{y}_b = \begin{bmatrix} I_3 & O_3 \end{bmatrix} \begin{bmatrix} \boldsymbol{\eta} \\ \boldsymbol{\nu} \end{bmatrix}. \tag{4.13}$$

The corresponding controllability and observability matrices are given by

$$\mathbf{C}_b = \begin{bmatrix} O_3 & J(\psi)M^{-1} & \cdots & J(\psi)(-M^{-1}D)^4 M^{-1} \\ M^{-1} & -M^{-1}DM^{-1} & \cdots & (-M^{-1}D)^5 M^{-1} \end{bmatrix}, \tag{4.14}$$

and

$$O_b = \begin{bmatrix} I_3 & O_3 \\ O_3 & J(\psi) \\ \vdots & \vdots \\ O_3 & J(\psi)(-M^{-1}D)^4 \end{bmatrix}. \tag{4.15}$$

The matrices defined in (4.14) and (4.15) have full row and column ranks, respectively. Therefore, the system (4.12) is both pointwise controllable and observable. Therefore, by using Theorem 4.1.1, we define a locally asymptotically stable SDARE controller for (4.12) as follows

$$\boldsymbol{u} = -R^{-1}M^{-1} \begin{bmatrix} \Pi_{21}(\psi) & \Pi_{22}(\psi) \end{bmatrix} \begin{bmatrix} \boldsymbol{\eta} \\ \boldsymbol{\nu} \end{bmatrix} - J^T(\psi)\boldsymbol{b}. \tag{4.16}$$

The control law (4.16) can be described as a state feedback law with a feedforward term '$-J^T(\psi)\boldsymbol{b}$'. Moreover, $\Pi_{21}(\psi)$ and $\Pi_{22}(\psi)$ comes from

$$\Pi_c(\psi) = \begin{bmatrix} \Pi_{11}(\psi) & \Pi_{12}(\psi) \\ \Pi_{21}(\psi) & \Pi_{22}(\psi) \end{bmatrix}. \tag{4.17}$$

which is the symmetric solution of the SDARE associated with (4.1) and (4.12). From (4.13), it is clear that we can only measure the position of the vessel and its velocities are not available for feedback. But we can also write (4.16) as

$$\boldsymbol{u} = -R^{-1}M^{-1} \begin{bmatrix} \Pi_{21}(\psi) & \Pi_{22}(\psi)J^T(\psi) \end{bmatrix} \begin{bmatrix} \boldsymbol{\eta} \\ \dot{\boldsymbol{\eta}} \end{bmatrix} - J^T(\psi)\boldsymbol{b}. \tag{4.18}$$

This control law can be seen as PD-type control law with feedforward term '$-J^T(\psi)\boldsymbol{b}$'.

Stability analysis of the controller (4.16)

The local asymptotic stability of the state feedback SDARE controller follows from Theorem 4.1.1. We prove by using the LMI based technique discussed in Chapter

3 that the SDARE feedback controller stabilizes the vessel globally asymptotically around the origin. We can write the SDARE state feedback controller, (4.16), as

$$\boldsymbol{u} = -\begin{bmatrix} K_1(\psi) & K_2(\psi) \end{bmatrix} \begin{bmatrix} \boldsymbol{\eta} \\ \boldsymbol{\nu} \end{bmatrix} - J^T(\psi)\boldsymbol{b}. \tag{4.19}$$

The closed loop system (4.12) and (4.19) is given by

$$\begin{bmatrix} \dot{\boldsymbol{\eta}} \\ \dot{\boldsymbol{\nu}} \end{bmatrix} = \underbrace{\begin{bmatrix} O_3 & J(\psi) \\ -M^{-1}K_1(\psi) & * \end{bmatrix}}_{A_{cl}(\psi)} \begin{bmatrix} \boldsymbol{\eta} \\ \boldsymbol{\nu} \end{bmatrix}. \tag{4.20}$$

It is a well-known fact that the SDARE controller results in an asymptotically stable closed loop matrix, see for instance [7]. Therefore, the closed loop system matrix (4.20) is pointwise Hurwitz. Using the LMI approach (see Chapter 3 for more details), it turns out that there exists an SPD matrix P such that

$$A_{cl}^T(\psi)P + PA_{cl}(\psi) + \begin{bmatrix} 0 & 0 \\ 0 & I_3 \end{bmatrix} \leq 0, \ \forall\, \psi \in [0, 2\pi]. \tag{4.21}$$

Now we consider the quadratic Lyapunov function: $V(\boldsymbol{x}) = \boldsymbol{x}^T P \boldsymbol{x}$. Differentiating w.r.t. ‘t’, we get

$$\begin{aligned} \dot{V}(\boldsymbol{x}) &= \boldsymbol{x}^T(A_{cl}^T(\psi)P + PA_{cl}(\psi))\boldsymbol{x}, \\ &\leq \boldsymbol{x}^T \begin{bmatrix} 0 & 0 \\ 0 & -I_3 \end{bmatrix} \boldsymbol{x}, \text{ using (4.21)}, \\ &\leq -\boldsymbol{\nu}^T\boldsymbol{\nu}, \\ &\leq 0. \end{aligned}$$

Since $\dot{V}(\boldsymbol{x}) \leq 0$, therefore, we use LaSalle’s invariance principle to further analyze the stability of the closed loop system. For this we first find the set of points where $\dot{V}(\boldsymbol{x}) = 0$.

$$\begin{aligned} E_l &= \{\boldsymbol{x} : \dot{V}(\boldsymbol{x}) = 0\}, \\ &= \{\boldsymbol{\nu} = 0, \ \boldsymbol{\eta} \text{ is free}\}. \end{aligned}$$

Now we need the invariant sets of the closed loop system. To show that the origin is the only equilibrium point of the closed loop system, we need to show that no solution other than the trivial solution stays identically in E_l, *i.e.*, $\boldsymbol{\eta}(t) \equiv 0$ and $\boldsymbol{\nu}(t) \equiv 0$ for all ‘t’.

Let $\boldsymbol{\eta}(t)$ and $\boldsymbol{\nu}(t)$ be a solution pair of the closed loop system (4.20) that belongs identically to E_l. Then

$$\begin{aligned} \boldsymbol{\nu}(t) \equiv 0, \ &\Rightarrow \ \dot{\boldsymbol{\nu}}(t) \equiv 0, \\ &\Rightarrow \ -M^{-1}K_1(\psi)\boldsymbol{\eta}(t) \equiv 0. \end{aligned} \tag{4.22}$$

To show that $\boldsymbol{\eta}(t) \equiv 0$, we need to prove that $K_1(\psi)$ is a non-singular matrix. We prove this by contradiction. Suppose that it is singular then $\exists\ \boldsymbol{\nu} \neq 0$ such that

$$M^{-1}K_1(\psi)\boldsymbol{\nu} = 0,$$
$$\Rightarrow \begin{bmatrix} O_3 & J(\psi) \\ -M^{-1}K_1(\psi) & * \end{bmatrix}\begin{bmatrix} \boldsymbol{\nu} \\ 0 \end{bmatrix} = 0 \begin{bmatrix} \boldsymbol{\nu} \\ 0 \end{bmatrix}.$$

This implies that $\lambda = 0$ is an eigenvalue of the closed loop system matrix in (4.20). But it is a well-known fact that the closed system (4.20) is pointwise asymptotically stable (all eigenvalues lie in the left half plane). Therefore, it is a contradiction. Hence, $K_1(\psi)$ is nonsingular.

Therefore, from (4.22), we conclude that the only solution of the closed loop system which stays identically in E_l is the trivial solution. Hence $(\boldsymbol{\eta}^*, \boldsymbol{\nu}^*) = (0, 0)$ is a globally asymptotically stable equilibrium point of the the closed loop system (4.20) which means that the SDARE controller (4.19) globally asymptotically stabilizes the vessel.

II. Disturbance vector $\boldsymbol{b}$ is unknown

We now assume that the LF disturbances are slowly varying (as described by the first order Markov process $\dot{\boldsymbol{b}} = -T^{-1}\boldsymbol{b} + \Psi \boldsymbol{w}_b$) but unknown and should be estimated. The LF motion in this case, in the SDC form, is described as

$$\begin{bmatrix} \dot{\boldsymbol{\eta}} \\ \dot{\boldsymbol{\nu}} \\ \dot{\boldsymbol{b}} \end{bmatrix} = \begin{bmatrix} O_3 & J(\psi) & O_3 \\ O_3 & -M^{-1}D & M^{-1}J^T(\psi) \\ O_3 & O_3 & -T^{-1} \end{bmatrix}\begin{bmatrix} \boldsymbol{\eta} \\ \boldsymbol{\nu} \\ \boldsymbol{b} \end{bmatrix} + \begin{bmatrix} O_3 \\ M^{-1} \\ O_3 \end{bmatrix}\boldsymbol{u} + \begin{bmatrix} O_3 \\ O_3 \\ \Psi \end{bmatrix}\boldsymbol{w}_b, \tag{4.23}$$

$$\boldsymbol{y}_b = \begin{bmatrix} I_3 & O_3 & O_3 \end{bmatrix}\begin{bmatrix} \boldsymbol{\eta} \\ \boldsymbol{\nu} \\ \boldsymbol{b} \end{bmatrix} + \boldsymbol{v}. \tag{4.24}$$

The controllability and observability matrices for (4.23)-(4.24) are given by

$$\mathbf{C}_b = \begin{bmatrix} O_3 & J(\psi)M^{-1} & \cdots & J(\psi)(-M^{-1}D)^7M^{-1} \\ M^{-1} & -M^{-1}DM^{-1} & \cdots & (-M^{-1}D)^8M^{-1} \\ O_3 & O_3 & \cdots & O_3 \end{bmatrix}, \tag{4.25}$$

and

$$\mathcal{O}_b = \begin{bmatrix} I_3 & O_3 & O_3 \\ O_3 & J(\psi) & O_3 \\ O_3 & -J(\psi)M^{-1}D & J(\psi)M^{-1}J^T(\psi) \\ \vdots & \vdots & \vdots \end{bmatrix}. \tag{4.26}$$

Since the matrices M, D, and $J^T(\psi)$ are non-singular, the controllability matrix (4.25) has rank 6. This means that only the states $\boldsymbol{\eta}$ and $\boldsymbol{\nu}$ are controllable. This is not restrictive as the bias forces are always uncontrollable. The observability matrix (4.26) has full rank for all $\psi \in \mathbb{R}$. An SDARE associated with (4.23) is given by

$$\Pi_c(\psi)A_b(\psi) + A_b^T(\psi)\Pi_c(\psi) + Q - \Pi_c(\psi)B_bR^{-1}B_b^T\Pi_c(\psi) = 0. \tag{4.27}$$

Using Theorem 4.1.1, a locally asymptotically stable SDARE-based suboptimal control law is given by

$$\boldsymbol{u} = -R^{-1}M^{-1}\begin{bmatrix} \Pi_{21}(\psi) & \Pi_{22}(\psi) & \Pi_{23}(\psi) \end{bmatrix}\begin{bmatrix} \boldsymbol{\eta} \\ \boldsymbol{\nu} \\ \boldsymbol{b} \end{bmatrix}. \tag{4.28}$$

The gain of the SDARE controller is defined by

$$K_c(\psi) = R^{-1}M^{-1}\begin{bmatrix} \Pi_{21}(\psi) & \Pi_{22}(\psi) & \Pi_{23}(\psi) \end{bmatrix}, \tag{4.29}$$

where $\Pi_{21}(\psi)$, $\Pi_{22}(\psi)$, and $\Pi_{23}(\psi)$ are obtained from the solution of the SDARE (4.27). The control law (4.28) can be described as a state feedback controller. From (4.24), we notice that only the LF position and heading can be measured by the sensors. Therefore, a state estimator is required to estimate the complete state. A suboptimal locally asymptotically stable SDARE controller for the system (4.23)-(4.24) will be

$$\boldsymbol{u} = -R^{-1}M^{-1}\begin{bmatrix} \Pi_{21}(\hat{\psi}) & \Pi_{22}(\hat{\psi}) & \Pi_{23}(\hat{\psi}) \end{bmatrix}\begin{bmatrix} \hat{\boldsymbol{\eta}} \\ \hat{\boldsymbol{\nu}} \\ \hat{\boldsymbol{b}} \end{bmatrix}. \tag{4.30}$$

Since the system (4.23)-(4.24) is pointwise observable, the corresponding dual system will be pointwise controllable. Therefore, we can design a suboptimal locally asymptotically stable SDARE observer, see [7]. The following theorem states this result.

Theorem 4.2.1. (The SDARE state estimator) *Assume that a system in SDC form*

$$\dot{\boldsymbol{x}} = A(\boldsymbol{x})\boldsymbol{x} + B(\boldsymbol{x})\boldsymbol{u}, \tag{4.31}$$

$$\boldsymbol{y} = C(\boldsymbol{x})\boldsymbol{x}, \tag{4.32}$$

is such that $\boldsymbol{f}(\boldsymbol{x}) = A(\boldsymbol{x})\boldsymbol{x}$ *and* $\frac{\partial f(x)}{\partial x_j},\ j = 1, 2, ..., n$ *are continuous in* $\boldsymbol{x}$ *for all* $\|\boldsymbol{x}\| \leq \hat{r},\ \hat{r} > 0$ *and* $\boldsymbol{x} = 0$ *is a stable equilibrium point of (4.31). Assume further that the pair* $(A(\boldsymbol{x}), C(\boldsymbol{x}))$ *is pointwise detectable and the matrices* $A(\boldsymbol{x})$ *and* $C(\boldsymbol{x})$ *are locally Lipschitz for all* $\boldsymbol{x} \in \Omega \subseteq \mathcal{B}_{\hat{r}}(0)$, *where* Ω *is a nonempty neighborhood of the origin. Then the estimated state given by*

$$\dot{\hat{\boldsymbol{x}}} = A(\hat{\boldsymbol{x}})\hat{\boldsymbol{x}} + B(\hat{\boldsymbol{x}})\boldsymbol{u} + K_o(\hat{\boldsymbol{x}})(\boldsymbol{y} - \hat{\boldsymbol{y}}), \tag{4.33}$$

will converge locally asymptotically to the state. In (4.33), $K_o(\hat{\boldsymbol{x}})$ *is the observer gain and is given by*

$$K_o(\hat{\boldsymbol{x}}) = \Pi_o(\hat{\boldsymbol{x}})C^T V^{-1}. \tag{4.34}$$

In (4.34), $\Pi_o(\hat{\boldsymbol{x}})$ *is the solution of the dual SDARE*

$$\Pi_o(\hat{\boldsymbol{x}})A^T(\hat{\boldsymbol{x}}) + A(\hat{\boldsymbol{x}})\Pi_o(\hat{\boldsymbol{x}}) + U - \Pi_o(\hat{\boldsymbol{x}})C^T V^{-1} C\Pi_o(\hat{\boldsymbol{x}}) = 0, \tag{4.35}$$

associated with the system (4.31)-(4.32).

Proof. See [7]. □

An SDARE observer for the system (4.23)-(4.24) is given by

$$\begin{bmatrix} \dot{\hat{\boldsymbol{\eta}}} \\ \dot{\hat{\boldsymbol{\nu}}} \\ \dot{\hat{\boldsymbol{b}}} \end{bmatrix} = \begin{bmatrix} O_3 & J(\hat{\psi}) & O_3 \\ O_3 & -M^{-1}D & M^{-1}J^T(\hat{\psi}) \\ O_3 & O_3 & -T^{-1} \end{bmatrix} \begin{bmatrix} \hat{\boldsymbol{\eta}} \\ \hat{\boldsymbol{\nu}} \\ \hat{\boldsymbol{b}} \end{bmatrix} + \begin{bmatrix} O_3 \\ M^{-1} \\ O_3 \end{bmatrix} \boldsymbol{u} + K_o(\hat{\psi})(\boldsymbol{y}_\eta - \hat{\boldsymbol{y}}_\eta), \quad (4.36)$$

$$\hat{\boldsymbol{y}}_\eta = \begin{bmatrix} I_3 & O_3 & O_3 \end{bmatrix} \begin{bmatrix} \hat{\boldsymbol{\eta}} \\ \hat{\boldsymbol{\nu}} \\ \hat{\boldsymbol{b}} \end{bmatrix}. \quad (4.37)$$

The third term in (4.36) corrects the observer model by a nonlinear feedback of the difference between the measured output $\boldsymbol{y}_\eta$ and the estimated output $\hat{\boldsymbol{y}}_\eta$. The observer gain $K_o(\hat{\psi})$ in (4.36) is defined by

$$K_o(\hat{\psi}) = \begin{bmatrix} \Pi_{11}(\hat{\psi}) \\ \Pi_{21}(\hat{\psi}) \\ \Pi_{31}(\hat{\psi}) \end{bmatrix} \cdot V^{-1}, \quad (4.38)$$

where Π_{i1}, $i = 1, 2, 3$ are obtained from the solution of the corresponding dual SDARE of the form (4.35).

So far we have defined a suboptimal locally asymptotically stable nonlinear control law (4.30) and a suboptimal locally asymptotically stable nonlinear observer (4.36). A combination of both is called a nonlinear compensator. The separation properties for combination of linear controllers and observers are well defined, see for instance [60]. The separation principles for the nonlinear compensators are not well established yet. The following theorem from [7] states one particular result about stability of an SDARE compensator.

Theorem 4.2.2. (The SDARE state compensator) *Assume that the system in SDC form (4.31)-(4.32) is such that $\boldsymbol{f}(\boldsymbol{x}) = A(\boldsymbol{x})\boldsymbol{x}$ and $\frac{\partial f(\boldsymbol{x})}{\partial x_j}$, $j = 1, 2, ..., n$ are continuous in $\boldsymbol{x}$ for all $\|\boldsymbol{x}\| \leq \hat{r}$, $\hat{r} > 0$. Assume further that $A(\boldsymbol{x})$ and $B(\boldsymbol{x})$ are continuous. Let the matrices $A(\boldsymbol{x})$, $B(\boldsymbol{x})$, and $C(\boldsymbol{x})$ are chosen such that the pair $(A(\boldsymbol{x}), C(\boldsymbol{x}))$ is detectable and the pair $(A(\boldsymbol{x}), B(\boldsymbol{x}))$ is stabilizable for all $\boldsymbol{x} \in \Omega \subseteq \mathcal{B}_{\hat{r}}(0)$, where Ω is a nonempty neighborhood of the origin.*

Then $(\boldsymbol{x}, \boldsymbol{e}) = (0, 0)$ is a locally asymptotically stable point. Here, $\boldsymbol{e} = \boldsymbol{x} - \hat{\boldsymbol{x}}$ is the error between the state $\boldsymbol{x}$ from (4.31) and the state estimate $\hat{\boldsymbol{x}}$ from (4.33).

Proof. See [7]. □

A combination of the SDARE controller (4.30) and observer (4.36) is an SDARE pseudo-linear compensator illustrated in a block diagram shown in Figure 4.1 and is given by

$$\begin{bmatrix} \dot{\boldsymbol{x}} \\ \dot{\hat{\boldsymbol{x}}} \end{bmatrix} = \begin{bmatrix} A_b(\psi) & -B_bK_c(\hat{\psi}) \\ K_o(\hat{\psi})C_b & A_b(\hat{\psi}) - B_bK_c(\hat{\psi}) - K_o(\hat{\psi})C_b \end{bmatrix} \begin{bmatrix} \boldsymbol{x} \\ \hat{\boldsymbol{x}} \end{bmatrix} + \begin{bmatrix} E_b & O \\ O & K_o(\hat{\psi}) \end{bmatrix} \begin{bmatrix} \boldsymbol{w}_b \\ \boldsymbol{v} \end{bmatrix} \boldsymbol{w}_b. \quad (4.39)$$

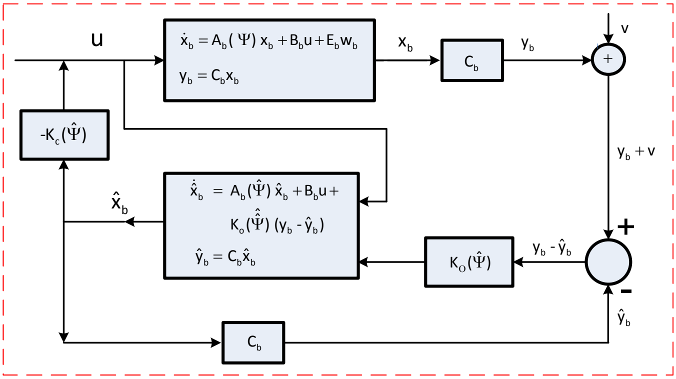

Figure 4.1: A nonlinear compensator for LF model

4.2.2 Nonlinear Regulation Problem for the Complete Model

Now, we take into account the effect of the wave frequency (WF) motion in the measurement. The WF motion in each of the *surge*, *sway*, and *yaw* directions is modeled as a second order harmonic oscillation, see Chapter 2 for more details. The WF motion model is given by

$$\begin{bmatrix} \dot{\xi}_1 \\ \dot{\xi}_2 \end{bmatrix} = \begin{bmatrix} O_3 & I_3 \\ -\Omega^2 & -2Z\Omega \end{bmatrix} \begin{bmatrix} \xi_1 \\ \xi_2 \end{bmatrix} + \begin{bmatrix} O_3 \\ \Sigma \end{bmatrix} \boldsymbol{w}_\xi, \tag{4.40}$$

$$\boldsymbol{y}_\xi = \begin{bmatrix} I_3 & O_3 \end{bmatrix} \begin{bmatrix} \xi_1 \\ \xi_2 \end{bmatrix}, \tag{4.41}$$

where the diagonal matrix $\Omega = \text{diag}\{\omega_{01}, \omega_{02}, \omega_{03}\}$ is such that each of the ω_{0i}'s represents the dominating wave frequency and the diagonal matrix $Z = \text{diag}\{\zeta_1, \zeta_2, \zeta_3\}$ is such that each of the ζ_i's represents the relative damping ratio in *surge*, *sway*, and *yaw* direction,respectively. The diagonal matrix $\Sigma = \text{diag}\{\sigma_1, \sigma_2, \sigma_3\}$ scales the noise vector $\boldsymbol{w}_b$ and its elements represents the wave intensity in each degree of freedom.

The response of the WF disturbances is incorporated in the model by assuming that the total ship motion is the sum of the LF motion and the WF motion components. The precept of the DP problem is to attenuate only the LF motion. Therefore, the WF motion component must be removed from the measured output when designing an output feedback controller. As mentioned earlier, there are various methods for wave filtering. We use the state estimation technique for wave filtering. For this, we augment the LF and WF models and assume that the superposition principle holds true, so that we can add the outputs of both the LF and WF models. The complete (augmented) model can be written as

$$\begin{bmatrix} \dot{\boldsymbol{\eta}} \\ \dot{\boldsymbol{\nu}} \\ \dot{\boldsymbol{b}} \\ \dot{\boldsymbol{\xi}}_1 \\ \dot{\boldsymbol{\xi}}_2 \end{bmatrix} = \begin{bmatrix} O_3 & J(\psi) & O_3 & O_3 & O_3 \\ O_3 & -M^{-1}D & M^{-1}J^T(\psi) & O_3 & O_3 \\ O_3 & O_3 & -T^{-1} & O_3 & O_3 \\ O_3 & O_3 & O_3 & O_3 & I_3 \\ O_3 & O_3 & O_3 & -\Omega^2 & -2Z\Omega \end{bmatrix} \begin{bmatrix} \boldsymbol{\eta} \\ \boldsymbol{\nu} \\ \boldsymbol{b} \\ \boldsymbol{\xi}_1 \\ \boldsymbol{\xi}_2 \end{bmatrix} + \begin{bmatrix} O_3 \\ M^{-1} \\ O_3 \\ O_3 \\ O_3 \end{bmatrix} \boldsymbol{u}$$

$$+ \begin{bmatrix} O_3 & O_3 \\ O_3 & O_3 \\ \Psi & O_3 \\ O_3 & O_3 \\ O_3 & \Sigma \end{bmatrix} \begin{bmatrix} \boldsymbol{w}_b \\ \boldsymbol{w}_\xi \end{bmatrix}, \quad (4.42)$$

$$\begin{aligned} \boldsymbol{y} &= \boldsymbol{y}_b + \boldsymbol{y}_\xi + \boldsymbol{v} \\ &= \begin{bmatrix} I_3 & O_3 & O_3 & I_3 & O_3 \end{bmatrix} \begin{bmatrix} \boldsymbol{\eta} \\ \boldsymbol{\nu} \\ \boldsymbol{b} \\ \boldsymbol{\xi}_1 \\ \boldsymbol{\xi}_2 \end{bmatrix} + \boldsymbol{v}. \end{aligned} \quad (4.43)$$

The controllability matrix of (4.42) is given by

$$\mathbf{C} = \begin{bmatrix} O_3 & J(\psi)M^{-1} & -J(\psi)M^{-1}DM^{-1} & \cdots & -J(\psi)(M^{-1}D)^{13}M^{-1} \\ M^{-1} & -M^{-1}DM^{-1} & (M^{-1}D)^2M^{-1} & \cdots & (M^{-1}D)^{14}M^{-1} \\ O_3 & O_3 & O_3 & \cdots & O_3 \\ O_3 & O_3 & O_3 & \cdots & O_3 \\ O_3 & O_3 & O_3 & \cdots & O_3 \end{bmatrix}, \quad (4.44)$$

Since the matrices $J(\psi)$, M, and D have full row rank for all $\psi \in \mathbb{R}$, the controllability matrix has rank 6. This means that only $\boldsymbol{\eta}$ and $\boldsymbol{\nu}$ are controllable states while the slowly varying disturbances and wave frequency motion are not controllable. This is not restrictive as the objective is to control only the low frequency motion. Using Theorem 4.1.1, a locally asymptotically stable SDARE controller for (4.42) is defined by

$$\begin{aligned} \boldsymbol{u} &= -R^{-1}B^T\Pi_c(\psi)\boldsymbol{x} \\ &= -R^{-1}M^{-1} \begin{bmatrix} \Pi_{21}(\psi) & \Pi_{22}(\psi) & \Pi_{23}(\psi) & \Pi_{24}(\psi) & \Pi_{25}(\psi) \end{bmatrix} \begin{bmatrix} \boldsymbol{\eta} \\ \boldsymbol{\nu} \\ \boldsymbol{b} \\ \boldsymbol{\xi}_1 \\ \boldsymbol{\xi}_2 \end{bmatrix}, \end{aligned} \quad (4.45)$$

where $\Pi_{2i}(\psi),\ i = 1,2,3,4,5$ are obtained from the SDARE associated with (4.1) and (4.42). Again as we know that only the position measurement is available. Therefore, to realize the controller (4.45), we need estimates of the states. Then this control law will be

$$\boldsymbol{u} = -R^{-1}M^{-1}\begin{bmatrix} \Pi_{21}(\hat{\psi}) & \Pi_{22}(\hat{\psi}) & \Pi_{23}(\hat{\psi}) & \Pi_{24}(\hat{\psi}) & \Pi_{25}(\hat{\psi}) \end{bmatrix}\begin{bmatrix} \hat{\boldsymbol{\eta}} \\ \hat{\boldsymbol{\nu}} \\ \hat{\boldsymbol{b}} \\ \hat{\boldsymbol{\xi}}_1 \\ \hat{\boldsymbol{\xi}}_2 \end{bmatrix}. \quad (4.46)$$

Before addressing the observability of (4.42), we recall the following result from [74].

Theorem 4.2.3. *Consider the system*

$$\dot{\boldsymbol{x}}_1 = A_1\boldsymbol{x}_1, \quad (4.47)$$

$$\dot{\boldsymbol{x}}_2 = A_1\boldsymbol{x}_2, \quad (4.48)$$

$$\boldsymbol{y} = C_1\boldsymbol{x}_1 + C_2\boldsymbol{x}_2, \quad (4.49)$$

where $x_1 \in \mathbb{R}^{n_1}$ and $x_2 \in \mathbb{R}^{n_2}$ are states and $\boldsymbol{y} \in \mathbb{R}^p$ is the output of the system. If A_1 and A_2 have no common eigenvalues, i.e.*,*

$$\sigma(A_1) \cap \sigma(A_2) = \phi, \quad (4.50)$$

then the system (4.47)-(4.49) is observable iff (C_1, A_1) *and* (C_2, A_2) *are both observable.*

Proof. See [74]. □

The systems (4.23) and (4.40), respectively, describe the slowly varying low frequency and wave frequency motions with different eigenfrequencies. Therefore, the system matrices $A_b(\psi)$ and A_ξ in (4.23) and (4.40) do not have any common eigenvalues. Moreover, the observability matrices (4.26) and

$$O_\xi = \begin{bmatrix} I_3 & O_3 \\ O_3 & I_3 \\ \vdots & \vdots \end{bmatrix} \quad (4.51)$$

have full row ranks. Therefore, the subsystems $(A_b(\psi), C_b)$ and (A_ξ, C_ξ) of the system (4.42) are observable. This means that by Theorem 4.2.3, we can conclude that the system (4.42)-(4.43) is pointwise observable for all $\psi \in \mathbb{R}$.

An SDARE observer for the system (4.42)-(4.43) is defined by

$$\begin{bmatrix} \dot{\hat{\boldsymbol{\eta}}} \\ \dot{\hat{\boldsymbol{\nu}}} \\ \dot{\hat{\boldsymbol{b}}} \\ \dot{\hat{\boldsymbol{\xi}}}_1 \\ \dot{\hat{\boldsymbol{\xi}}}_2 \end{bmatrix} = \begin{bmatrix} O_3 & J(\hat{\psi}) & O_3 & O_3 & O_3 \\ O_3 & -M^{-1}D & M^{-1}J^T(\hat{\psi}) & O_3 & O_3 \\ O_3 & O_3 & -T^{-1} & O_3 & O_3 \\ O_3 & O_3 & O_3 & O_3 & I_3 \\ O_3 & O_3 & O_3 & -\Omega^2 & -2Z\Omega \end{bmatrix} \begin{bmatrix} \hat{\boldsymbol{\eta}} \\ \hat{\boldsymbol{\nu}} \\ \hat{\boldsymbol{b}} \\ \hat{\boldsymbol{\xi}}_1 \\ \hat{\boldsymbol{\xi}}_2 \end{bmatrix} + \begin{bmatrix} O_3 \\ M^{-1} \\ O_3 \\ O_3 \\ O_3 \end{bmatrix} \boldsymbol{u}$$

$$+ K_o(\hat{\psi})(\boldsymbol{y} - \hat{\boldsymbol{y}}), \tag{4.52}$$

$$\hat{\boldsymbol{y}} = \begin{bmatrix} I_3 & O_3 & O_3 & I_3 & O_3 \end{bmatrix} \begin{bmatrix} \hat{\boldsymbol{\eta}} \\ \hat{\boldsymbol{\nu}} \\ \hat{\boldsymbol{b}} \\ \hat{\boldsymbol{\xi}}_1 \\ \hat{\boldsymbol{\xi}}_2 \end{bmatrix}. \tag{4.53}$$

The observer gain $K_o(\hat{\psi})$ in (4.52) is given by

$$\begin{aligned} K_o(\hat{\psi}) &= \Pi_o(\hat{\psi})C^T V^{-1} \\ &= \begin{bmatrix} \Pi_{11}(\hat{\psi}) + \Pi_{14}(\hat{\psi}) \\ \Pi_{21}(\hat{\psi}) + \Pi_{24}(\hat{\psi}) \\ \Pi_{31}(\hat{\psi}) + \Pi_{34}(\hat{\psi}) \\ \Pi_{41}(\hat{\psi}) + \Pi_{44}(\hat{\psi}) \\ \Pi_{51}(\hat{\psi}) + \Pi_{54}(\hat{\psi}) \end{bmatrix} \cdot V^{-1} \end{aligned} \tag{4.54}$$

where $\Pi_{i1}(\hat{\psi})$ and $\Pi_{i4}(\hat{\psi})$, $i = 1, 2, 3, 4, 5$ are obtained from the solution of the dual SDARE associated with the (4.42)-(4.43).

A combination of the nonlinear controller (4.46) and the nonlinear observer (4.52) is called a nonlinear compensator and is shown in Figure 4.2. The nonlinear SDARE compensator is given by

$$\begin{bmatrix} \dot{\boldsymbol{x}} \\ \dot{\hat{\boldsymbol{x}}} \end{bmatrix} = \begin{bmatrix} A(\psi) & -BK_c(\hat{\psi}) \\ K_o(\hat{\psi})C & A(\hat{\psi}) - BK_c(\hat{\psi}) - K_o(\hat{\psi})C \end{bmatrix} \begin{bmatrix} \boldsymbol{x} \\ \hat{\boldsymbol{x}} \end{bmatrix} + \begin{bmatrix} E & O \\ O & K_o(\hat{\psi}) \end{bmatrix} \begin{bmatrix} \boldsymbol{w} \\ \boldsymbol{v} \end{bmatrix}. \tag{4.55}$$

Before concluding this section, it is important to mention that in reality, the WF model is considered as a disturbance to the model. For designing a control law, it is desired that the effects of the WF disturbances do not enter into the feedback loop. In this particular example, it is required that no part of the disturbance vectors $\boldsymbol{\xi}_1$ and $\boldsymbol{\xi}_2$ enters in the control action. Here, the controller gain matrix turns out to have the form, $K_c(\hat{\psi}) = [K_{c1}(\hat{\psi}), K_{c2}(\hat{\psi}), K_{c3}(\hat{\psi}), O_3, O_3]$ which ensures the attenuation of the disturbance; in the feedback the product term, $K_c(\psi)\hat{\boldsymbol{x}}$, eliminates $\hat{\boldsymbol{\xi}}_1$ and $\hat{\boldsymbol{\xi}}_2$ from the feedback loop.

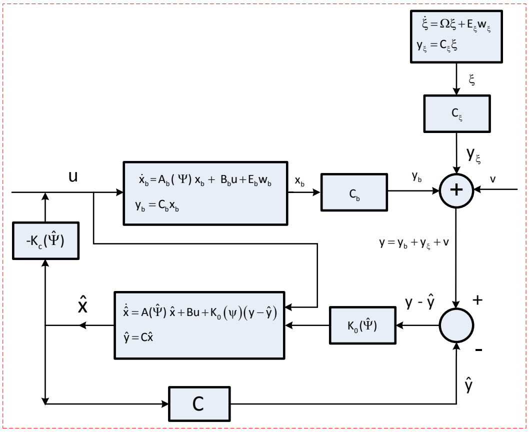

Figure 4.2: Nonlinear compensator

4.3 Simulation Results

Suppose the objective is to design a controller to stabilize the vessel around the origin. By the stabilized mode we mean that the vessel is positioned at rest at $(x, y) = (0, 0)$ and its heading is along the positive $x-$axis.

For numerical simulations to illustrate the effectiveness of the SDARE controllers and observers designed in the previous subsection, we use the data of a supply vessel from [51]. For simplicity of numerics, Bis-scaled [25] normalized parameters of the vessel model are used. The normalized matrices M and D are:

$$M = \begin{bmatrix} 1.1274 & 0 & 0 \\ 0 & 1.8902 & -0.0744 \\ 0 & -0.0744 & 0.1278 \end{bmatrix}, \quad D = \begin{bmatrix} 0.0358 & 0 & 0 \\ 0 & 0.1183 & -0.0124 \\ 0 & -0.0124 & 0.0308 \end{bmatrix}. \tag{4.56}$$

We assume that the ship is at a point $(x, y) = (-10, -10)$ making an angle $\psi(= 4\,\text{rad})$ with the positive x-axis. The control objective is to steer the system to the stable equilibrium position or the desired set-point, $(x, y) = (0, 0)$ and heading along the positive x-axis.

First we consider the nominal case, *i.e.*, when the disturbance vector $\boldsymbol{b}$ is known. Suppose $\boldsymbol{b} = [0.05, 0.05, 0.01]^T$ and we use the control law (4.18) in (4.12). We present the simulation results corresponding to the following weighting matrices.
$Q = 10^3\,\text{diag}\{0.1, 1, 0.1, 0, 0, 0\}$ and $R = 10^2\, I_3$.

Figure 4.3 shows the position and heading profiles as they evolve with time. It is clear that the regulation to the desired point is steady and smooth. Figure 4.4 shows: (a) the trajectory profile of the vessel, (b) the cost functional profile, and (c) the norm of the state vector. Figure 4.5 shows change in the heading of the vessel along the trajectory. Figure 4.6 shows the controller recommended force in each degree of freedom of the vessel. Once more, it is clear that the actuator input to the vessel is steady and smooth with a smooth overshoot.

As we have already mentioned that the weighting matrices can be tuned to improve the performance of the controller. We elaborate this feature in the following. For instance, we penalize the velocities and take $Q = 10^3\,\mathrm{diag}\{0.1, 1, 0.1, 1, 1, 1\}$. Figures 4.7 and 4.8 show the control input signals and the heading orintation of the vessel corresponding to the new weighting matrix Q. It is clear that new profiles for the heading orientation and the control input signal are smoother than the previous profiles. To emphasize more on tuning factor, we include another heading orientation profile corresponding to $R = 10^0\, I_3$, see Figure 4.9.

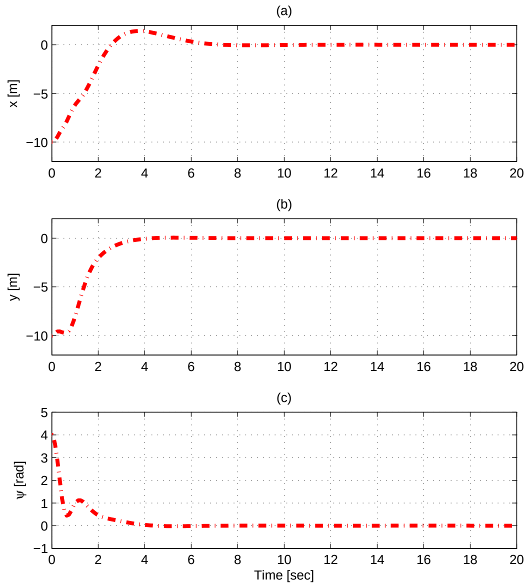

Figure 4.3: The position and heading profiles of the vessel as obtained from the closed loop system (4.12) and (4.18)

.

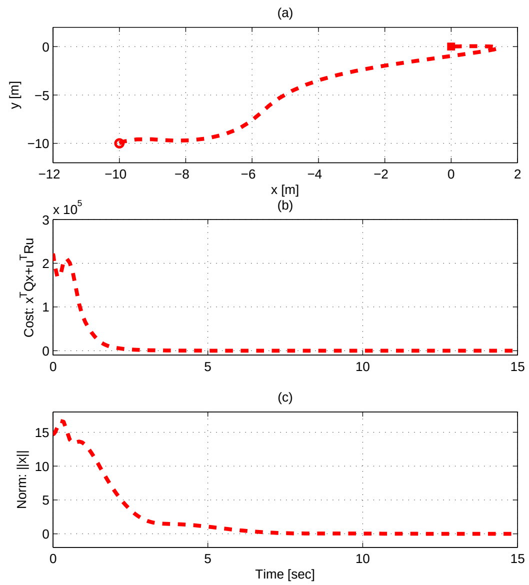

Figure 4.4: The evolution of the trajectory, cost, and the norm (of the state vector) profiles associated with the vessel as obtained from the closed loop system (4.12) and (4.18).

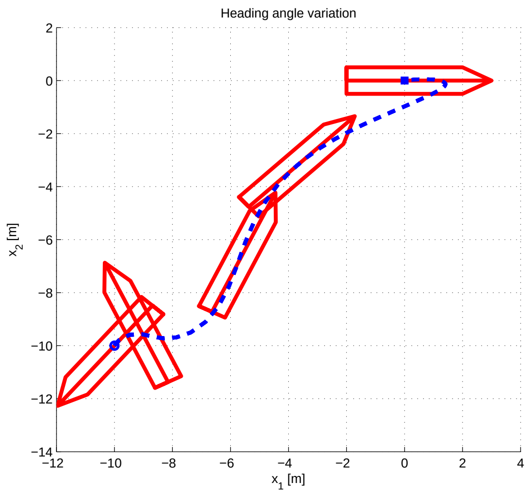

Figure 4.5: The heading orientation over the trajectory of the vessel as obtained from the closed loop system (4.12) and (4.18).

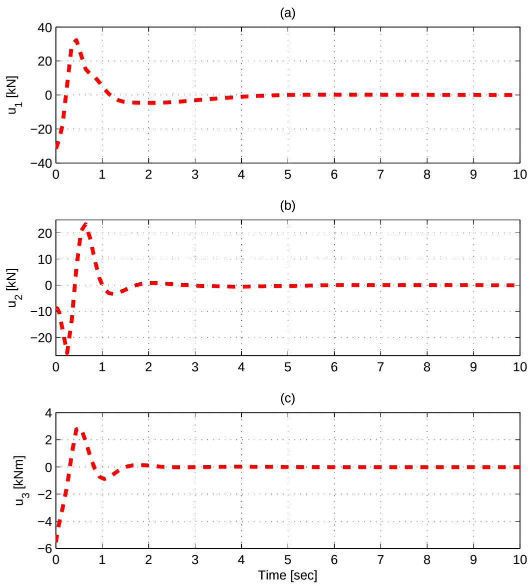

Figure 4.6: The profiles of the individual components of the control input vector as obtained from (4.18).

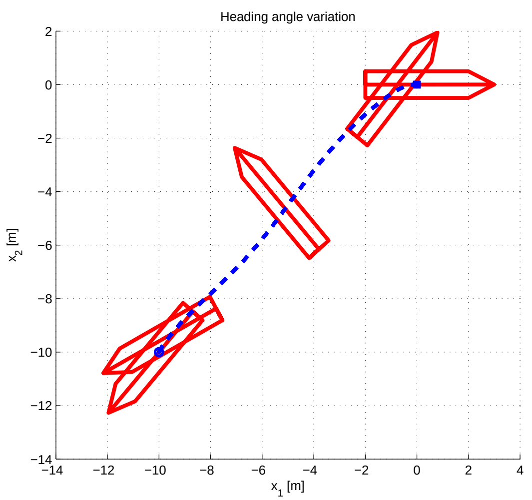

Figure 4.7: The heading orientation over the trajectory of the vessel as obtained from the closed loop system (4.12) and (4.18) after changing the weighting matrices Q and R.

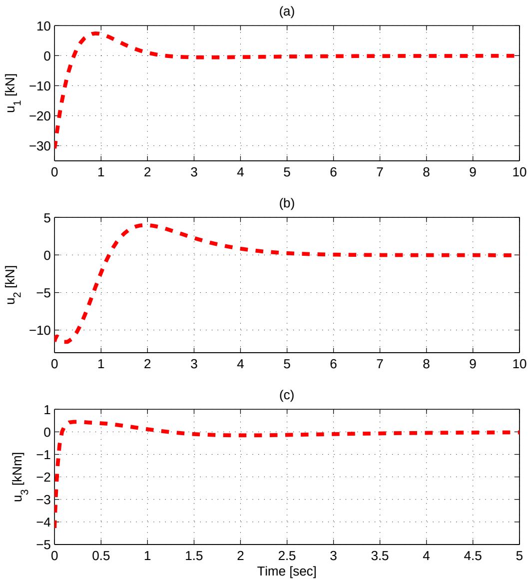

Figure 4.8: The profiles of the individual components of the control input vector as obtained from (4.18) after changing the weighting matrices Q and R.

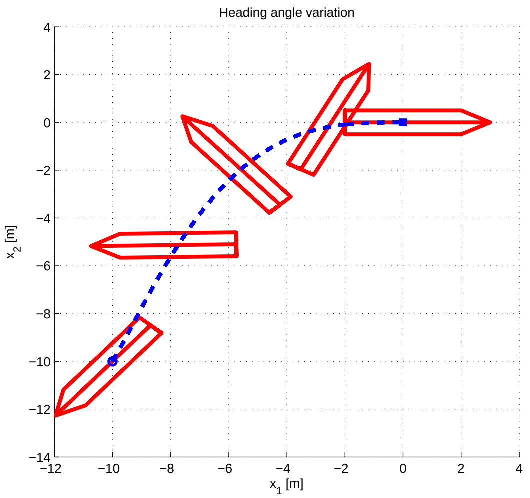

Figure 4.9: The heading orientation over the trajectory of the vessel as obtained from the closed loop system (4.12) and (4.18) after further changing the weighting matrices Q and R.

Next, we consider the case when the bias vector $\boldsymbol{b}$ is unknown. We consider exactly the same situation regarding the control objective and the initial position of the vessel, as in the nominal case. The simulation results show the performance of the SDARE-based control law and the SDARE observer to achieve the desired objective.

For the simulation results shown in the following figures, we use the bias time constant as $T = \text{diag}\{100, 100, 100\}$ while the controller weighting matrices are

$$Q = 10^{-1}\ \text{diag}\{100, 100, 10, 1, 1, 1, 0, 0, 0\} \text{ and } R = 10^{-1}\ \text{diag}\{1, 1, 0.01\},$$

and the observer weighting matrices are

$$U = 10^{0}\,\text{diag}\{1, 1, 1, 1, 1, 1, 1, 1, 10\} \text{ and } V = 10^{-2}\ \text{diag}\{1, 1, 1\}.$$

Figure 4.10 shows the measured position and heading profiles and their estimates obtained from the SDARE observer. As desired, the profiles show a steady and smooth estimation of the noisy measurements. Figure 4.11 shows the profiles of linear velocity in *surge* and *sway* directions and the angular *yaw* velocity and their estimates. Figure 4.12 shows the profiles of the bias estimates in *surge*, *sway*, and *yaw* directions. Figure 4.13 shows: (a) the trajectory profile, (b) the cost functional profile, and (c) the norm of the state vector and its estimate. Figure 4.14 shows the heading orientation with the trajectory. The profile shows a smooth and steady path and orientation of the vessel. Figure 4.15 shows the control input signals from the controller in each degree of freedom. The profiles show that the controller adjusts in the start and then signals become steady and smooth. From all these figures, we see that the SDARE compensator states show nice asymptotic convergence to the desired point.

To emphasize the role of the weighting matrices, we include some more simulations. For instance, we take

$$Q = 10^{-2}\ \text{diag}\{100, 100, 10, 1, 1, 1, 0, 0, 0\} \text{ and } R = 10^{-3}\ \text{diag}\{1, 1, 0.01\}.$$

This means that we reduce the penalty on both the vectors $\boldsymbol{x}$ and $\boldsymbol{u}$. Figures 4.16 and 4.17 show the corresponding profiles of the trajectory and the control input signals. The vessel takes a relatively longer route but its smoother than the one we obtained with the previous weighting matrices. The control input signals are also amplified as expected.

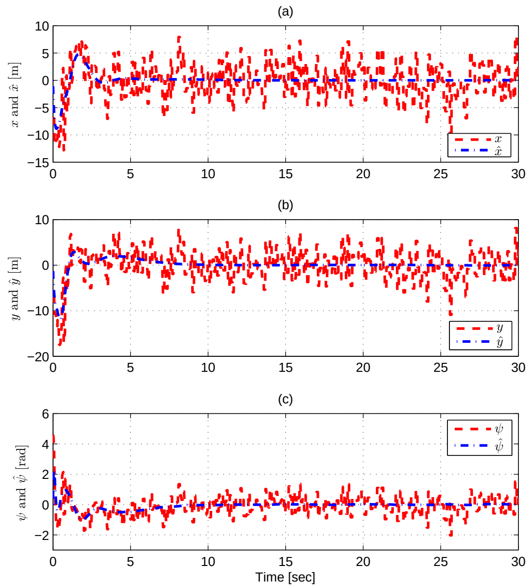

Figure 4.10: The profiles of the actual and the estimated position and orientation as obtained from (4.39).

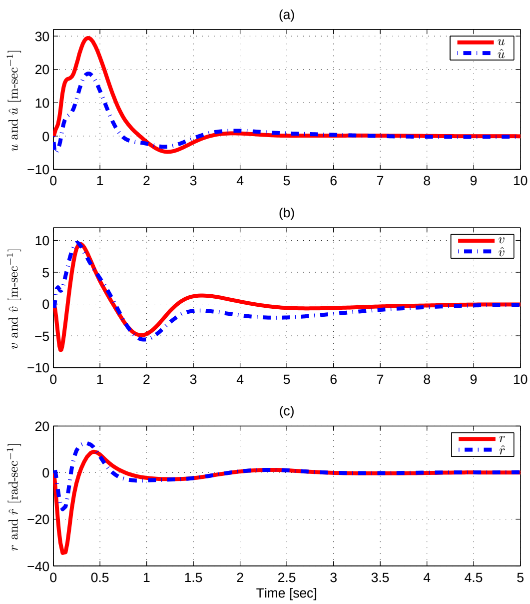

Figure 4.11: The actual and the estimated surge, sway, and yaw velocities as obtained from (4.39).

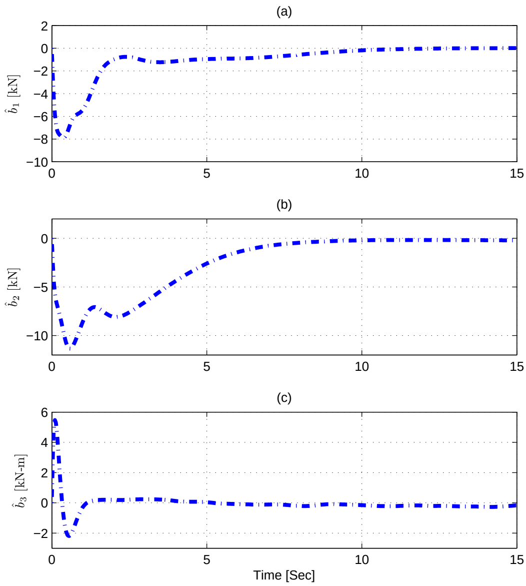

Figure 4.12: The bias estimates in surge, sway, and yaw directions as obtained from (4.39).

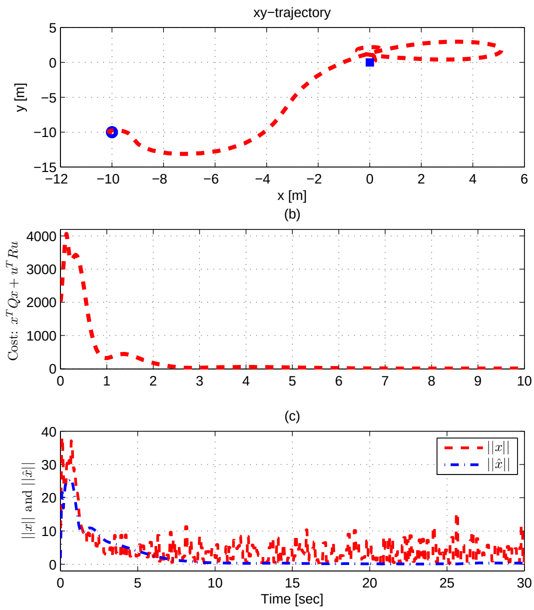

Figure 4.13: The trajectory and the profiles of the cost functional and the norms of the measured state and its estimate as obtained from (4.39).

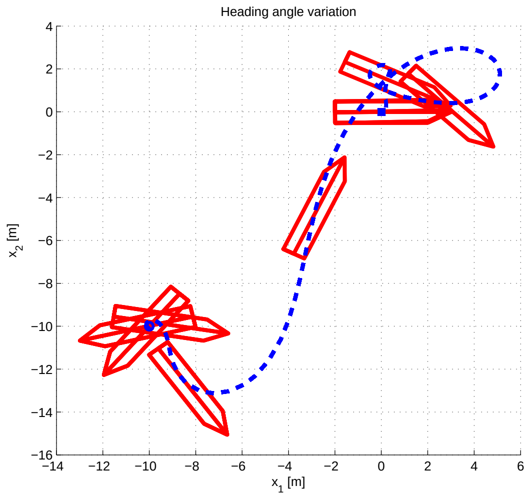

Figure 4.14: The heading orientation along the trajectory as obtained from (4.39).

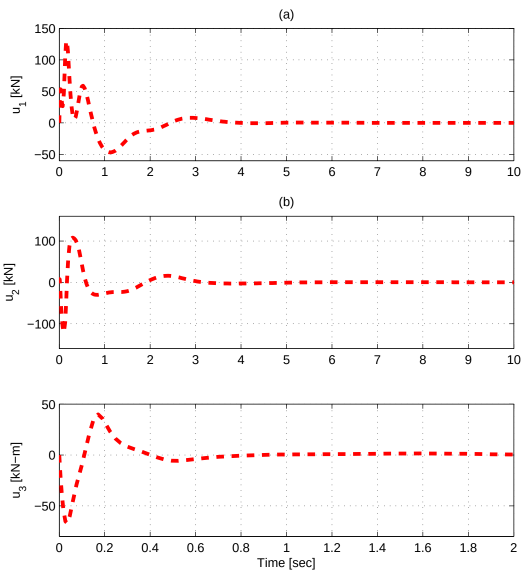

Figure 4.15: The control input signals for each degree of freedom as computed from (4.30).

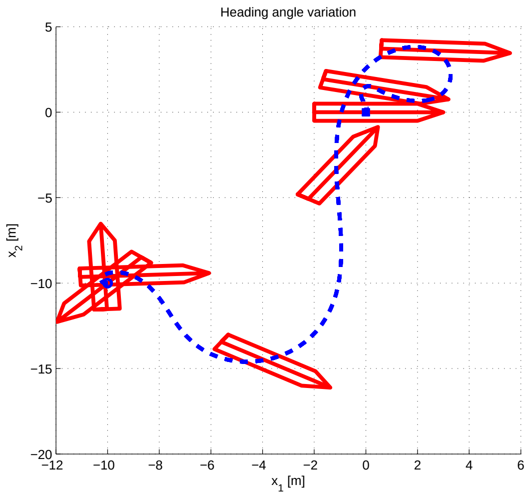

Figure 4.16: The heading orientation along the trajectory as obtained from (4.39) after changing weighting matrices Q and R and the observer tuning matrices U and V.

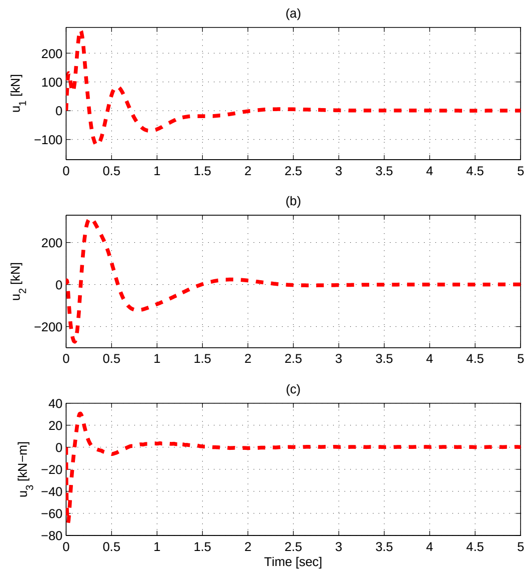

Figure 4.17: The control input signals for each degree of freedom as computed from (4.30) after changing weighting matrices Q and R and the observer tuning matrices U and V.

Finally, we consider the case when the WF motion is also playing a role. For the simulation results shown in the following figures, we use the bias time constant as $T = \text{diag}\{100, 100, 100\}$, the dominating wave frequencies as $\Omega = \text{diag}\{0.9, 0.9, 0.9\}$, the relative damping ratios as $Z = \text{diag}\{0.2, 0.2, 0.2\}$, the controller weighting matrices as

$$Q = 10^{-1}\,\text{diag}\{100, 100, 10, 1, 1, 1, O_{1\times 9}\}, \text{ and } R = 10^{-1}\,\text{diag}\{1, 1, 0.01\}$$

and the observer weighting matrices as

$$U = 10^{0}\,\text{diag}\{1, 1, 1, 1, 1, 1, 1, 1, 10, 1, 1, 1, 1, 1, 1\} \text{ and } V = 10^{-1}\,\text{diag}\{1, 1, 1\}.$$

Figure 4.18 shows the profiles of the measured position and heading, and their estimates obtained from the SDARE observer. The profiles depict a smooth and steady regulation of the vessel to the desired position. Figure 4.19 shows the velocity profiles of the vessel motion and their estimates along surge, sway, and yaw directions. Figure 4.20 shows the bias estimates obtained from the SDARE observer. Figure 4.21 shows: (a) the trajectory of the vessel motion, (b) the cost functional profile, and (c) the norm of the measured state vector and its estimate. In Figure 4.22, we show the heading orientation along the trajectory. The traectory and orientation are nice and smooth. Figure 4.23 shows the control input signal in each degree of freedom computed from (4.46). As in the previous case, the control signals need some adjustment in the beginning and then become smooth and steady.

To further elaborate the importance of the weighting matrices, we add some more simulation results. Now, Lets take the matrices

$$Q = 10^{-2}\,\text{diag}\{100, 100, 10, 1, 1, 1, O_{1\times 9}\} \text{ and } R = 10^{-3}\,\text{diag}\{1, 1, 0.01\}.$$

Figures 4.24 and 4.25 show the corresponding trajectory and control input signals. It can be seen that the vessel follows a relatively longer path but its slightly better than the previous path. The control input signals are amplified with this choice of the tuning matrices.

Further lets modify the observer weighting matrix U: we now take

$$U = 10^{0}\,\text{diag}\{10, 10, 10, 1, 1, 1, 1, 1, 10, 1, 1, 1, 1, 1, 1\}.$$

Figures 4.26 and 4.27 show the corresponding profiles of the trajectory and the control input signals. The trajectory profile has further improved and control input profiles show an increased control input.

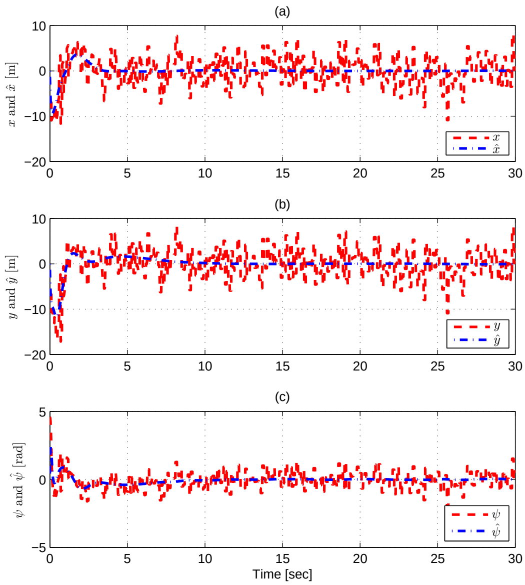

Figure 4.18: The position and heading profiles of the vessel motion as obtained from the compensator (4.55).

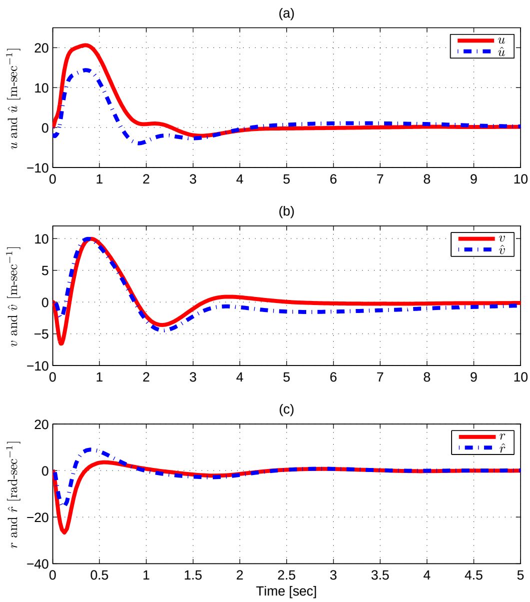

Figure 4.19: The velocities and their estimates along surge, sway, and yaw directions as obtained from (4.55).

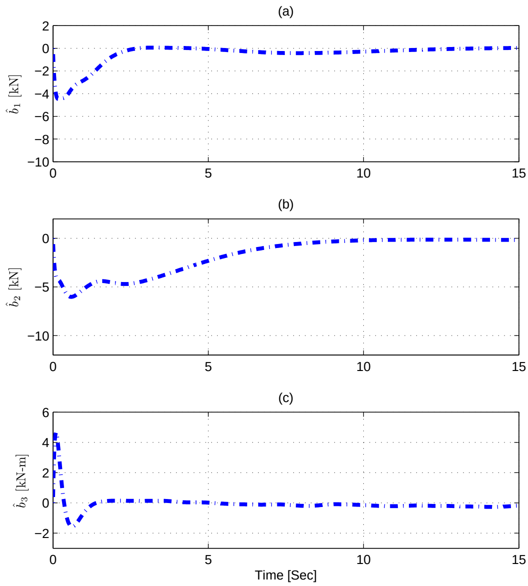

Figure 4.20: The bias estimates in surge, sway, and yaw directions as obtained from (4.55).

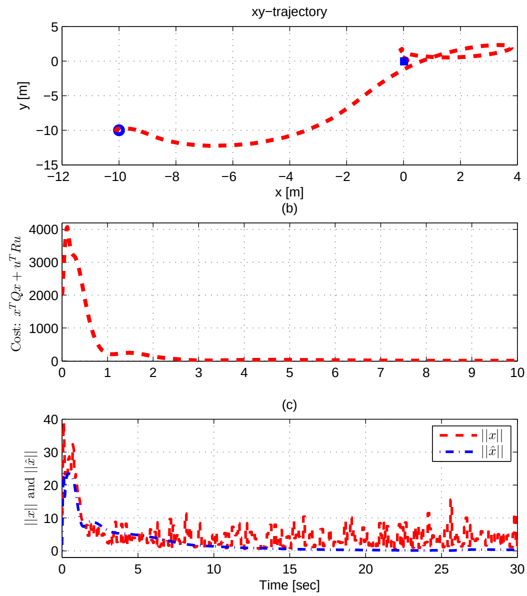

Figure 4.21: The trajectory and profile of the cost functional and the norms of the measured state vector and its estimate corresponding to the closed loop system (4.55).

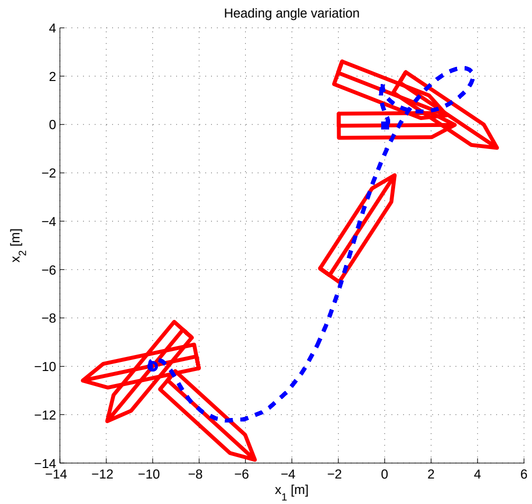

Figure 4.22: The heading orientation along the trajectory as obtained from (4.55).

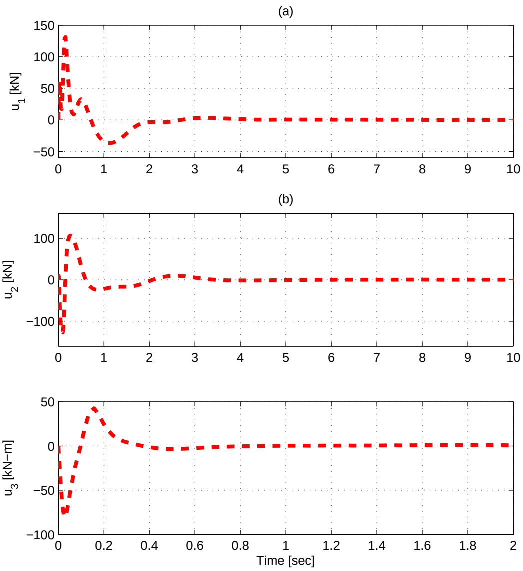

Figure 4.23: The control input signals for each degree of freedom as obtained from (4.46).

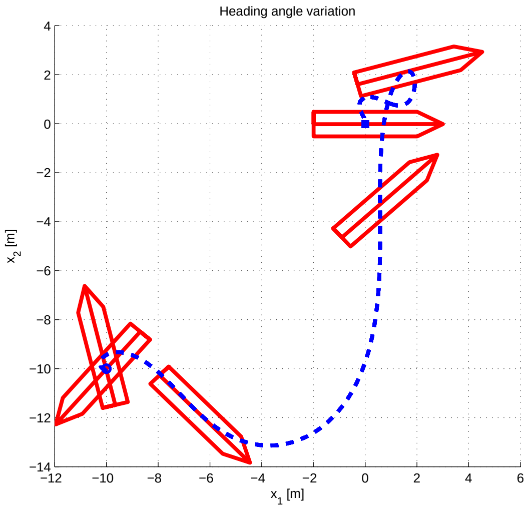

Figure 4.24: The heading orientation along the trajectory as obtained from (4.55) after changing weighting matrices Q and R and the observer tuning matrices U and V.

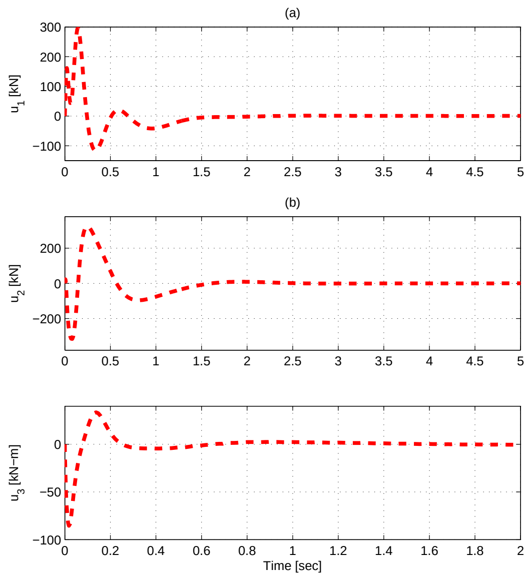

Figure 4.25: The control input signals for each degree of freedom as obtained from (4.46) after changing weighting matrices Q and R.

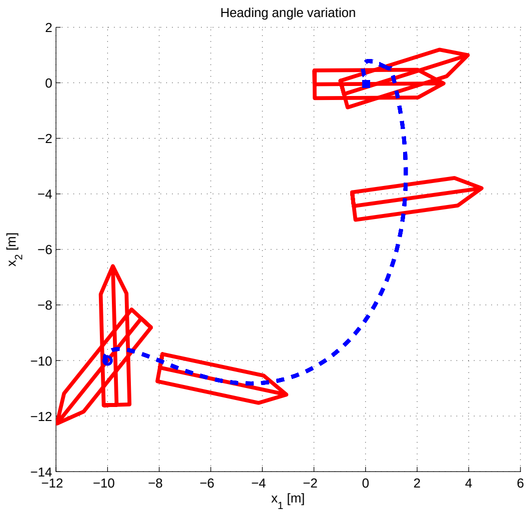

Figure 4.26: The heading orientation along the trajectory as obtained from (4.55) after further changing weighting matrices Q and R and the observer tuning matrices U and V.

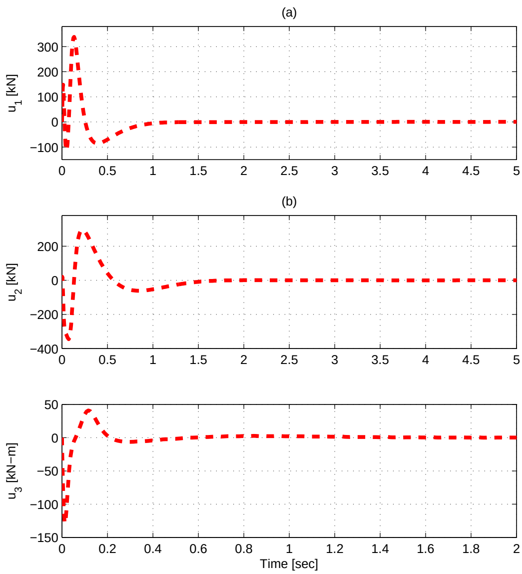

Figure 4.27: The control input signals for each degree of freedom as obtained from (4.46) after further changing weighting matrices Q and R and the observer tuning matrices U and V.

4.4 Conclusions

We study the regulation problem of a DP vessel by using the SDARE technique. We extend the concept of the LQR problem to nonlinear system by using the SDC parametrization. This gives rise to an SDARE which must be solved to obtain a suboptimal solution of the nonlinear regulation problem.

The DP vessel model shows that only the position and heading measurements are available from the sensors. This is an inadequate information for the SDARE control design problem which requires complete state knowledge. Using the stabilizability and detectability of the vessel model together with the duality concept, we propose a suboptimal locally asymptotically stable SDARE observer. The combination of the locally asymptotically stable SDARE regulator and SDARE observer is a locally asymptotically stable SDARE compensator.

We divide the study of the DP vessel regulation problem in two steps. First, we study the LF motion regulation without taking into account the WF motions. We begin by considering a nominal case (the bias disturbance vector is known or its estimate is available) and come up with a PD-type control law with a feedforward term. The controller is proved to be globally asymptotically stable by using the LMIs and the Lyapunov stability theory.

Afterwards, we assume that the bias vector is unknown and the measured signals from the sensors are contaminated by noise. We combine the concept of the SDARE regulation and estimation (to estimate the position, velocity, and bias vectors) to come up with a locally asymptotically stable SDARE compensator. Second, we take into account both the LF and WF motions and use again the SDARE method to address the regulation and estimation problems. A locally asymptotically stable compensator is obtained by combining locally asymptotically stable controller and estimator. We use the data of a supply vessel for simulation experiments. Simulation results presented in this chapter confirm the asymptotic stability of the SDARE regulator and the SDARE estimator.

Chapter 5

The Fourier Series Interpolation Method[1]

In Chapter 4, the controller and observer gains are state dependent. They are required to be determined by online solving the concerned SDAREs. These SDAREs have a special form in which the coefficient matrix depends on a single state component in a periodic way. In this chapter, we propose a new method for solving these SDAREs. This method is based on the Fourier series. This method reduces the online computation time for the solution of these SDAREs by performing the major computational task offline.

The earliest traces of the use of the algebraic Riccati equation in control related problems can be found in the works on the solution of the LQ optimal control and filtering problem [41] and on approximation methods in optimal control [67]. To date its scope has been extended to address problems of nonlinear state regulation and estimation, estimator based feedback control synthesis, $H_\infty-$control, H_2-control, and nonlinear filter design, for instance see [7], [14], [31], [52], and [66]. Recently, the state dependent Riccati equation based technique has been used in nonlinear optimal vehicle control in [2].

The SDARE has emerged in many practical applications. Especially, the SDARE has become an important research topic in ongoing developments in the areas of control and estimation theory. It has been regarded as an efficient tool to tackle problems related with the nonlinear control design, filtering, synthesis, and analysis. Consequently, emphasis has been put on developing computationally efficient solution methods for the SDARE.

In a broader perspective, we divide the solution methods in two categories: iterative and direct. Both type of methods have positive and negative features. Mainly, the direct methods are computationally faster than the iterative methods, especially when the problem is poorly conditioned or when a good-quality initial guess is not available.

[1]This work has been published in the proceedings of the UKACC International Conference on Control (CONTROL 2010), see [57].

On the other hand, the direct methods require more storage capacity than the iterative methods. Some of the well-known direct methods are the Taylor series method [7], the generalized eigenvector approach [15], the matrix sign function method [17], the information filter algorithm [39], and the Schur decomposition method [49]. Some of the well-known iterative methods are the Kleinman algorithm [3], the interpolation methods [7], the Newton-method and its modified forms [9, 18, 40], solution via spectral factorization, the doubling algorithm [13, 44], and the Chandrasekhar algorithm [72].

In (4.5), we observe that the controller gain is not fixed but it varies with the state of the system. The computation of the controller gain requires the solution of the SDARE (4.6). Therefore, in the feedback loop, the controller gain is computed online. As pointed out in [12] the reduction in the online computation time of the solution of the SDARE is a major issue because of its high computational cost. In this chapter, we propose the Fourier series based numerical method for the solution of the SDARE of type (4.7) which reduces the online computations. Henceforth, we call this method the Fourier series interpolation (FSI) method. This method of solution is computationally very simple and hence, it is valuable in the situations where online computation of the solution of the SDARE is required.

5.1 The Fourier Series Interpolation (FSI) Method

First we explain why it is reasonable to use the Fourier series for the solution of the algebraic Riccati equations of the type (4.7). Then we will illustrate the details of the FSI method. For a general formulation of the FSI method, we make a slight change of notation in the SDARE (4.7). We consider the following form

$$\Pi(x_1)A(x_1) + A^T(x_1)\Pi(x_1) + Q - \Pi(x_1)BR^{-1}B^T\Pi(x_1) = 0, \tag{5.1}$$

where $x_1 \in \mathbb{R}$, without loss of generality, is the first component of the state vector $\boldsymbol{x} \in \mathbb{R}^n$, $A(\cdot) \in \mathbb{R}^{n\times n}$ is a C^∞ function[2], $\Pi(\cdot) \in \mathbb{R}^{n\times n}$, and $B \in \mathbb{R}^{n\times m}$.

The matrix function $A(\cdot)$ is smooth and $\theta-$periodic, *i.e.*, $A(x_1) = A(x_1 + \theta)$ for all $x_1 \in \mathbb{R}$. The solution matrix $\Pi(\cdot)$, provided it exists, is also a smooth and $\theta-$periodic function, see [16]. At this point, we recall two important results from [35] which endorse the idea of using the Fourier series for finding an approximate solution of the SDARE (5.1). First, we recall the Fourier convergence theorem due to Dirichlet.

Theorem 5.1.1. (The Fourier Convergence Theorem) *Let f be a piecewise smooth function on the interval $-L \le x \le L$, then the Fourier series of f converges*
1. to $f(x)$, if f is continuous at $x \in (-L, L)$.
2. *to the average of the two limits,*

$$\frac{1}{2}[f(x+) + f(x-)],$$

if f has a jump discontinuity at $x \in (-L, L)$, where $f(x-)$ and $f(x+)$ means, respectively, the left and the right hand limits of the function f at point x.

[2] $C^\infty(\mathbb{R}, \mathbb{R}^{n\times m}) := \{A : \mathbb{R} \longrightarrow \mathbb{R}^{n\times m} \mid \text{A is } C^k \text{ for all } \ k \ge 0\}$.

The periodic extension of a $2L$–periodic function is always admissible. The following corollary gives the necessary and sufficient condition for the continuity of the periodic extension of a piecewise smooth function.

Corollary 5.1.1. *For a $2L$–periodic piecewise smooth function f, the periodic extension of f is continuous for all $x \in \mathbb{R}$ if and only if f is continuous and $f(-L) = f(L)$.*

In the context of the vessel model, the solution $\Pi_c(\psi)$ of the SDARE (4.7) is a smooth matrix function with period θ. Therefore, by the above results, it is possible to represent the matrix function $\Pi(\cdot)$ in the form of a Fourier series. This means that the Fourier series of $\Pi(\cdot)$ exists and converges to $\Pi(x_1)$ for all $x_1 \in \mathbb{R}$. Thus we write

$$\Pi(x_1) = \frac{A_0}{2} + \sum_{k=1}^{\infty}\left(A_k \cos\left(\frac{2k\pi x_1}{\theta}\right) + B_k \sin\left(\frac{2k\pi x_1}{\theta}\right)\right). \tag{5.2}$$

The Fourier coefficients $A_0, A_k \in \mathbb{R}^{n\times n}$ and $B_k \in \mathbb{R}^{n\times n}$ for $k = 1, 2, 3, ...$, are defined by

$$A_k = \frac{2}{\theta}\int_{-\frac{\theta}{2}}^{\frac{\theta}{2}} \Pi(x_1)\cos\left(\frac{2k\pi x_1}{\theta}\right) dx_1,\ k = 0, 1, 2, 3, ... \tag{5.3}$$

and

$$B_k = \frac{2}{\theta}\int_{-\frac{\theta}{2}}^{\frac{\theta}{2}} \Pi(x_1)\sin\left(\frac{2k\pi x_1}{\theta}\right) dx_1,\ k = 1, 2, 3, ... \tag{5.4}$$

Let us now recall a well-known result by Riemann and Lebesgue which is stated in the following lemma.

Lemma 5.1.1. (The Riemann-Lebesgue Lemma) *If f is an integrable function on $[-\frac{\theta}{2}, \frac{\theta}{2}]$ then*

$$\lim_{k\to\infty}\int_{-\frac{\theta}{2}}^{\frac{\theta}{2}} f(x)\sin kx\, dx = 0,$$

and

$$\lim_{k\to\infty}\int_{-\frac{\theta}{2}}^{\frac{\theta}{2}} f(x)\cos kx\, dx = 0,$$

From the fact that the series on the right hand side of (5.2) is convergent and from the statement of the Lemma 5.1.1, it follows that the Fourier coefficients with sufficiently high indices are negligibly small (their norms are of order zero) and can be left out. Therefore, for any small positive number ϵ, there exists an integer N' such that $||A_n||_2 < \epsilon$ and $||B_n||_2 < \epsilon$, $\forall n > N'$. We use the spectral matrix norm in this chapter.

We explain the procedure to compute the Fourier coefficients as follows. First, we decide a stopping criterion for the computation of the Fourier coefficients. We define a tolerance level say $\epsilon' > 0$, such that the process of the computation of the Fourier series coefficients stops when

$$\left\|\Pi(x_1) - \left(\frac{A_0}{2} + \sum_{k=1}^{N}\left(A_k \cos\left(\frac{2k\pi x_1}{\theta}\right) + B_k \sin\left(\frac{2k\pi x_1}{\theta}\right)\right)\right)\right\|_2 < \epsilon', \tag{5.5}$$

is satisfied for all $x_1 \in [-\frac{\theta}{2}, \frac{\theta}{2})$.

Then, we start with $N = 1$ such that there are $2N+1(= 3)$ Fourier coefficients to be determined. Equation (5.2) holds identically true for all $x_1 \in [-\frac{\theta}{2}, \frac{\theta}{2})$. Take $m > 2N+1$ points $x_{1_t} \in [-\frac{\theta}{2}, \frac{\theta}{2})$, $t = 1, 2, ..., m$. To each point $x_{1_t} \in [-\frac{\theta}{2}, \frac{\theta}{2})$, there corresponds an equation of the following form

$$\frac{A_0}{2} + \sum_{k=1}^{N} \left(A_k \cos\left(\frac{2k\pi x_{1_t}}{\theta}\right) + B_k \sin\left(\frac{2k\pi x_{1_t}}{\theta}\right)\right) = \Pi(x_{1_t}). \tag{5.6}$$

In this way, we get the following nonhomogeneous system of m linear matrix equations

$$\begin{bmatrix} \frac{1}{2} & \cos\frac{2\pi x_{1_1}}{\theta} & \cdots & \cos\frac{2N\pi x_{1_1}}{\theta} & \sin\frac{2\pi x_{1_1}}{\theta} & \cdots & \sin\frac{2N\pi x_{1_1}}{\theta} \\ \frac{1}{2} & \cos\frac{2\pi x_{1_2}}{\theta} & \cdots & \cos\frac{2N\pi x_{1_2}}{\theta} & \sin\frac{2\pi x_{1_2}}{\theta} & \cdots & \sin\frac{2N\pi x_{1_2}}{\theta} \\ \vdots & \vdots & \vdots & \vdots & \vdots & \vdots & \vdots \\ \frac{1}{2} & \cos\frac{2\pi x_{1_m}}{\theta} & \cdots & \cos\frac{2N\pi x_{1_m}}{\theta} & \sin\frac{2\pi x_{1_m}}{\theta} & \cdots & \sin\frac{2N\pi x_{1_m}}{\theta} \end{bmatrix} \begin{bmatrix} A_0 \\ A_1 \\ \vdots \\ A_N \\ B_1 \\ \vdots \\ B_N \end{bmatrix} = \begin{bmatrix} \Pi_1 \\ \Pi_2 \\ \vdots \\ \Pi_m \end{bmatrix},$$

where $\Pi_i = \Pi(x_{1_i})$. We can write this in short form as

$$\mathcal{A}\mathcal{X} = \mathcal{B} \tag{5.7}$$

However, note that the dimensions of the matrices in (5.7) do not conform with the usual matrix multiplication rules. We use the Kronecker matrix product to remove this discrepancy. For this we multiply the matrix $\mathcal{A}$ from right by I_n in the Kronecker sense. This results in

$$(\mathcal{A} \otimes I_n)\mathcal{X} = \mathcal{B}. \tag{5.8}$$

The equation (5.8) can be solved in the least-squares sense, minimize $\left\|(\mathcal{A}\otimes I_n)\mathcal{X} - \mathcal{B}\right\|^2$. The solution $\mathcal{X}$ to this problem yields $2N + 1$ Fourier coefficients. The Fourier series approximation of the solution of the SDARE (5.1) is then given by

$$\Pi(x_1) \approx \frac{A_0}{2} + \sum_{k=1}^{N} \left(A_k \cos\left(\frac{2k\pi x_1}{\theta}\right) + B_k \sin\left(\frac{2k\pi x_1}{\theta}\right)\right). \tag{5.9}$$

Now the stopping criterion (5.5) is tested. This can be done by plotting $\epsilon' - g(x_1)$ vs x_1 on the interval $[-\frac{\theta}{2}, \frac{\theta}{2})$, where $g(x_1)$ is the LHS of (5.5). To get a smooth sketch, we take enough points on the interval. This will also ensure that we did not overlook any sharp peaks or discontinuities. If the stopping criterion is satisfied (plot lies above x_1-axis) then we stop. Otherwise, we repeat the above procedure for the next integer value of $N(= 2)$ and so on, and continue until the stopping criterion is satisfied. The algorithm for finding the Fourier coefficients is summarized below[3].

Algorithm 5.1.1: COMPUTATION OF THE FOURIER COEFFICIENTS (FCs)

input: The tolerance parameter ϵ' and an integer $N(=1)$.

assumption: The m number of interpolation points must satisfy $m > 2N + 1$.

output: The Fourier Coefficients $A_0, A_1, A_2, ..., A_N, B_1, B_2, ..., B_N$.

for $N \leftarrow 1$ **to** *some finite large natural number*
step 1: Take $m > 2N + 1$.

step 2: Take $x_{t_i} \in [-\frac{\theta}{2}, \frac{\theta}{2}),\ \ i = 1, 2, 3, ...m.$

step 3: Solve (5.1) at m interpolation points to get $\Pi_1, \Pi_2, ..., \Pi_m$. (i)

step 4: Use statement (i) of this algorithm and (5.6) to get (5.7).

step 5: $\begin{cases}\text{Use Kronecker matrix product to get a linear system of}\\ \text{equations (5.8).}\end{cases}$

step 6: $\begin{cases}\text{Solve the linear system (5.8) to get the desired Fourier}\\ \text{coefficients.}\end{cases}$

if *the tolerance condition is satisfied*
then $\begin{cases}\textit{Fourier Coefficients } A[0], A[1], ..., A[N], B[1], B[2], ..., B[N]\\ \textit{are obtained.}\end{cases}$
else
continue the for loop until tolerance condition is satisfied.

The main step of the algorithm is step 6 of the *for* loop. The repetition of the loop continues until the stopping criteria is satisfied. We conclude this section with the following remark about the above algorithm.

Remark 5.1.1. *We take the number m of distict points in* $[-\frac{\theta}{2}, \frac{\theta}{2})$*, greater than the number of Fourier coefficients* $2N+1$ *to be determined to generate an over-determined system of linear equations. The system (5.8) has a solution because* $rank(\mathcal{A} \otimes I_n) = rank(\mathcal{A} \otimes I_n, \mathcal{B})$*.*

5.2 Performance Analysis

In this section we explain why the FSI method is effectively a better method for online computation of the solution of the SDARE than "care" in terms of computation time. We do so on the basis of flop count. Equations (4.20), (4.39) and (4.55) describe the feedback dynamics of the SDARE nonlinear compensator. The presence of $K_c(\hat{\psi})$ and $K_o(\hat{\psi})$ therein indicates that two SDAREs have to be solved at each iteration when the ode systems (4.20), (4.39) and (4.55) are solved numerically. This demands a computationally efficient method for finding the solution of the SDARE.

[3] The author is thankful to Professor Donald Kreher for his help on the pseudocode environment.

We compare the FSI method with the Schur decomposition method [15]. The MATLAB routine "care" is based on this method. For each ψ, the SDARE (4.7) reduces to a continuous time algebraic Riccati equation (CARE)

$$\Pi A + A^T \Pi + Q - \Pi B R^{-1} B^T \Pi = 0, \tag{5.10}$$

We solve the closed loop system equations by using the MATLAB solver *ode45*. During the process of computation of the numerical solution of the closed loop system, MATLAB routine "care" is called multiple times to solve (5.10). In the following we explain some details of the Schur decomposition method for a better understanding of the computational complexity of this method.

The Schur decomposition method requires two major computations for solving the SDARE. First step is the reduction of the Hamiltonian matrix to an ordered real Schur form (RSF). The Hamiltonian matrix associated with (5.10) is given by

$$\mathcal{H} = \begin{bmatrix} A & -BR^{-1}B^T \\ -Q & -A^T \end{bmatrix}. \tag{5.11}$$

The following result ensures that the Hamiltonian matrix (5.11) does not have any eigenvalue on the imaginary axis.

Theorem 5.2.1. (Relationship between the Hamiltonian Matrix and the Riccati Equations) *Let (A,B) be stabilizable and (A,Q) be detectable. Then the Hamiltonian matrix $\mathcal{H}$ has n eigenvalues with negative real parts, no eigenvalues on the imaginary axis, and n eigenvalues with positive real parts. In this case the CARE (5.10) has a unique stabilizing solution* Π.

Now using the QR-factorization, $\mathcal{H}$ can be transformed into RSF form according to the following result.

Theorem 5.2.2. (The Real Schur Triangularization Theorem) *Let $\mathcal{H}$ be a $2n \times 2n$ Hamiltonian matrix. Then there exists a $2n \times 2n$ matrix Q_{rs} such that*

$$Q_{rs}^T \mathcal{H} Q_{rs} = R_{rs} = \begin{bmatrix} R_{11} & R_{12} & \cdots & R_{1k} \\ 0 & R_{22} & \cdots & R_{2k} \\ \vdots & \vdots & \vdots & \vdots \\ 0 & 0 & 0 & R_{kk} \end{bmatrix}, \tag{5.12}$$

where each R_{ii} is either a scalar or a 2×2 matrix. The scalar diagonal entries correspond to real eigenvalues, and each 2×2 matrix on the diagonal has a pair of complex conjugate eigenvalues. The matrix R_{rs} is known as the RSF of $\mathcal{H}$.

The eigenvalues in (5.12) are not ordered so an additional step is made to get an ordered RSF which is important for the next step which uses the invariant subspace of the stable eigenvalues of $\mathcal{H}$ to solve (5.10). The following definition and subsequent theorem and corollary summarize the concluding step of the Schur decomposition method.

Definition 5.2.1. (Basis of an Invariant Subspace from RSF) *Let*

$$Q_{rs}^T \mathcal{H} Q_{rs} = R_{rs} = \begin{bmatrix} R_{11} & R_{12} \\ 0 & R_{22} \end{bmatrix}, \tag{5.13}$$

and let us assume that eigenvalues of R_{11} and R_{22} respectively are the negative and positive eigenvalues of the Hamiltonian matrix $\mathcal{H}$. Then the first p columns of Q_{rs}, where p is the order of R_{11}, form an orthonormal basis for the invariant subspace associated with the stable eigenvalues of $\mathcal{H}$.

Theorem 5.2.3. *A matrix Π is a solution of the CARE (5.10) if and only if the columns of $\begin{pmatrix} I \\ \Pi \end{pmatrix}$ span an n-dimensional invariant subspace of the Hamiltonian matrix $\mathcal{H}$.*

Corollary 5.2.1. *If the columns of $\begin{pmatrix} \Pi_1 \\ \Pi_2 \end{pmatrix}$ span an n-dimensional invariant subspace of the Hamiltonian matrix $\mathcal{H}$ associated with the CARE (5.10) and Π_1 is invertible, then $\Pi = \Pi_2\Pi_1^{-1}$ is a solution of the CARE (5.10).*

The Schur method is based on reduction of the Hamiltonian matrix $\mathcal{H}$ to RSF which is done by QR factorization. The exact flop count is not possible as QR-factorization is an iterative procedure. However, by the empirical observations it is assumed that on average each eigenvalue requires 2 QR-factorizations, [15]. The QR-factorization of a matrix requires $O(n^3)$ flops which means that the RSF obtained in the first step of the Schur decomposition method also requires $O(n^3)$ flops. The ordering of the eigenvalues in RSF requires *O(n)* flops. In the second step, the computation of $\Pi = \Pi_2\Pi_1^{-1}$ is done by using the least-squares algorithm and this also requires $O(n^3)$ flops. Therefore the Schur decomposition requires $O(n^3)$ flops each time CARE (5.10) is solved online. On the other hand, the FSI method requires simple matrix addition ($O(n^2)$ flops) and scalar-matrix multiplication ($O(n^2)$ flops). Therefore, the FSI method requires $O(n^2)$ flops when the online solution of (5.10) is computed by this method.

The computationally expensive task in FSI method is the computation of the Fourier coefficients which is done offline, only once. From the algorithm given in Section 5.1, we see that the computation of the Fourier coefficients involve two major steps. First, the computation of the solution of the SDARE at a known (m) number of points. Second, the solution of a linear system of equations. Each requires $O(n^3)$ flops.

Based on the foregoing discussion, we conclude that the FSI method reduces the online computations in a feedback dynamics based on an SDARE control law. In Table 5.1, by using the simulation results discussed in Section 4.3, we quantitatively demonstrate that the FSI method reduces the online computation time for the solution of the SDARE. Each of the closed loop systems (4.20), (4.39) and (4.55) are solved with the MATLAB routine *ode45* on a time interval $[0, 30]$. Table 5.1 shows a comparison between the computer time required to solve the closed loop systems with the FSI method and by the MATLAB routine “care”. We notice that with the increase in the size of the system, the performance of the FSI method is still comparable to its performance with a lower order system. The simulations have been performed on an Intel Centrino duo running at the frequency of 2 GHz having 2 GB RAM.

Table 5.1: Performance Analysis

	Online comput. time (sec) with "care"	Online comput. time (sec) with FSI method	Percentage (%) reduc. in online computation time
For (4.20)	11	6	45
	11	6.8	37
	118	48	59
For (4.39)	96	67	30
	274	192	32
For (4.55)	191	90	53
	467	252	46
	495	276	44

Looking at the profile summary obtained from the MATLAB, we notice that "care" is called *2164*, *2479*, and *17948* times when (4.20) is solved on interval $[0, 30]$. It is called *12352* and *34406* times when (4.39) is solved on interval $[0, 30]$ and it is called *12406*, *34547*, and *34405* times when (4.55) is solved on interval $[0, 30]$ for each $K_c(\hat{\psi})$ and $K_o(\hat{\psi})$. The times for the offline computations of the Fourier series coefficients are 0.1, 0.13, and 0.15 seconds, respectively. This computational evidence supports the argument made on the basis of the flop counts earlier in this section. That is the FSI method is capable of solving the CARE faster than the Schur decomposition method. Particularly, this is useful in situations where the online solution of the Riccati equation is required.

Chapter 6

Port-Hamiltonian Formulation and Passivity Based Control Design[1]

This chapter focuses on the design of the control law for dynamic positioning assuming that the filtering and estimation problems have been solved, *i.e.*, the measured output contains only the noise free LF position and heading measurements and the disturbances vector is either known or its estimate is available. The Port-Hamiltonian framework is a very useful concept which offers more capacity to improve the performance of the controllers and to analyze stability properties. Passivity-based techniques were first introduced in [38], [53], and [87] in the early 1970's. These techniques have been used since then in many applications, for instance in underwater vehicles [4], the control of electrical machines [21], the design of power system stabilizers [61], adaptive control for rigid robots [63], underactuated mechanical systems [64], power converters [69], and magnetic levitation systems [70].

A nice feature of the passivity-based control design is the physical meaning of the resulting control laws and concepts, such as storage energy or dissipation, which play a fundamental role in analyzing stability and the performance of the controller. Stability properties, based on the Lyapunov theory, can easily be studied for the closed loop systems obtained. The passivity based approach has two versions. The classical Euler Lagrange (EL-PBC) allows the change in the potential energy function and the generalized inertia matrix, see [65]. In the last decade, the Interconnection and Damping Assignment Passivity Based Control (IDA-PBC) methodology has emerged as an easy and a (quasi) step-by-step methodology to obtain passivity based controllers, see for instance [65]. IDA-PBC also allows changes in the interconnection matrix.

This chapter introduces the port-Hamiltonian model of a vessel with 3 degrees of freedom in a horizontal plane. The obtained port-Hamiltonian equations are the

[1]This work has been published in the proceedings of the Dynamic Positioning Conference DP2010 in Houston, see [55]. It is also to appear at the IET Journal of Control Theory and Applications, see [56].

starting point for the design of controllers using the IDA-PBC technique. The main contribution of this chapter is a family of passivity-based controllers, in the port-Hamiltonian framework, which uses the energy shaping of the closed loop system to ensure (local/global) asymptotic stability. The resulting control laws are of output-feedback form and are robust in presence of eventual disturbances.

6.1 Hamiltonian-Based Control

6.1.1 Port-Hamiltonian Modeling

A large class of physical systems of interest in control applications can be modeled in the general form of port-Hamiltonian systems (PHS), see [84]. PHS generalize the Hamiltonian formalism of classical mechanics to physical systems connected in a power-preserving way and encodes the detailed energy transfer and storage in the systems, and is thus suitable for control schemes based on IDA-PBC.

A PHS can be written, in an implicit form, as

$$\dot{\boldsymbol{x}} = (\mathcal{J}(\boldsymbol{x}) - \mathcal{R}(\boldsymbol{x}))\partial H(\boldsymbol{x}) + G(\boldsymbol{x})\boldsymbol{u}, \tag{6.1}$$

where $\boldsymbol{x} \in \mathbb{R}^n$ is the state (or Hamiltonian variables) vector, $\mathcal{J}(\boldsymbol{x}) \in \mathbb{R}^{n\times n}$ is the skew-symmetric interconnection matrix ($\mathcal{J} = -\mathcal{J}^T$), $\mathcal{R}(\boldsymbol{x}) \in \mathbb{R}^{n\times n}$ is the dissipation (or damping) matrix (symmetric positive semi-definite, $\mathcal{R} = \mathcal{R}^T \geq 0$), $G(\boldsymbol{x}) \in \mathbb{R}^{n\times m}$ is the external connection matrix, $\boldsymbol{u} \in \mathbb{R}^m$ is the control input vector, and $H(\boldsymbol{x})$ is the Hamiltonian (energy or storage) function[2]. In this formulation, the matrix $\mathcal{R}$ describes the energy losses of the system, the interconnection matrix $\mathcal{J}$ describes the flow of energy inside the system, and the port matrix G describes the flow of energy from outside (for instance from the controller) to the system. In a passivity based control design approach, the controller can be considered as a source injecting energy into the system.

The so-called passive output, $\boldsymbol{y} \in \mathbb{R}^m$, is given by

$$\boldsymbol{y} = G^T(\boldsymbol{x})\partial H(\boldsymbol{x}), \tag{6.2}$$

and the product $\boldsymbol{u}^T\boldsymbol{y}$ usually has unity of power. In the literature on port-Hamiltonian systems, the so-called passive output is a relative degree one output.

6.1.2 The IDA-PBC Technique

The Interconnection and Damping Assignment Passivity Based Control (IDA-PBC), [65], is a technique for designing controllers based on the port-Hamiltonian framework. It uses the passive stability properties to ensure the convergence of the system to the desired fixed point.

The main idea behind the IDA-PBC is to define a new closed loop (or target) system with a Hamiltonian structure. The design problem summarizes into finding a

[2]The $\partial_{\boldsymbol{x}}$ (or ∂, if no confusion arises) operator defines the gradient of a function of $\boldsymbol{x}$, and in what follows we will take it as a column vector.

control law such that the system behaves as

$$\dot{\boldsymbol{x}} = (\mathcal{J}_d - \mathcal{R}_d)\partial H_d, \tag{6.3}$$

where $\mathcal{J}_d(\boldsymbol{x}) = -\mathcal{J}_d^T(\boldsymbol{x})$, $\mathcal{R}_d(\boldsymbol{x}) = \mathcal{R}_d^T(\boldsymbol{x}) \geq 0$ and $H_d(\boldsymbol{x})$ has a minimum at the desired regulation point $\boldsymbol{x}^d$, $\boldsymbol{x}^d = \arg\min(H_d(\boldsymbol{x}))$. The stability of this system can easily be proved by using H_d as a Lyapunov function ($\dot{H}_d(\boldsymbol{x}) = -(\partial H_d)^T \mathcal{R}_d \partial H_d \leq 0$, see for instance, [62] and [65] for a detailed discussion).

The design procedure reduces to finding matrices $\mathcal{J}_d(\boldsymbol{x})$ and $\mathcal{R}_d(\boldsymbol{x})$ and a desired closed loop energy function $H_d(\boldsymbol{x})$, which solve the so-called matching equation

$$(\mathcal{J} - \mathcal{R})\partial H + G\boldsymbol{u} = (\mathcal{J}_d - \mathcal{R}_d)\partial H_d. \tag{6.4}$$

Then, the control law becomes

$$\boldsymbol{u} = \left(G^T G\right)^{-1} G^T \left((\mathcal{J}_d - \mathcal{R}_d)\partial H_d - (\mathcal{J} - \mathcal{R})\partial H\right). \tag{6.5}$$

A drawback of the IDA-PBC controllers is that they are, in general, not able to reject disturbances. To remove this discrepancy of the control design, usually a dynamic extension of the system is introduced to obtain an integral action on the output error. Extension of the closed loop dynamics in the IDA-PBC framework can be done, in a natural way, only for passive outputs, see [62]. A completely different approach addresses non-passive outputs (or higher relative degree one outputs). In this case, a Hamiltonian based controller with an integral action can be obtained via a change of variables, see [20].

Let us assume that the $\boldsymbol{x}_o \in \mathbb{R}^r$ are the higher relative degree one (or non-passive) outputs. The main idea is to introduce a new variable $\boldsymbol{z}_e \in \mathbb{R}^r$, which is used to enforce the equilibrium point of the closed loop system to the desired one, and a change of variables $\boldsymbol{z} = f(\boldsymbol{x}, \boldsymbol{z}_e) \in \mathbb{R}^{n-r}$ to cast the target system in a Hamiltonian structure as follows

$$\begin{bmatrix} \dot{\boldsymbol{x}}_o \\ \dot{\boldsymbol{z}} \\ \dot{\boldsymbol{z}}_e \end{bmatrix} = \begin{bmatrix} J_o - R_o & J_{zo} - R_{zo} & J_e \\ -J_{zo}^T - R_{zo}^T & J_z - R_z & O_3 \\ -J_e^T & O_3 & O_3 \end{bmatrix} \partial H_{de}. \tag{6.6}$$

The power-preserving interconnection structure of the proposed target system is defined by $J_o = -J_o^T \in \mathbb{R}^{r\times r}$, $J_z = -J_z^T \in \mathbb{R}^{(n-r)\times(n-r)}$, $J_{zo} \in \mathbb{R}^{r\times(n-r)}$ and $J_e \in \mathbb{R}^{r\times r}$. Dissipation is given by $R_o = R_o^T \in \mathbb{R}^{r\times r}$, $R_z = R_z^T \in \mathbb{R}^{(n-r)\times(n-r)}$, and $R_{zo} \in \mathbb{R}^{r\times(n-r)}$. Finally, the Hamiltonian function, H_{de} takes the form

$$H_{de} = H_d(\boldsymbol{x}_o, \boldsymbol{z}) + \frac{1}{2}\boldsymbol{z}_e^T K_e \boldsymbol{z}_e, \tag{6.7}$$

where H_d has a minimum at the desired regulation point $(\boldsymbol{x}_o^d, f(\boldsymbol{x}_o^d, 0), 0)$.

Following the idea of the IDA-PBC technique, the stability is guaranteed if the dissipative matrix is positive semidefinite, i.e., $R_o \geq 0$, $R_z > 0$ and $R_o - R_{zo}R_z^{-1}R_{zo}^T \geq 0$.

The key point of the PHS structure in (6.6) is that the existence of a minimum of H_{de} in $\boldsymbol{x}_o^d$, implies $\partial_{\boldsymbol{x}_o} H_d|_{\boldsymbol{x}_o^d} = 0$ which, evaluated in the $\boldsymbol{z}_e$ dynamics,

$$\dot{\boldsymbol{z}}_e = -J_e^T \partial_{\boldsymbol{x}_o} H_d \tag{6.8}$$

ensures that $\boldsymbol{x}_o^d$ is an equilibrium point.

6.2 Dynamic Positioning Problem

A dynamic positioning (DP) system is a computer controlled system which automatically maintains a vessel's position and heading by using propellers and thrusters. The computer program contains a mathematical model of the vessel which includes information pertaining to the wind and current drag of the vessel and the location of the thrusters. This knowledge, combined with the sensor information, helps the computer calculate the required steering angle and thruster output for each thruster.

Generally, in DP problems, only position and heading measurements are available. This leads to the use of observers to estimate the state (mainly the velocities and the bias term) which are required for feedback into the control law. This problem is studied in many papers. Some examples include a nonlinear observer designed in [26], a passivity-based scheme considered in [29] and [51], and the Luenberger observer used in [76].

Furthermore, the measured position and heading signals are noisy and, also, with two different frequency components (see Figure 2.5, Chapter 2). The total ship motion can be seen as a superposition of a low frequency component (due to the wind, sea currents and thruster forces and moments) and an oscillatory term (the so-called wave-induced wave frequency motion), which represents the effect of the waves. See [24] for more details.

However, DP only considers the slow variations and, consequently, the motion due to the waves should be removed before it enters in the controller algorithm. Kalman filtering techniques were proposed in [30] and [34]. See [27] for a recent overview. As pointed out in [29], Kalman filters require the use of a linear model, and the nonlinear motion should be linearized at various operation points. To overcome this drawback, a wave-frequency observer is added to compensate the wave disturbances, see [29] and [51].

Due to the important role of the estimation and filtering process, the motion control system in the DP problem can be grouped in two basic subsystems: the observer system (or wave filter), and the controller, see Figure 6.1.

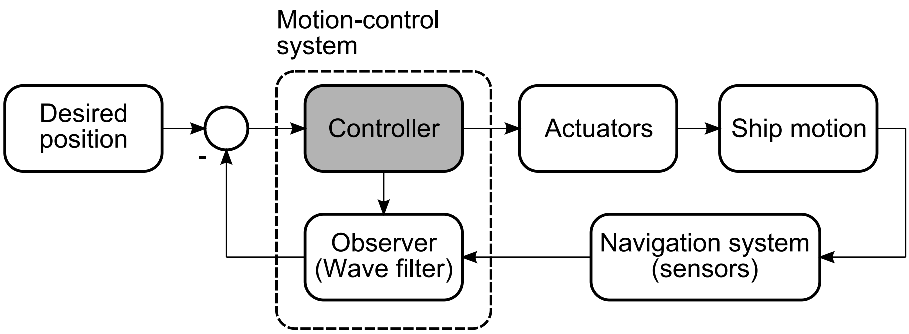

Figure 6.1: Basic scheme of components of a ship motion-control system.

Various controllers have been proposed to stabilize the ship to the desired position. PI controllers are often used [24], however more advanced techniques are applied to this problem resulting in interesting control algorithms. Backstepping design, which also includes the observer stage, is presented in [26] and [74]. In [51] the stability of a PD-type controller with a passive observer is proved using a separation principle argument. Recently, sampled-data control theory has also been applied to the DP problem for designing the control law [42]. As mentioned at the start of this chapter, we assume that the estimation and filtering problem has been solved and our focus is the control design for dynamic positioning using the port-Hamiltonian framework.

6.3 Ship Model in Port-Hamiltonian Framework

6.3.1 Ship Model in Cartesian Coordinates

We recall here the vessel model from Chapter 2. In this chapter, we consider a model in the following form.

$$\begin{bmatrix} \dot{\boldsymbol{\eta}} \\ \dot{\boldsymbol{\nu}} \end{bmatrix} = \begin{bmatrix} O_3 & J(\psi) \\ O_3 & -M^{-1}D \end{bmatrix} \begin{bmatrix} \boldsymbol{\eta} \\ \boldsymbol{\nu} \end{bmatrix} + \begin{bmatrix} O_3 \\ M^{-1} \end{bmatrix} \boldsymbol{\tau} + \begin{bmatrix} O_3 \\ M^{-1}J^T(\psi) \end{bmatrix} \boldsymbol{b}. \tag{6.9}$$

The details of the vectors and the matrices in (6.9) are given in Chapter 2. The environmental disturbances due to the sea currents, waves, and wind are represented by $\boldsymbol{b} = [b_1\ b_2\ b_3]^T \in \mathbb{R}^3$ in the Earth-fixed reference frame. This bias term is constant in the Earth-fixed reference frame, under assumption of constant or slowly varying currents.

In this chapter, it is assumed that these natural effects (sometimes called bias forces and moments), which can also be modeled as a first-order Markov process, [24, Chapter 3, page:89], are either known or an estimate of the bias vector is available. We assume that the measurement system gives us noise free position and orientation measurements and that the wave frequency (WF) components from the measured output are filtered or estimated. Hence, in this chapter, we skip the dynamics of the bias and the WF components.

The main goal in the dynamic positioning problem is to stabilize the ship in a given $\boldsymbol{\eta}$-coordinate. Without loss of generality, our objective is to design an appropriate control law $\boldsymbol{\tau}$ which stabilizes the system to the origin $(x, y, \psi) = (0, 0, 0)$. Additionally, as the measurement of the relative velocity vector is not available, the control law should be independent of $\boldsymbol{\nu}$, and must be able to reject unknown disturbances or uncertainties.

6.3.2 Ship Model in Port-Hamiltonian Coordinates

We can write the system described in (6.9) in a PHS form (6.1) by using as a state $\boldsymbol{x}^T = [\boldsymbol{q}^T, \boldsymbol{p}^T] \in \mathbb{R}^6$, where $\boldsymbol{q} = [q_1\ q_2\ q_3]^T \in \mathbb{R}^3$ represents the Earth-fixed position and heading, and the momentum $\boldsymbol{p} = [p_1\ p_2\ p_3]^T \in \mathbb{R}^3$, is defined as $\boldsymbol{p} = M\boldsymbol{\nu}$. Substituting $\boldsymbol{\eta} = \boldsymbol{q}$ and $\boldsymbol{\nu} = M^{-1}\boldsymbol{p}$ in (6.9), we get the following system

$$\dot{\boldsymbol{x}} = (\mathcal{J}(q_3) - \mathcal{R})\,\partial H + G_\tau \boldsymbol{\tau} + G_b(q_3)\boldsymbol{b} \tag{6.10}$$

with the following interconnection and damping matrices

$$\mathcal{J}(q_3) = \begin{bmatrix} O_3 & J(q_3) \\ -J^T(q_3) & O_3 \end{bmatrix}, \qquad \mathcal{R} = \begin{bmatrix} O_3 & O_3 \\ O_3 & D \end{bmatrix}, \tag{6.11}$$

the external connection matrices

$$G_\tau = \begin{bmatrix} O_3 \\ I_3 \end{bmatrix}, \qquad G_b(q_3) = \begin{bmatrix} O_3 \\ J^T(q_3) \end{bmatrix}, \tag{6.12}$$

and the Hamiltonian function given by

$$H = \frac{1}{2}\boldsymbol{p}^T M^{-1} \boldsymbol{p}. \tag{6.13}$$

Note that the Hamiltonian function contains only a *kinetic* energy term, associated with the momentum variable. A *potential* energy, artificially added by the controller will play a key role to stabilize the ship in the desired position. From (6.2), we observe that the passive output for the system (6.10) is the velocity vector which does not correspond to the actual output of the system, the position and the orientation. This is an important consideration for the control design, especially for the dynamic IDA-PBC control design in Section 6.5.

Two different energy functions are proposed in this chapter. We start by illustrating the methodology using a quadratic and a trigonometric Hamiltonian function and recover a simple classical IDA-PBC controller which guarantees asymptotic stability. The energy shaping, based on a trigonometric function, improves the heading control. These controllers do not produce the desired regulation properties in the presence of unknown disturbances. Consequently, in order to achieve the desired performance, a dynamic extension is proposed, and it results in a control law that can be interpreted as a nonlinear version of the conventional PID controller. A salient feature of the proposed controllers is that they do not require the relative velocity measurements and, thanks to a dynamic extension, they also ensure a good regulation behavior even in presence of disturbances or unknown (or non-estimated) terms.

6.4 Classical IDA-PBC Design

A family of output feedback controllers can be obtained via the IDA-PBC methodology. In the design process, a nominal case is considered (i.e., where the disturbances are assumed to be completely known), and then the stability against an unknown disturbance vector is also analyzed.

As presented in Section 6.1, the control laws are obtained from matching the dynamical system (6.10) with the target dynamics (6.3). To solve this, the desired interconnection matrix is fixed as in (6.10), i.e.,

$$\mathcal{J}_d = \begin{bmatrix} O_3 & J(q_3) \\ -J^T(q_3) & O_3 \end{bmatrix}, \tag{6.14}$$

the dissipation matrix set as

$$\mathcal{R}_d = \begin{bmatrix} O_3 & O_3 \\ O_3 & R_p \end{bmatrix}, \tag{6.15}$$

where $R_p \in \mathbb{R}^{3\times 3}$ is a symmetric positive definite matrix ($R_p = R_p^T > 0$), and the closed loop energy function, $H_d(\boldsymbol{x})$, is shaped as

$$H_d(\boldsymbol{q}, \boldsymbol{p}) = \Psi(\boldsymbol{q}) + \frac{1}{2}\boldsymbol{p}^T M^{-1} \boldsymbol{p}, \tag{6.16}$$

where $\Psi(\boldsymbol{q})$ has a minimum at the origin, i.e., $\partial_{\boldsymbol{q}}\Psi|_{\boldsymbol{q}^*=0} = 0$ and $\partial^2_{\boldsymbol{q}}\Psi|_{\boldsymbol{q}^*} = 0 > 0$. This implies that the desired energy function has the minimum at the desired stabilizing point $(\boldsymbol{q}^*, \boldsymbol{p}^*) = (0, 0)$. From a physical point of view, the controller adds some *potential* energy, in the $\boldsymbol{q}$ coordinates, with respect to the original Hamiltonian function (6.13).

From the resulting matching equation (6.4), the equality corresponding to the first row is automatically satisfied while, from the second equality, we obtain the following control law

$$\boldsymbol{\tau} = -J^T(q_3)(\partial_{\boldsymbol{q}}\Psi + \boldsymbol{b}) - (R_p - D)M^{-1}\boldsymbol{p}. \tag{6.17}$$

From the $\boldsymbol{q}$ dynamics in (6.10), we get $\boldsymbol{p} = MJ^T(q_3)\dot{\boldsymbol{q}}$, and defining $K_D := R_p - D$, the state feedback algorithm (6.17) takes the form

$$\boldsymbol{\tau} = -\, J^T(q_3)\partial_{\boldsymbol{q}}\Psi - K_D J^T(q_3)\dot{\boldsymbol{q}} - J^T(q_3)\boldsymbol{b}, \tag{6.18}$$

which can be seen as a nonlinear output feedback PD (Proportional-Derivative) controller with a feed-forward term, $-J^T(q_3)\boldsymbol{b}$. Notice that with the choice $R_p = D$, the controller simplifies because $K_D = 0$. But, we keep the general result because, as we point out in the simulations that by increasing the dissipation of the system, the performance of the closed loop system improves considerably .

Proposition 6.4.1. *Consider the dynamical system (6.10) in a closed loop with the control law (6.18), where the origin $\boldsymbol{q} = 0$ is a local minimum of $\Psi(\boldsymbol{q})$, and that the bias vector $\boldsymbol{b}$ and the matrix D are known. Then, the desired regulation point $(\boldsymbol{q}^*, \boldsymbol{p}^*) = (0, 0)$ is locally asymptotically stable. Furthermore, if $\boldsymbol{q} = 0$ is the global minimum of $\Psi(\boldsymbol{q})$, then $(\boldsymbol{q}^*, \boldsymbol{p}^*) = (0, 0)$ is globally asymptotically stable.*

Proof. Substituting (6.18) in (6.10), we get a PHS in the form (6.3) with (6.14) and (6.15) as follows:

$$\begin{aligned}
\dot{\boldsymbol{x}} =& \begin{bmatrix} O_3 & J(q_3) \\ -J^T(q_3) & -D \end{bmatrix}\begin{bmatrix} O_3 \\ M^{-1}\boldsymbol{p} \end{bmatrix} + \begin{bmatrix} O_3 \\ I_3 \end{bmatrix}\begin{bmatrix} -J^T(q_3) & -K_D J^T(q_3) \end{bmatrix}\partial H_d + \\
& \begin{bmatrix} O_3 \\ -J^T(q_3) \end{bmatrix}\boldsymbol{b} + \begin{bmatrix} O_3 \\ J^T(q_3) \end{bmatrix}\boldsymbol{b} \\
=& \begin{bmatrix} J(q_3)M^{-1}\boldsymbol{p} \\ -J^T(q_3)\partial_{\boldsymbol{q}}H_d - R_{\boldsymbol{p}}\partial_{\boldsymbol{p}}H_d \end{bmatrix} \\
=& \begin{bmatrix} O_3 & J(q_3) \\ -J^T(q_3) & -R_p \end{bmatrix}\begin{bmatrix} \partial_{\boldsymbol{q}}H_d \\ \partial_{\boldsymbol{p}}H_d \end{bmatrix} \\
=& (\mathcal{J}_d - \mathcal{R}_d)\,\partial H_d.
\end{aligned} \tag{6.19}$$

Using the Hamiltonian function (6.16) as a Lyapunov function, we get

$$\begin{aligned}
\dot{H}_d =& (\partial H_d)^T\,\dot{\boldsymbol{x}} \\
=& (\partial H_d)^T \begin{bmatrix} O_3 & J(q_3) \\ -J^T(q_3) & -R_p \end{bmatrix}\partial H_d \\
=& \begin{bmatrix} \left(\partial_{\boldsymbol{q}}\Psi\right)^T & \left(M^{-1}\boldsymbol{p}\right)^T \end{bmatrix}^T \begin{bmatrix} O_3 & O_3 \\ O_3 & -R_p \end{bmatrix}\begin{bmatrix} \partial_{\boldsymbol{q}}\Psi \\ M^{-1}\boldsymbol{p} \end{bmatrix} \\
=& -\,\boldsymbol{p}^T\left(M^{-1}\right)^T R_p M^{-1}\boldsymbol{p} \le 0.
\end{aligned} \tag{6.20}$$

Since $\dot{H}_d$ is negative semidefinite, equilibrium point theorems do not establish asymptotic stability of the closed loop system (6.19). However, invoking LaSalle's invariance principle, asymptotic stability can be proved.

The set of points at which $\dot{H}_d$ vanishes is

$$E_l = \{(\boldsymbol{q}, \boldsymbol{p}) : \boldsymbol{p} = 0 \text{ and } \boldsymbol{q} \text{ is free}\}. \tag{6.21}$$

The invariant points of the closed loop system (6.19) are given by

$$M_l = \{(\boldsymbol{q}^*, \boldsymbol{p}^*) : \boldsymbol{p}^* = 0 \text{ and } \boldsymbol{q}^* \text{ is such that } \partial_{\boldsymbol{q}} \Psi(\boldsymbol{q})|_{\boldsymbol{q}^*} = 0\}. \tag{6.22}$$

In case, $\boldsymbol{q}^* = 0$ is the global minimum of the function $\Psi(\boldsymbol{q})$ then the set M_l consists of only the origin $(\boldsymbol{q}^*, \boldsymbol{p}^*) = (0, 0)$. This means that the largest invariant subset M_l of E_l is a singleton set. Hence the closed loop system (6.19) converges globally asymptotically to the desired point. In case, $\boldsymbol{q}^* = 0$ is only a local minima of $\Psi(\boldsymbol{q})$ then the set M_l may consists of multiple points. The closed loop system then converges locally asymptotically to the set M_l. □

The role of the energy function in this study is similar to that of a Lyapunov function. From the Lyapunov stability theory, we know that the stability properties of a dynamical system and the minima of the Lyapunov function have a close connection. In the sequel, we explain how this connection can be exploited to improve the performance of the controllers in this study. In (6.18), we have a rather general expression for the control law depending on $\Psi(\boldsymbol{q})$. What follows are two special cases, a quadratic and a trigonometric, of the control law depending upon two different energy shapings.

6.4.1 A Quadratic Energy Shaping

The simplest function with a global minimum at the origin has a quadratic form: $\Psi(\boldsymbol{q}) = \frac{1}{2}\boldsymbol{q}^T K \boldsymbol{q}$, where $K = K^T > 0$ is a gain matrix. It is easy to see that $\boldsymbol{q} = 0$ is the only minimum of $\Psi(\boldsymbol{q})$ and the desired energy function (6.16) becomes

$$H_{d1}(\boldsymbol{q}, \boldsymbol{p}) = \frac{1}{2}\boldsymbol{q}^T K \boldsymbol{q} + \frac{1}{2}\boldsymbol{p}^T M^{-1} \boldsymbol{p}, \tag{6.23}$$

which implies, from (6.18), the following control law

$$\boldsymbol{\tau} = -J^T(q_3)(K\boldsymbol{q} + \boldsymbol{b}) - K_D J^T(q_3)\dot{\boldsymbol{q}}. \tag{6.24}$$

Using Proposition 6.4.1, we can conclude that the closed loop system (6.10) with (6.24), is globally asymptotically stable.

6.4.2 A Trigonometric Energy Shaping

Inspired by the energy function of a pendulum, we propose to shape the desired Hamiltonian containing a trigonometric function with the form

$$\Psi(\boldsymbol{q}) = \frac{1}{2}\boldsymbol{q}_{12}^T C_{12} \boldsymbol{q}_{12} + c_3(1 - \cos q_3), \tag{6.25}$$

where $\boldsymbol{q}_{12} = [q_1\ q_2]^T$, $C_{12} = \mathrm{diag}\{c_1, c_2\}$ and $c_1, c_2, c_3 > 0$. This function, has multiple local minima at $\boldsymbol{q} = (0, 0, a2\pi)$, where $a \in \mathbb{Z}$. With this choice the desired energy function (6.16) becomes

$$H_{d2}(\boldsymbol{q}, \boldsymbol{p}) = \frac{1}{2}\boldsymbol{q}_{12}^T C_{12}\boldsymbol{q}_{12} + c_3(1 - \cos q_3) + \frac{1}{2}\boldsymbol{p}^T M^{-1}\boldsymbol{p}. \tag{6.26}$$

Figure 6.2 illustrates the difference between the two proposed energy shapings (6.23) and (6.26) in terms of the level surfaces.

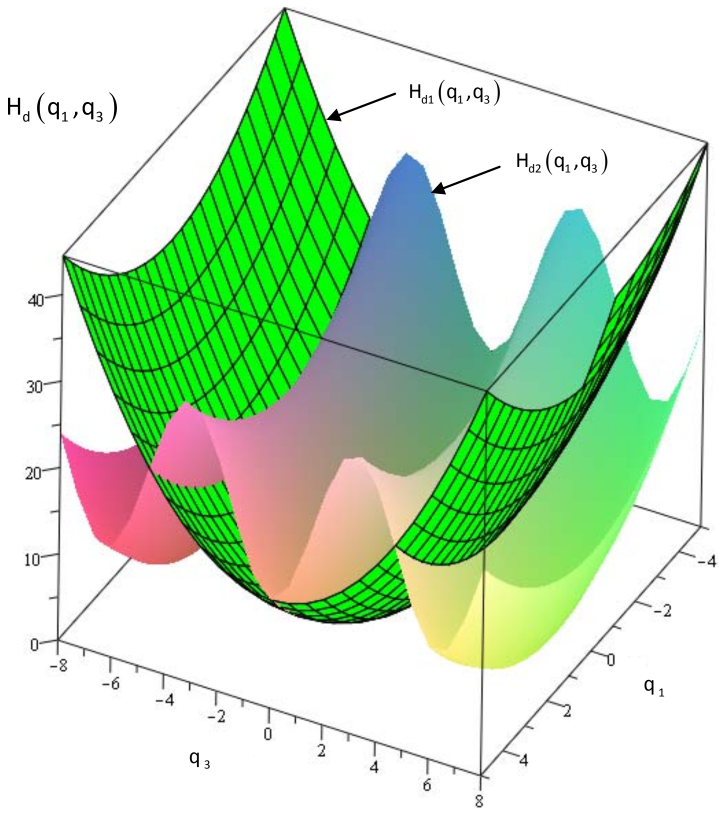

Figure 6.2: Comparison between the quadratic and the trigonometric functions, H_{d1} and H_{d2}, respectively, in the coordinates q_1 and q_3.

The main motivation for this kind of energy shaping is that, for certain applications where there are no constraints (for instance, links with external objects), stabilization in $q_3 = 0$ or $q_3 = 2\pi$ is exactly the same. Figure 6.3, shows a possible scenario, where the path for stabilizing in $q_3 = 2\pi$ is shorter than stabilizing in $q_3 = 0$.

The Hamiltonian (6.26) with the target closed loop system defined by (6.14) and

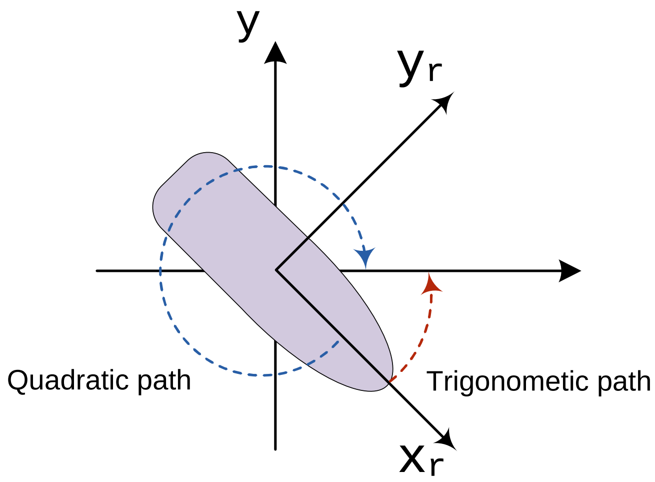

Figure 6.3: A possible scenario when it is advantageous to use the trigonometric energy function instead of the quadratic energy function.

(6.15), implies that the control law (6.18) takes the final form as

$$\boldsymbol{\tau} = -J^T(q_3)C\begin{bmatrix} q_1 \\ q_2 \\ \sin q_3 \end{bmatrix} - K_D J^T(q_3)\dot{\boldsymbol{q}} - J^T(q_3)\boldsymbol{b}, \tag{6.27}$$

where $C = \text{diag}\{c_1, c_2, c_3\}$ is a positive definite gain matrix.

As in the previous subsection, using Proposition 6.4.1, we can conclude that the closed loop system (6.10) with (6.27), is (locally) asymptotically stable.

6.5 Extended IDA-PBC Design

6.5.1 Motivating Problem

The control law (6.18) assumes that $\boldsymbol{b}$ is known and that (6.10) perfectly models the ship motion. In practical situations, the ship model only represents some simple dynamics of the actual system and furthermore the bias vector, $\boldsymbol{b}$, has to be estimated. Let us study the influence of unmodeled behaviors, wrong estimations or, in the general case, the presence of disturbances.

In order to analyze the performance of the proposed passivity-based controller, we study the following perturbed system

$$\begin{bmatrix} \dot{\boldsymbol{q}} \\ \dot{\boldsymbol{p}} \end{bmatrix} = \begin{bmatrix} O_3 & J(q_3) \\ -J^T(q_3) & -D \end{bmatrix}\partial H + \begin{bmatrix} O_3 \\ I_3 \end{bmatrix}\boldsymbol{\tau} + \begin{bmatrix} O_3 \\ J^T(q_3) \end{bmatrix}\boldsymbol{b} + \begin{bmatrix} O_3 \\ I_3 \end{bmatrix}\boldsymbol{\Delta}, \tag{6.28}$$

where $\boldsymbol{\Delta} \in \mathbb{R}^3$ is a vector which represents the disturbances. As a first approximation, and only to motivate the use of the extended dynamics, we consider this vector as a constant.

The system (6.28) in a closed loop with (6.18) results in the following system

$$\begin{bmatrix} \dot{\boldsymbol{q}} \\ \dot{\boldsymbol{p}} \end{bmatrix} = \begin{bmatrix} O_3 & J(q_3) \\ -J^T(q_3) & -R_p \end{bmatrix} \partial H_d + \begin{bmatrix} O_3 \\ I_3 \end{bmatrix} \boldsymbol{\Delta}, \tag{6.29}$$

which has an equilibrium point which satisfies $\partial\Psi|_{\boldsymbol{q}=\boldsymbol{q}^*} = J(q_3^*)\boldsymbol{\Delta}$ and $\boldsymbol{p}^* = 0$. It implies that in presence of disturbances, the closed-loop system (6.28) with control law (6.18) has a different equilibrium than $(0, 0)$. However, stability should also be further analyzed.

Moreover, in the special case where the disturbances are also affected by $J^T(q_3)$ given by

$$\begin{bmatrix} \dot{\boldsymbol{q}} \\ \dot{\boldsymbol{p}} \end{bmatrix} = \begin{bmatrix} O_3 & J(q_3) \\ -J^T(q_3) & -D \end{bmatrix} \partial H + \begin{bmatrix} O_3 \\ I_3 \end{bmatrix} \boldsymbol{\tau} + \begin{bmatrix} O_3 \\ J^T(q_3) \end{bmatrix} \boldsymbol{b} + \begin{bmatrix} O_3 \\ J^T(q_3) \end{bmatrix} \boldsymbol{\Delta}, \tag{6.30}$$

it can be seen that some stability properties still remain. With the control law (6.24), global asymptotic stability can be proved by shifting the Hamiltonian function to the new equilibrium point, i.e., with

$$\tilde{H}_{d1} = \frac{1}{2}(\boldsymbol{q} - \boldsymbol{q}^*)^T K(\boldsymbol{q} - \boldsymbol{q}^*) + \frac{1}{2}\boldsymbol{p}^T M^{-1}\boldsymbol{p} \tag{6.31}$$

as a Lyapunov function, where $q^* = K^{-1}\boldsymbol{\Delta}$. See Appendix A for more details.

Similarly, the control law (6.27) derived by using the trigonometric energy shaping in (6.30), gives the following closed-loop system

$$\begin{bmatrix} \dot{\boldsymbol{q}} \\ \dot{\boldsymbol{p}} \end{bmatrix} = \begin{bmatrix} O_3 & J(q_3) \\ -J^T(q_3) & -R_p \end{bmatrix} \begin{bmatrix} \partial_{\boldsymbol{q}} H_{d2} \\ \partial_{\boldsymbol{p}} H_{d2} \end{bmatrix} + \begin{bmatrix} O_3 \\ J^T(q_3) \end{bmatrix} \boldsymbol{\Delta}, \tag{6.32}$$

where $\partial_{\boldsymbol{q}} H_{d2} = C \begin{bmatrix} q_1 \\ q_2 \\ \sin q_3 \end{bmatrix}$ and $\partial_{\boldsymbol{p}} H_{d2} = M^{-1}\boldsymbol{p}$. The new set of equilibrium points of (6.32) is

$$\boldsymbol{q}^* = \left[\frac{\Delta_1}{c_1}, \frac{\Delta_2}{c_2}, \arcsin\left(\frac{\Delta_3}{c_3}\right) - 2k\pi\right]^T, \text{ and } \boldsymbol{p}^* = 0, \ k \in \mathbb{Z}. \tag{6.33}$$

The new set of equilibrium points (6.33) is not a set of minima of (6.26). Unlike the quadratic case, shifting of (6.26) to the new equilibrium (6.33) does not make them a set of minima of the shifted Hamiltonian function. This is because of the presence of transcendental term in (6.26). Therefore, we require another Hamiltonian function for the stability analysis of (6.32).

We seek another Hamiltonian function (energy shaping) $\tilde{H}_{d2}(\boldsymbol{q}, \boldsymbol{p})$ which has a minimum value at $(\boldsymbol{q}^*, 0)$, *i.e.*, we require

$$\partial_{\boldsymbol{q}} \tilde{H}_{d2}(\boldsymbol{q}, \boldsymbol{p})|_{\boldsymbol{q}^*} = 0, \quad \partial_{\boldsymbol{p}} \tilde{H}_{d2}(\boldsymbol{q}, \boldsymbol{p})|_{\boldsymbol{p}^*} = 0, \quad \text{and} \quad \partial^2 \tilde{H}_{d2}(\boldsymbol{q}, \boldsymbol{p})|_{(\boldsymbol{q}^*, \boldsymbol{p}^*)} > 0. \tag{6.34}$$

Let us define

$$\tilde{H}_{d2}(\boldsymbol{q},\boldsymbol{p}) = \frac{1}{2}c_1\left(q_1 - \frac{\Delta_1}{c_1}\right)^2 + \frac{1}{2}c_2\left(q_2 - \frac{\Delta_2}{c_2}\right)^2 + c_3\tilde{\psi}_3(q_3) + \frac{1}{2}\boldsymbol{p}^T M^{-1}\boldsymbol{p}, \tag{6.35}$$

where $\tilde{\psi}_3(q_3)$ is such that

$$\begin{aligned} \partial_{q_3}\tilde{\psi}_3|_{q_3^*} &= 0, \\ \Rightarrow \qquad \partial_{q_3}\tilde{\psi}_3 &= \sin q_3 - \frac{\Delta_3}{c_3}. \end{aligned}$$

Integrating both sides,

$$\tilde{\psi}_3(q_3) = -\cos q_3 - \frac{\Delta_3}{c_3}q_3 + e_1,$$

where e_1 is a constant of integration. Without loss of generality, we take $e_1 = 1$, then

$$\tilde{\psi}_3(q_3) = 1 - \cos q_3 - \frac{\Delta_3}{c_3}q_3. \tag{6.36}$$

Therefore, the new desired energy function is

$$\tilde{H}_{d2}(\boldsymbol{q},\boldsymbol{p}) = \frac{1}{2}c_1\left(q_1 - \frac{\Delta_1}{c_1}\right)^2 + \frac{1}{2}c_2\left(q_2 - \frac{\Delta_2}{c_2}\right)^2 + c_3\left(1 - \cos q_3 - \frac{\Delta_3}{c_3}q_3\right) + \frac{1}{2}\boldsymbol{p}^T M^{-1}\boldsymbol{p}. \tag{6.37}$$

The Hessian of $\tilde{H}_{d2}(\boldsymbol{q},\boldsymbol{p})$ is given by

$$\begin{aligned} \partial^2\tilde{H}_{d2} &= \begin{bmatrix} \partial^2_{\boldsymbol{q}}\tilde{H}_{d2} & \partial^2_{\boldsymbol{qp}}\tilde{H}_{d2} \\ \partial^2_{\boldsymbol{pq}}\tilde{H}_{d2} & \partial^2_{\boldsymbol{p}}\tilde{H}_{d2} \end{bmatrix} \\ &= \begin{bmatrix} \partial^2_{\boldsymbol{q}}\tilde{H}_{d2} & O_3 \\ O_3 & M^{-1} \end{bmatrix}, \end{aligned}$$

where

$$\partial^2_{\boldsymbol{q}}\tilde{H}_{d2} = \begin{bmatrix} c_1 & 0 & 0 \\ 0 & c_2 & 0 \\ 0 & 0 & c_3\cos q_3 \end{bmatrix}.$$

Using the Schur complement argument, the Hessian, $\partial^2\tilde{H}_{d2}|_{(\boldsymbol{q}^*,\boldsymbol{p}^*)}$ is positive definite *iff* $\partial^2_{\boldsymbol{q}}\tilde{H}_{d2}|_{(\boldsymbol{q}^*,\boldsymbol{p}^*)} > 0$. This requires

$$\begin{aligned} & c_3\cos q_3^* > 0, \\ \Rightarrow \qquad & c_3\cos\left(\sin^{-1}\frac{\Delta_3}{c_3}\right) > 0, \\ \Rightarrow \qquad & \sqrt{1-\left(\frac{\Delta_3}{c_3}\right)^2} > 0, \\ \Rightarrow \qquad & \frac{\Delta_3}{c_3} < 1. \end{aligned}$$

Using the LaSalle's principle, local asymptotic stability of this new set of equilibria can be proved with the Hamiltonian function

$$\tilde{H}_{d2}(\boldsymbol{q},\boldsymbol{p}) = \frac{1}{2}(\boldsymbol{q}_{12}-\boldsymbol{q}_{12}^*)^T C_{12}(\boldsymbol{q}_{12}-\boldsymbol{q}_{12}^*) + c_3\left(1-\cos q_3 - q_3\frac{\Delta_3}{c_3}\right) + \frac{1}{2}\boldsymbol{p}^T M^{-1}\boldsymbol{p}, \tag{6.38}$$

which has local minima if $\frac{\Delta_3}{c_3} < 1$. More details of this result have been explained in Appendix A. Figure 6.4 explains this condition for existence of the set of minima for the energy function (6.38).

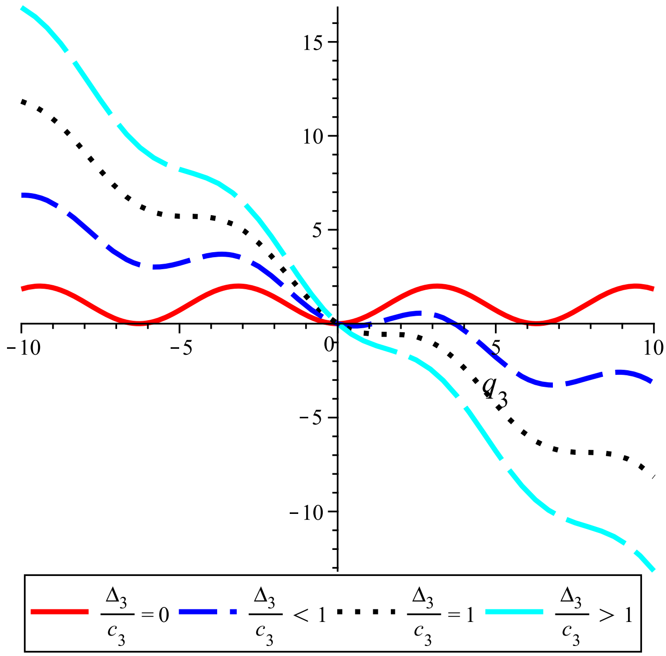

Figure 6.4: Visualization of the condition for existence of the set of minima of (6.38).

Summarizing, the presence of unknown disturbances results in a bad positioning of the ship. Although a high gain in the K and C matrices (in controllers (6.24) and (6.27), respectively) implies stabilization close to the desired equilibrium point. This may not be a rational strategy due to practical limitations of the propulsion units. This discrepancy in the desired performance of the control law motivates the use of a dynamic extension in order to achieve the stabilization at the desired point.

6.5.2 Target Extended System

In [5], it has been proved that if a system cannot be stabilized by using the classical IDA-PBC approach then it is impossible to stabilize the system by dynamic extension. This result is not restrictive in our case; our system is stabilizable but the discrepancy is that it does not stabilize to the desired equilibrium point. To overcome this drawback, we introduce an integral action by dynamic extension.

A dynamic extension for a non passive output, maintaining the port-Hamiltonian structure, is possible by means of a change of coordinates. The controller is designed for a nominal case, without disturbances, and then the presence of unknown terms is analyzed. Following the idea in [20], we introduce a new state variable, $\boldsymbol{z}_e \in \mathbb{R}^3$, which is used to enforce the equilibrium point of the closed-loop system to the desired one, and a change of variables $\boldsymbol{z} = f(\boldsymbol{q}, \boldsymbol{p}, \boldsymbol{z}_e)$. We define the target system, with the form of (6.6), as

$$\begin{bmatrix} \dot{\boldsymbol{q}} \\ \dot{\boldsymbol{z}} \\ \dot{\boldsymbol{z}}_e \end{bmatrix} = \begin{bmatrix} O_3 & J(q_3) & J(q_3) \\ -J^T(q_3) & -R_z & O_3 \\ -J^T(q_3) & O_3 & O_3 \end{bmatrix} \begin{bmatrix} \partial_{\boldsymbol{q}} H_{de} \\ \partial_{\boldsymbol{z}} H_{de} \\ \partial_{\boldsymbol{z}_e} H_{de} \end{bmatrix}, \tag{6.39}$$

where $R_z = R_z^T \geq 0$, is a 3×3 matrix to be defined. The desired Hamiltonian function is defined as

$$H_{de}(\boldsymbol{q}, \boldsymbol{z}, \boldsymbol{z}_e) = \Psi(\boldsymbol{q}) + \frac{1}{2}\boldsymbol{z}^T M^{-1} \boldsymbol{z} + \frac{1}{2}\boldsymbol{z}_e^T K_e \boldsymbol{z}_e \tag{6.40}$$

where $K_e = \text{diag}\{k_{e1}, k_{e2}, k_{e3}\} > 0$. As earlier in the classical IDA-PBC design, $\Psi(\boldsymbol{q})$ must be designed with a minimum in the desired regulation point. Then, the Hamiltonian function (6.40) has a minimum at $(\boldsymbol{q}^*, \boldsymbol{z}^*, \boldsymbol{z}_e^*) = (\boldsymbol{q}^*, 0, 0)$.

Matching the $\boldsymbol{q}$ dynamics, from (6.10) and (6.39), the change of variables $\boldsymbol{z}$ is defined as

$$\boldsymbol{z} = \boldsymbol{p} - M K_e \boldsymbol{z}_e. \tag{6.41}$$

The state feedback control law is obtained from the second row of (6.39) and the time derivative of (6.41),

$$\begin{aligned} \boldsymbol{\tau} &= -K_P J^T(q_3)\partial_{\boldsymbol{q}}\Psi - K_D M^{-1}\boldsymbol{p} + K_I \boldsymbol{z}_e - J^T(q_3)\boldsymbol{b} && (6.42) \\ \dot{\boldsymbol{z}}_e &= -J^T(q_3)\partial_{\boldsymbol{q}}\Psi && (6.43) \end{aligned}$$

where we define

$$\begin{aligned} K_P &:= (MK_e + I_3), && (6.44) \\ K_D &:= R_z - D, && (6.45) \\ K_I &:= K_e. && (6.46) \end{aligned}$$

Similarly to the classical IDA-PBC controller in the previous section, using $\boldsymbol{p} = MJ^T(q_3)\dot{\boldsymbol{q}}$, the control law (6.42)-(6.43) takes the following form

$$\boldsymbol{\tau} = -K_P J^T(q_3)\partial_{\boldsymbol{q}}\Psi - K_I \int J^T(q_3)\partial_{\boldsymbol{q}}\Psi \mathrm{d}t - K_D J^T(q_3)\dot{\boldsymbol{q}} - J^T(q_3)\boldsymbol{b} \tag{6.47}$$

which has the same structure as a nonlinear PID controller with a feed-forward term, $-J^T(q_3)\boldsymbol{b}$.

Proposition 6.5.1. *Assume that $\boldsymbol{q}$ is measurable, and that the disturbances vector $\boldsymbol{b}$ and the matrices M and D are known. If $K_e = \text{diag}\{k_{e1}, k_{e2}, k_{e3}\} > 0$, and $\Psi(\boldsymbol{q})$ has* *a (local) minimum at the origin,* $\boldsymbol{q} = 0$*, then the system (6.10) in a closed loop with (6.47), is (locally) asymptotically stable at the point* $(\boldsymbol{q}, z, z_e) = (0, 0, 0)$*.*

Furthermore, if $\boldsymbol{q} = 0$ *is a global minimum of* $\Psi(\boldsymbol{q})$*, then the origin of (6.47) is globally asymptotically stable.*

Proof. The closed-loop system (6.10) with (6.47) takes the form of (6.39). Then, the Hamiltonian function (6.40) is a Lyapunov-candidate function and its time derivative is

$$\dot{H}_{de} = -z^T \left(M^{-1}\right)^T R_z M^{-1} z \leq 0. \tag{6.48}$$

Then, the stability can be proved invoking LaSalle's invariance principle as we already show in proof of Proposition 6.4.1. □

Equation (6.47) is a rather general formulation of the control law. What follows are two special cases depending on two different formulations of the energy shaping (6.40).

6.5.3 A Quadratic Energy Shaping

Let us first take the same quadratic energy shaping as in Section 6.4, $\Psi(\boldsymbol{q}) = \frac{1}{2}\boldsymbol{q}^T K \boldsymbol{q}$ with $K = \mathrm{diag}\{k_1, k_2, k_3\} > 0$, the Hamiltonian function (6.40) becomes

$$H_{de1}(\boldsymbol{q}, z, z_e) = \frac{1}{2}\boldsymbol{q}^T K \boldsymbol{q} + \frac{1}{2} z^T M^{-1} z + \frac{1}{2} z_e^T K_e z_e. \tag{6.49}$$

with a global minimum at the origin, $(0, 0, 0)$. The control law (6.42)-(6.43) becomes

$$\begin{aligned} \boldsymbol{\tau} &= -K_P J^T(q_3) K \boldsymbol{q} + K_I z_e - K_D J^T(q_3)\dot{\boldsymbol{q}} - J^T(q_3)\boldsymbol{b} && (6.50)\\ \dot{z}_e &= -J^T(q_3) K \boldsymbol{q}. && (6.51) \end{aligned}$$

From Proposition 6.5.1 the controller (6.50)-(6.51) ensures the global asymptotic stability.

6.5.4 A Trigonometric Energy Shaping

The trigonometric energy shaping proposed in the previous section can also be considered for the extended controller. Taking again

$$\Psi(\boldsymbol{q}) = \frac{1}{2}\boldsymbol{q}_{12}^T C_{12} \boldsymbol{q}_{12} + c_3 \left(1 - \cos q_3\right), \tag{6.52}$$

where $\boldsymbol{q}_{12} = [q_1 \ q_2]^T$ and $C_{12} = \mathrm{diag}\{c_1, c_2\}$, and $c_1, c_2, c_3 > 0$ the desired Hamiltonian function (6.40) becomes

$$H_{de2}(\boldsymbol{q}, z, z_e) = \frac{1}{2}\boldsymbol{q}_{12}^T C_{12} \boldsymbol{q}_{12} + c_3 \left(1 - \cos q_3\right) + \frac{1}{2} z^T M^{-1} z + \frac{1}{2} z_e^T K_e z_e. \tag{6.53}$$

As previously mentioned, this function has multiple local minima at $\boldsymbol{q}^* = (0, 0, a2\pi)$, $a \in \mathbb{Z}$. Using Proposition 6.5.1, this case ensures local asymptotic stability, and the control law (6.42)-(6.43) becomes

$$\begin{aligned}\boldsymbol{\tau} &= -K_P J^T(q_3) C \begin{bmatrix} q_1 \\ q_2 \\ \sin q_3 \end{bmatrix} + K_I z_e - K_D J^T(q_3)\dot{\boldsymbol{q}} - J^T(q_3)\boldsymbol{b} && (6.54)\\ \dot{z}_e &= -J^T(q_3) C \begin{bmatrix} q_1 \\ q_2 \\ \sin q_3 \end{bmatrix} && (6.55)\end{aligned}$$

where $C = \text{diag}\{c_1, c_2, c_3\}$.

6.5.5 Analysis in Presence of Disturbances

The main contribution of the extended dynamics excels in the presence of unknown disturbances. As before, let us analyze the closed-loop system in the presence of disturbances. First, we consider constant (or, at least, very slow) disturbances. Taking the perturbed system (6.28) with the designed control law (6.47), we obtain

$$\begin{bmatrix} \dot{\boldsymbol{q}} \\ \dot{z} \\ \dot{z}_e \end{bmatrix} = \begin{bmatrix} O_3 & J(q_3) & J(q_3) \\ -J^T(q_3) & -R_z & O_3 \\ -J^T(q_3) & O_3 & O_3 \end{bmatrix} \begin{bmatrix} \partial_{\boldsymbol{q}}\Psi \\ M^{-1}z \\ K_e z_e \end{bmatrix} + \begin{bmatrix} O_3 \\ I_3 \\ O_3 \end{bmatrix} \boldsymbol{\Delta}. \tag{6.56}$$

From the z_e dynamics, and due to $\partial_{\boldsymbol{q}}\Psi|_{\boldsymbol{q}^*} = 0$, this system has the following equilibrium point[3]

$$\begin{aligned}\boldsymbol{q}^* &= 0 && (6.57)\\ z^* &= M R_z^{-1} \boldsymbol{\Delta} && (6.58)\\ z_e^* &= -K_e R_z^{-1} \boldsymbol{\Delta}. && (6.59)\end{aligned}$$

Notice that, contrary to the classical controller as discussed in Section 6.5.1, in the presence of unknown disturbances, the origin is still the equilibrium in the position coordinates.

The question that now arises is about the stability of (6.56). A simple stability analysis is possible using the error coordinates $\tilde{z} = z - z^*$ and $\tilde{z}_e = z_e - z_e^*$. Shifting the energy function (6.40) to the new equilibria, we get

$$\tilde{H}_{de}(\boldsymbol{q}, \tilde{z}, \tilde{z}_e) = \Psi(\boldsymbol{q}) + \frac{1}{2}\tilde{z}^T M^{-1} \tilde{z} + \frac{1}{2}\tilde{z}_e^T K_e \tilde{z}_e, \tag{6.60}$$

and (6.56) can be written as

$$\begin{bmatrix} \dot{\boldsymbol{q}} \\ \dot{\tilde{z}} \\ \dot{\tilde{z}}_e \end{bmatrix} = \begin{bmatrix} O_3 & J(q_3) & J(q_3) \\ -J^T(q_3) & -R_z & O_3 \\ -J^T(q_3) & O_3 & O_3 \end{bmatrix} \begin{bmatrix} \partial_{\boldsymbol{q}}\Psi \\ M^{-1}\tilde{z} \\ K_e \tilde{z}_e \end{bmatrix}. \tag{6.61}$$

This closed-loop system still has the desired structure (6.6), with a energy function which has a minimum at (6.57)-(6.59). The asymptotic stability is automatically guaranteed.

[3]Notice that for the case of the trigonometric controller, the equilibria become $\boldsymbol{q}^* = (0, 0, a2\pi)$.

In a more realistic case, the disturbance could be considered as a vector which depends on time, i.e., $\boldsymbol{\Delta} = \boldsymbol{\Delta}(t)$. Then, we can no longer study the stability of an equilibrium point, and we only can expect that the solution of the system becomes bounded due to the special structure of the closed-loop system, that can be seen as a forced oscillator with damping in the $\tilde{z}$ coordinates.

6.6 Simulations

In order to test the performance of the designed controllers we performed some numerical simulations. For this validation we used the data of a supply ship from [26]. The (Bis-scaled non-dimensional [24]) matrices M and D are given by

$$M = \begin{bmatrix} 1.1274 & 0 & 0 \\ 0 & 1.8902 & -0.0744 \\ 0 & -0.0744 & 0.1278 \end{bmatrix}$$

and

$$D = \begin{bmatrix} 0.0358 & 0 & 0 \\ 0 & 0.1183 & -0.0124 \\ 0 & -0.0124 & 0.0308 \end{bmatrix}.$$

The bias vector has been set to $\boldsymbol{b} = [0.05, 0.05, 0.01]^T$. For all simulations, we considered that the initial conditions of the ship are $(q_1, q_2) = (-10, -10)$, and the heading angle $q_3 = 4$ rad, and the desired stabilization position is the origin. The desired heading direction is along the positive x-axis. More generally, the starting heading angle is set greater than π to show the ability of the so-called trigonometric controller to stabilize to the closer minimum, in this case 2π.

6.6.1 Simulation Results for the classical IDA-PBC design

In this subsection, we present the simulation results for the classical (quadratic and trigonometric) control laws (6.24) and (6.27), respectively. The gain matrices we used are $K = C = \text{diag}\{0.05, 0.05, 0.01\}$ and $R_p = \text{diag}\{0.75, 0.75, 0.1\}$. Precisely, for this system, we enlarged the damping (about one order of magnitude in the first and third components), to improve the performance. In Figure 6.5 we show the trajectories of the same classical controller (the quadratic case) with extra dissipation, setting R_p to the values proposed before, and keeping the original damping, $R_p = D$. This comparison justifies the use of the extra damping to obtain more suitable paths.

Figure 6.6 shows the trajectories of the position coordinates q_1 and q_2, and the heading angle, q_3, of the quadratic and the trigonometric versions. Both controllers stabilize the ship at the desired position and angle. The notable point is the difference in the orientation profiles. While the quadratic controller stabilizes the heading angle at $q_3 = 0$, the trigonometric controller does so at $q_3 = 2\pi$.

Figure 6.7 compares the trajectories in the q_1q_2-plane for two versions of the classical IDA-PBC design. In both cases, the performance is similar but, even though the controllers for the q_1 and q_2 coordinates are the same (with the same gain values),

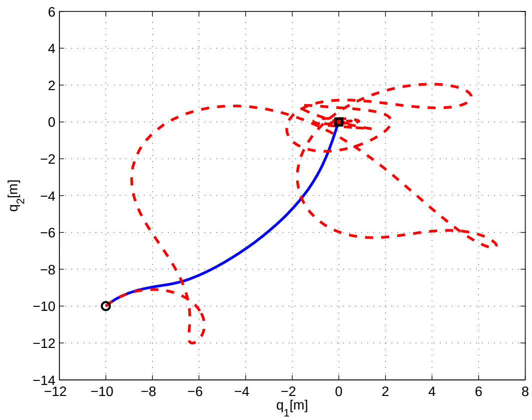

Figure 6.5: Simulation results: ship position trajectories in the q_1, q_2 plane, for the classical IDA-PBC (quadratic controller) design with extra damping (solid line) and the original damping coefficient (dashed line).

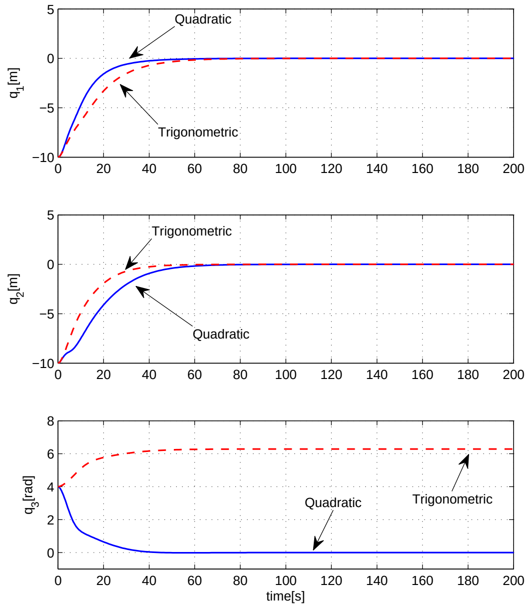

Figure 6.6: Simulation results: ship position coordinates, q_1 and q_2, and heading angle, q_3, for the quadratic (solid line) and trigonometric (dashed line) controllers of the classical IDA-PBC design.

the trajectories take different paths. This fact is associated with the different heading angle trajectories.

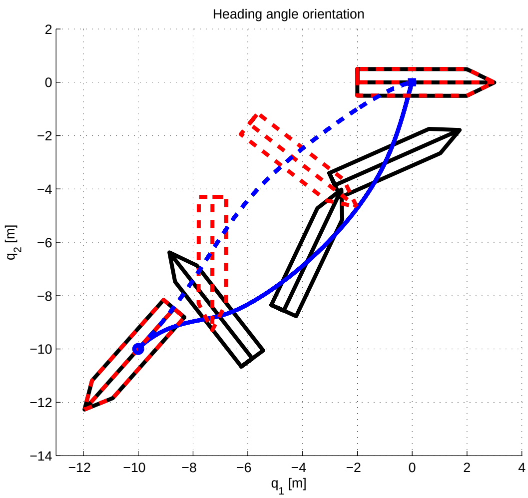

Figure 6.7: Simulation results: ship position trajectories in the q_1q_2-plane, for the quadratic (solid line) and trigonometric (dashed line) controllers of the classical IDA-PBC design together with the respective heading orientation.

6.6.2 Simulation Results in Presence of Disturbances

In this subsection, we present the simulation results in the presence of disturbances. The key point is to show that the controllers from the extended IDA-PBC design approach are able to reject unknown terms. For this scenario we assume that the disturbance due to the bias term, $\boldsymbol{b}$, is not available. Consequently, the feed-forward term, $J^T(q_3)\boldsymbol{b}$, is removed in all the tested controllers. The gain matrices for the classical controllers, (6.24) and (6.27), are the same as in the previous subsection. The corresponding gain matrices used for the controllers from extended IDA-PBC design, (6.51) and (6.55), are $R_z = \text{diag}\{0.75, 0.75, 0.4\}$, $K = C = \text{diag}\{0.05, 0.05, 0.025\}$ and $K_e = \text{diag}\{0.01, 0.01, 0.015\}$.

In Figure 6.8, $\boldsymbol{q}$ trajectories for the four controllers are plotted. Clearly the controllers from IDA-PBC design steer the ship to the desired equilibrium position while the controllers from the classical IDA-PBC design fails to do so and have a steady state error. This difference between the performance of both the controllers can also be seen from the respective trajectory profiles. See Figure 6.9.

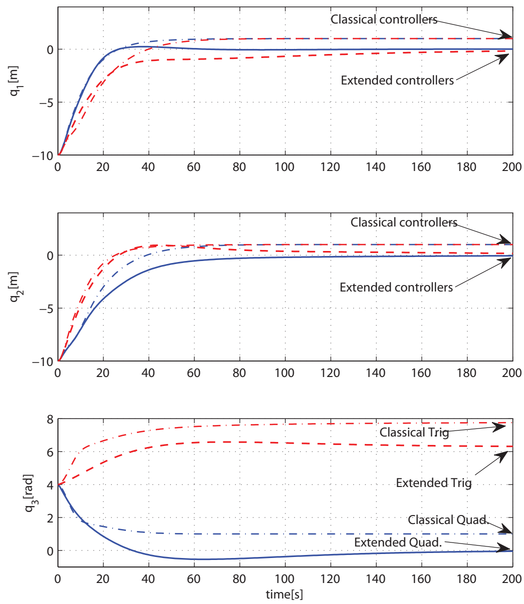

Figure 6.8: Simulation results: ship position coordinates, q_1 and q_2, and heading angle, q_3, for the both the quadratic and trigonometric versions of the controllers from the classical and extended IDA-PBC designs.

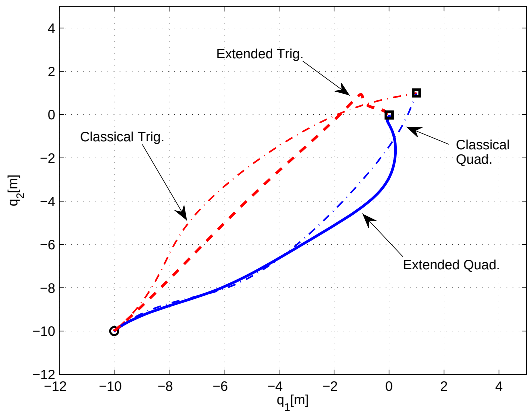

Figure 6.9: Simulation results: ship position trajectories in the q_1, q_2 plane, for the both the quadratic and trigonometric versions of the controllers from the classical and extended IDA-PBC designs.

6.7 Conclusions

A passivity-based approach called IDA-PBC is used to obtain a set of output feedback controllers for the dynamic positioning of a ship. This methodology is based on the port-Hamiltonian description which gives a physical interpretation of the dynamical systems. Under this point of view, the controller design problem is addressed as to shape the energy function of the closed loop system. After a general formulation we propose two different controllers: first with a quadratic energy function and second, inspired by the physics of a pendulum, with a trigonometric energy function. Also, the presence of disturbances is studied and it turns out that the control laws obtained by using the classical IDA-PBC methodology, do not stabilize the system at the desired position. This discrepancy is the starting point for a second set of controllers which consist of a dynamic extension of the system which provides stability at the desired regulation point, also in presence of disturbances. Simulations are done to validate and compare the performance of the controllers designed.

It is worth mentioning that the obtained control laws, with a general form of state feedback, can be easily converted to output feedback algorithms that only require the position measurement. Furthermore, they exhibit a simple structure that can be interpreted as non-linear versions of PID controllers. An important observation is that the trigonometric energy shaping improves the heading angle control. We also observe that by keeping the differential term, which physically increases the damping effect, in the controller formulation helps in getting a smoother trajectory profile.

Future work can be aimed at determining other energy functions, $\Psi(\boldsymbol{q})$, to improve the performance, as well as to consider the optimization of the resulting path. Further analysis depending on the nature of the disturbance vector (including the wave frequency and wind models) is required. Also, this work could be a starting point for a new design, using the port-Hamiltonian perspective, of the complete motion-control system (controller and observer) for a DP problem.

Chapter 7

Conclusions and Recommendations for Future Work

In this chapter, we summarize the main conclusions of this work and present some recommendations for future work based on our knowledge and experiences acquired during the process of reaching to this point. The first major topic studied in this thesis is the stability analysis of a special type of nonlinear system in which nonlinearity appears only in the dynamics of a single state variable. The study is based on the SDC framework which transforms the nonlinear system in a pseudo-linear form with a state dependent system matrix. The stability analysis of such systems is based on the properties of the system matrix. From the perspective of the DP system we are interested in the asymptotic behavior of the system. The local asymptotic stability of the system is easy to establish, the major concern always remains the analysis of the global asymptotic stability.

From the first counterexample discussed in Section 3.4.1, we can conclude that the conditions that the system matrix is continuous, pointwise Hurwitz, and exponentially bounded are not sufficient to ascertain the global asymptotic stability of the pseudo-linear system. In the prototype vessel model, the system matrix is a periodic function of the heading angle of the vessel. The periodicity assumption also ensures that the states of the system are bounded, *i.e.*, they will not blow up at finite time. Further research has proved that the extended set of conditions that the system matrix is continuous, pointwise Hurwitz, exponentially bounded, and periodic does not constitute the set of sufficient conditions for the global asymptotic stability of the pseudo-linear system. This fact is explained in the second counterexample presented in Section 3.5.1. This study concludes that more research is required to explore the set of sufficient conditions which establish the global asymptotic stability of the pseudo-linear systems with a system matrix depending on a single state variable.

The periodicity property of the vessel model has lured us to combine the Lyapunov stability theory with the LMIs to come up with a new approach to prove the global asymptotic stability of the pseudo-linear system which has a periodic system matrix. This approach has proved successful to establish the global asymptotic stability of the vessel model, in particular. Further research is required to investigate the additional features like for instance, the best solutions of the LMI feasibility problem, the impact of the number of LMIs on the solutions of the LMI feasibility problem, conditions for existence and non-existence of the solutions of the LMI feasibility problem, etc.

We present the SDARE technique for control design of the vessel model. The design objective is to stabilize the vessel at the desired equilibrium point. The SDARE technique gives a state feedback controller which means that the complete state of the system should be known. This is not the case for the vessel model in this work as only the noisy position and heading measurements are available through sensors (GPS and gyro). So it is required to estimate the remaining states of the vessel model. We have also used the SDARE technique to address the estimation problem. The SDARE technique has many characteristic features. It addresses the performance of the controller and the observer by specifying a performance index. The state and the control weights can be adjusted to influence the performance. For instance, an increase in the state weighting matrix Q results in a faster regulation of the vessel at the expense of a greater control effort. Generally, the SDC parametrization is not unique and this feature offers an extra degree of freedom for design and performance improvements. While the technique offers ways to use the results from linear system theory, it maintains the nonlinear character of the system which is not the case in linearization methods like the extended Kalman filter (EKF) etc.

The simulation results show promising performance of the SDARE technique when applied to address the regulation problem of a DP vessel. The controller and the observer gains can be tuned by using the weighting matrices, to obtain the desired performance. This study is limited to the regulation problem of the DP vessel. An extension of the SDARE technique to address the path following and trajectory tracking problems of the DP vessel remains still an open research topic.

We present the FSI method which is a fast solution method for the specific type of the SDARE associated with a pseudo-linear system whose system matrix depends on a single state variable in a periodic way. This method is based on the Fourier series and involves the concept of interpolation. The emphasis of the FSI method is on offline computation of the Fourier series coefficients. It has been shown that it makes the online computation of the solution of the SDARE faster by reducing the online computations. The method is particularly useful for the systems having a small time constant or fast dynamic response. For such systems, the actuators are required to have a faster dynamic response than the system they are controlling. The method was motivated by the periodicity of the pseudo-linear vessel model. The vessel system in this work is a slow system (with a large time constant), the FSI method has shown good results in comparison with the MATLAB routine “care” which uses the Schur decomposition to solve the SDARE. This work is limited to just one application of the FSI method on the vessel model. The search for more applications of the FSI method on physical systems is still open for future research.

In this work, the use of the port-Hamiltonian system formulation to study the control design problem of the DP vessel has revealed some important and interesting features. The Hamiltonian (storage) function is a powerful component in this formulation. We have seen that it not only simplifies the stability analysis but also offers more options to improve the performance of the controller. This can be done by using different formulations of the Hamiltonian function to design different controllers. The performance of the controllers can then be analyzed to see which one suits the desired performance objective. This fact is clear from the trigonometric and quadratic formulations of the Hamiltonian function. A better heading control of the vessel is obtained from the trigonometric controller than the quadratic controller.

The dissipation (damping) matrix in the desired dynamics in the IDA-PBC design technique is very important from the perspective of the tuning of the controller gain matrices. It makes it possible to manipulate the damping of the system. Through the controller action, we can increase the damping of the system and it eventually helps us to steer the vessel along a stable and smooth trajectory.

This study addresses only the regulation problem with passivity based approach using the port-Hamiltonian formulation. With the encouraging results obtained, the possible extension of this concept to address more involved problems like path following, trajectory tracking, and state estimation is a challenging and interesting topic for future research.

Appendix A

Proof of Asymptotic Stability of (6.32) at (6.33)

The objective is to show that (6.33) is an asymptotically stable equilibrium point of the perturbed closed loop system (6.32). For convenience of the reader, we recall both equations mentioned above.

$$\begin{bmatrix} \dot{\boldsymbol{q}} \\ \dot{\boldsymbol{p}} \end{bmatrix} = \begin{bmatrix} O_3 & J(q_3) \\ -J^T(q_3) & -R_p \end{bmatrix} \begin{bmatrix} \partial_{\boldsymbol{q}} H_{d2} \\ \partial_{\boldsymbol{p}} H_{d2} \end{bmatrix} + \begin{bmatrix} O_3 \\ J^T(q_3) \end{bmatrix} \boldsymbol{\Delta}, \tag{A.1}$$

where

$$H_{d2}(\boldsymbol{q}, \boldsymbol{p}) = \frac{1}{2}\boldsymbol{q}_{12}^T C_{12} \boldsymbol{q}_{12} + c_3(1 - \cos q_3) + \frac{1}{2}\boldsymbol{p}^T M^{-1} \boldsymbol{p}. \tag{A.2}$$

The equilibrium point of (A.1) is given by

$$\boldsymbol{q}^* = \begin{bmatrix} \frac{\Delta_1}{c_1} & \frac{\Delta_2}{c_2} & \arcsin\left(\frac{\Delta_3}{c_3}\right) - 2k\pi \end{bmatrix}^T, \text{ and } \boldsymbol{p}^* = 0,\ k \in \mathbb{Z}. \tag{A.3}$$

To prove the above mentioned asymptotic stability, we proceed as follows. Let us consider the following closed loop system.

$$\begin{bmatrix} \dot{\tilde{\boldsymbol{q}}} \\ \dot{\tilde{\boldsymbol{p}}} \end{bmatrix} = \begin{bmatrix} O_3 & J(q_3) \\ -J^T(q_3) & -R_p \end{bmatrix} \begin{bmatrix} \partial_{\tilde{\boldsymbol{q}}} \tilde{H}_{d2} \\ \partial_{\tilde{\boldsymbol{p}}} \tilde{H}_{d2} \end{bmatrix}, \tag{A.4}$$

where $\tilde{\boldsymbol{q}} = \begin{bmatrix} q_1 - q_1^* \\ q_2 - q_2^* \\ q_3 \end{bmatrix}$, $\tilde{\boldsymbol{p}} = \boldsymbol{p}$, and

$$\tilde{H}_{d2}(\tilde{\boldsymbol{q}}, \tilde{\boldsymbol{p}}) = \frac{1}{2}\tilde{\boldsymbol{q}}_{12}^T C_{12} \tilde{\boldsymbol{q}}_{12} + c_3\left(1 - \cos q_3 - \frac{\Delta_3}{c_3} q_3\right) + \frac{1}{2}\tilde{\boldsymbol{p}}^T M^{-1} \tilde{\boldsymbol{p}}. \tag{A.5}$$

As a first step, we use the LaSalle's invariance principle to prove asymptotic stability of (A.4). The energy function (A.5) is a scalar valued function and its first partial derivatives exist. Differentiating it w.r.t 't', we get

$$
\begin{aligned}
\dot{\tilde{H}}_{d2} &= \left(\partial \tilde{H}_{d2}\right)^T \dot{\tilde{\boldsymbol{x}}} \\
&= \left(\partial \tilde{H}_{d2}\right)^T \begin{bmatrix} O_3 & J(q_3) \\ -J^T(q_3) & -R_p \end{bmatrix} \partial \tilde{H}_{d2} \\
&= -\, \tilde{\boldsymbol{p}}^T \left(M^{-1}\right)^T R_p M^{-1} \tilde{\boldsymbol{p}} \leq 0,
\end{aligned}
\tag{A.6}
$$

where $\tilde{\boldsymbol{x}} = \begin{bmatrix} \tilde{\boldsymbol{q}} \\ \tilde{\boldsymbol{p}} \end{bmatrix}$. The set of points where $\dot{\tilde{H}}_{d2} = 0$ is given by

$$
\begin{aligned}
E_l =& \{\tilde{x} \in \mathbb{R}^6 : \dot{\tilde{H}}_{d2} = 0\} \\
=& \{\tilde{\boldsymbol{p}} = 0 \text{ and } \tilde{\boldsymbol{q}} \text{ is free}\}.
\end{aligned}
\tag{A.7}
$$

The equilibrium (invariant) points of (A.4) are

$$
\tilde{\boldsymbol{q}}^* = [\tilde{q}_1, \tilde{q}_2, \tilde{q}_3]^T = \left[0, 0, \arcsin(\frac{\Delta_3}{c_3}) - 2k\pi\right]^T, \text{and } \boldsymbol{p}^* = 0,\ k \in \mathbb{Z}. \tag{A.8}
$$

The largest invariant subset M_l of E_l consists of the equilibrium points (A.8). Hence, LaSalle's invariance principle implies that the closed loop system (A.4) converges locally asymptotically to either one of the equilibrium points.

As second step, we show that both the closed loop systems (A.1) and (A.4) are equivalent. It is a straightforward observation that $\tilde{\boldsymbol{q}}$ and $\boldsymbol{q}$ have the same dynamics. We show the equivalence of the dynamics of $\tilde{\boldsymbol{p}}$ and $\boldsymbol{p}$.

$$
\begin{aligned}
\dot{\tilde{\boldsymbol{p}}} &= -\, J^T(q_3)\partial_{\tilde{\boldsymbol{q}}}\tilde{H}_{d2} - R_p \partial_{\tilde{\boldsymbol{p}}}\tilde{H}_{d2} \\
&= -\, J^T(q_3)\partial_{\boldsymbol{q}} H_{d2} - R_p \partial_{\boldsymbol{p}} H_{d2} + J^T(q_3)\Delta \\
&= \dot{\boldsymbol{p}}.
\end{aligned}
\tag{A.9}
$$

Hence, (A.1) and (A.4) are equivalent. This implies that if (A.8) is an asymptotically stable equilibrium point of (A.4) then (A.3) is an asymptotically stable equilibrium point of (A.1).

Similarly, asymptotic stability of

$$
\begin{bmatrix} \dot{\boldsymbol{q}} \\ \dot{\boldsymbol{p}} \end{bmatrix} = \begin{bmatrix} O_3 & J(q_3) \\ -J^T(q_3) & -R_p \end{bmatrix} \begin{bmatrix} \partial_{\boldsymbol{q}} H_{d1} \\ \partial_{\boldsymbol{p}} H_{d1} \end{bmatrix} + \begin{bmatrix} O_3 \\ J^T(q_3) \end{bmatrix} \boldsymbol{\Delta}, \tag{A.10}
$$

where

$$
H_{d1}(\boldsymbol{q}, \boldsymbol{p}) = \frac{1}{2}\boldsymbol{q}^T C \boldsymbol{q} + \frac{1}{2}\boldsymbol{p}^T M^{-1} \boldsymbol{p}. \tag{A.11}
$$

w.r.t. the equilibrium point $(\boldsymbol{q}^*, \boldsymbol{p}^*) = (-K^{-1}\Delta, 0)$ follows. The asymptotic stability in this case will be global because the point $(\boldsymbol{q}^*, \boldsymbol{p}^*) = (-K^{-1}\Delta, 0)$ is global minimum of the shifted Hamiltonian function associated with (A.11).

Appendix B

Glossary

This appendix contains definitions and additional details of some notions used in this thesis.

BIS-Scaling

Scaling is done to normalize the vessel steering equations of motion. This helps to study the scaled models of the vessel and then compare and analyze the performance of the full scale vessel models. This idea is more economical both in terms of time and money, than doing the full scale experiments in the sea. There are two main methods of scaling: the *Prime-system* of SNAME introduced in 1950 and the *Bis-system* introduced in 1970 by Norrbin. The Prime-system uses the instantaneous velocity to normalize the time unit. Therefore, it is not used for the DP vessels or other low speed applications.

The Bis-system uses the length unit L_{pp} (length between fore and aft perpendiculars), body mass density ratio $\mu = \frac{m}{\rho\nabla}$, and the time unit $\sqrt{\frac{L_{pp}}{g}}$ as the basic scaling parameters. The parameters μ, ρ, ∇, and g represent the level of buouncy, mass density of the fluid, hull contour displacement, and acceleration due to gravity, respectively. The scaling parameters for other variables like velocity, acceleration, etc. can be found in terms of these basic scaling parameters.

First order wave-induced forces

First order wave-induced wave forces (loads or disturbances) are forces whose magnitude is proportional to the wave height and their frequency is the same as that of the incident waves. These forces are also called WF forces (disturbances or loads).

Gaussian white noise process

In Chapter 2, we have mentioned that the process and measurement uncertainties are stationary Gaussian random white noise process. For the convenience of the reader, some details of this concept are presented here. The vector $\boldsymbol{w}(t) = \begin{bmatrix} w_1(t) \\ w_2(t) \\ w_3(t) \end{bmatrix}$ consists of three uncorrelated independent Gaussian white noise processes: $w_1(t)$, $w_2(t)$, and $w_3(t)$. This implies the mean

$$E(w(t)) = 0, \tag{B.1}$$

and covariance

$$E\left(w(t)w^T(s)\right) = W\delta(t-s). \tag{B.2}$$

The δ in (B.2) represents the Dirac delta (or continuous time impulse response) function and is given by

$$\delta(t-s) = \begin{cases} \infty & \text{if } t = s \\ 0 & \text{if } t \neq s \end{cases} \tag{B.3}$$

Kronecker Product

Let $A \in \mathbb{R}^{m \times n}$ and $B \in \mathbb{R}^{p \times q}$. Then the Kronecker (direct or tensor) product of A and B is defined as the matrix

$$A \otimes B = \begin{bmatrix} a_{11}B & \cdots & a_{1m}B \\ \vdots & \ddots & \vdots \\ a_{m1}B & \cdots & a_{mn}B \end{bmatrix} \in \mathbb{R}^{mp \times nq}. \tag{B.4}$$

LaSalle's Invariance Theorem (Principle)

An important result in stability theory which was independently formulated by N. N. Krasovskii and E. A. Barbashin in Russian in 1959, see [11] for its translated version in English, and by J. P. LaSalle in 1960, see [48]. It is stated as follows

"Let $\Omega_0 \subset \Omega$ be a compact set that is positively invariant with respect to (3.2). Let $V : \Omega \longrightarrow \mathbb{R}$ be a continuously differentiable function such that $\dot{V}(\boldsymbol{x}) \leq 0$ in Ω_0. Let E be the set of all points in Ω_0 where $\dot{V}(\boldsymbol{x}) = 0$. Let M be the largest invariant set in E. Then every solution starting in Ω_0 approaches M as $t \to \infty$."

Second order wave-induced forces

Second order wave-induced wave forces (loads or disturbances) are forces whose magnitude is proportional to the square of the wave height. These forces are also called LF forces (disturbances or loads).

Bibliography

[1] M. F. Aarset, J. P. Strand, and T. I. Fossen. Nonlinear vectorial observer backstepping with integral action and wave filtering for ships. Proceedings of IFAC Conference on Control Applications in Marine Systems CAMS'98, October 20-27, 1998, Fukuoka, Japan.

[2] T. Acarman. Nonlinear optimal integrated vehicle control using individual braking torque and steering angle with on-line control allocation by using state-dependent Riccati equation technique. *Vehicle Sysytem Dynamics*, 47(2):155–177, 2009.

[3] B. D. O. Anderson. Second-order convergent algorithms for the steady-state Riccati equation. *International Journal of Control*, 28(2):295–306, 1978.

[4] A. Astolfi, D. Chhabra, and R. Ortega. Asymptotic stabilization of some equilibria of an underactuated underwater vehicle. *Systems & Control Letters*, 45(3):193–206, 2002.

[5] A. Astolfi and R. Ortega. Dynamic extension is unnecessary for stabilization via interconnection and damping assignment passivity-based control. *Systems & Control Letters*, 58(2):133–135, 2009.

[6] J. G. Balchen, N. A. Jenssen, and S. Sælid. Dynamic positioning using kalman filtering and optimal control theory. pages 183–186. Proceedings of IFAC/IFIP Symposium on Automation in Offshore Oil Field Operation,ly 6-11, 2008, Amsterdam, The Netherlands.

[7] H. T. Banks, B. M. Lewis, and H. T. Tran. Nonlinear feedback controllers and compensators: a state-dependent Riccati equation approach. *Computational Optimization and Applications*, 37(2):177–218, 2007.

[8] S. P. Banks and K. J. Mhana. Optimal control and stabilization of nonlinear systems. *IMA Journal of Mathematical Control and Information*, 9(3):179–196, 1992.

[9] P. Benner and R. Byers. An exact line search method for solving generalized contineous-time algebraic Riccati equation. *IEEE Transactions on Automatc Control*, 43(1):101–107, 1998.

[10] W. E. Boyce and R. C. DiPrima. *Elementary Differential Equations and Boundary Value Problems*. John Wiley & Sons, Inc., Eighth edition, 2004.

[11] J. L. Brenner. *Stability of Motion*. Stanford University Press, First edition, 1963.

[12] T. Çimen. State dependent Riccati equation control: A survey. pages 3761–3775. Proceedings of the International Federation of Automatic Control (IFAC) World Congress, July 6-11, 2008, Seoul, South Korea.

[13] E. K. W. Chu, H. Y. Fan, and W. W. Lin. A structure preserving doubling algorithm for continuous-time algebraic Riccati equations. *Linear Algebra and its Applications*, 396:55–80, 2005.

[14] J. R. Cloutier. State dependent Riccati equation technique: an overview. pages 932–936. Proceedings of American Control Conference, June 4-6, 1997, New Mexico, USA.

[15] B. N. Datta. *Numerical Methods for Linear Control Systems*. Elsevier Academic Press, 2003.

[16] D. F. Delchamps. Analytic feedback control and the algebraic Riccati equation. *IEEE Transactions on Automatic Control*, 29(11):1031–1033, 1984.

[17] D. E. Denman and A. N. Beavers Jr. The matrix sign function and computations in systems. *Applied Mathematics and Computations*, 2(1):63–94, 1976.

[18] L. Dieci. Some numerical considertions and Newton's method revisited for solving algebraic Riccati equations. 36(5):608–616, 1991.

[19] K. D. Do and J. Pan. *Control of Ships and Underactuated Vehicles*. Springer, 2009.

[20] A. Donaire and S. Junco. On the addition of the integral action to port-controlled Hamiltonian systems. *Automatica*, 45(8):1910–1916, 2009.

[21] A. Dòria-Cerezo. *Modeling, Simulation and Control of a Doubly-Fed Induction Machine Controlled by a Back-to-Back Converter*. PhD thesis, Univesitat Politècnica de Catalunya, Barcelona, Spain, 2006.

[22] O. M. Faltinsen. *Hydrodynamics of High Speed Marine Vehicles*. Cambridge University Press, 2005.

[23] H. Faÿ. *Dynamic Positioning Systems: Principles, Design and Applications*. Ēditions Technip, 1990.

[24] T. I. Fossen. *Guidance and Control of Ocean Vehicles*. John Wiley & Sons, Inc., 1994.

[25] T. I. Fossen. *Marine Control Systems: Guidance, Navigation and Control of Ships, Rigs and Underwater Vehicles*. John Wiley & Sons, Inc., 2002.

[26] T. I. Fossen and Å. Grøvlen. Nonlinear output feedback control of dynamically positioned ships using vectorial observer backstepping. *IEEE Transactions on Control Systems Technology*, 6(1):121–128, 1998.

[27] T. I. Fossen and T. Perez. Kalman filtering for positioning and heading control of ships and offshore rigs. *IEEE Control Systems Magazine*, 29(6):32–46, 2009.

[28] T. I. Fossen, S. I. Sagatun, and A. J. Sørensen. Identification of dynamically positioned ships. *Modeling, Identification, and Control*, 17(2):153–165, 1996.

[29] T. I. Fossen and J. P. Strand. Passive nonlinear observer design for ship using Lyapunov methods: Full-scale experiments with a supply vessel. *Automatica*, 35(1):3–16, 1999.

[30] T-K. P. Fung and M. J. Grimble. Dynamic ship positioning using a self-tuning Kalman filter. *IEEE Transactions on Automatic Control*, 28(3):339–350, 1983.

[31] W. L. Garrard and J. M. Jordan. Design of nonlinear automatic flight control systems. *Automatica*, 13(5):497–505, 1977.

[32] H. Giacomini, J. Llibr, and M. Viano. On the nonexistence, existence, and uniqueness of limit cycles. *Nonlinearity*, 9(2):501–516, 1996.

[33] G. Golub and C. F. Van Loan. *Matrix Computations*. The Johns Hopkins University Press, Baltimore, USA, Third edition, 1996.

[34] M. J. Grimble, R. J. Patton, and D. S. Wise. Use of Kalman filtering techniques in dynamic ship-positioning systems. *IEE Proceedings*, 127(3):93–102, 1980.

[35] R. Haberman. *Elementary Applied Partial Differenrial Equations With Fourier Series and Boundary Value Problems*. Prentice Hall.

[36] K. D. Hammett, C. D. Hall, and D. B. Ridgely. Controllability issues in nonlinear state dependent Riccati equation control. *Journal of Guidance, Control, and Dynamics*, 21(5):767–773, 1998.

[37] A. D. Hansen. *Predictive Controller Design and Identification in Connection with Steering Dynamics*. PhD thesis, Technical University of Denmark, Denmark, 1996.

[38] D. Hill and P. J. Moylan. The stability of nonlinear dissipative systems. *IEEE Transactions on Automatic Control*, 21(5):708–711, 1976.

[39] K. Hiramoto, H. Doki, and G. Obinata. Optimal sensor/actuator placement for active vibration control using explicit solution of algebraic Riccati equation. *Journal of Sound and Vibration*, 229(5):1057–1075, 2000.

[40] J. Imae, H. Sagami, T. Kobayashi, and G. zhai. Nonlinear control design method based on state-dependent Riccati equation SDRE via quasi-newton method. Proceedings of the 43rd IEEE Conference on Decision and Control, December 14-17, 2004, Atlantis, The Bahamas.

[41] R. E. Kalman. Contributions to the theory of optimal control. *Boletin Sociedad Matemática Mexicana*, 5:102–119, 1960.

[42] H. Katayama. Nonlinear sampled-data stabilization of dynamically positioned ships. *IEEE Transactions on Control Systems Technology*, 18(2):463–468, 2010.

[43] H. K. Khalil. *Nonlinear Systems*. Prentice Hall, Third edition, 2002.

[44] M. Kimura. Doubling algorithm for continuous-time algebraic Riccati equation. *International Journal of Systems Science*, 20(2):191–202, 1989.

[45] V. Lakshmikantham, V. M. Matrosov, and S. Sivasundaram. *Vector Lyapunov Functions and Stability Analysis of Nonlinear Systems*. Kluwer, 1991.

[46] W. Langson. Optimal and suboptimal control of a class of nonlinear systems. Master's thesis, Graduate College of the University of Illinois Urbana-Champaign, USA, November 1997.

[47] W. Langson and A. Alleyne. A stability result with application to nonlinear regulation. *Journal of Dynamic Systems, Measurement, and Control*, 124(3):452–456, 2002.

[48] J. P. LaSalle. Some extensions of liapunov's second method. *IRE Transactions on Circuit Theory*, CT-7(4):520–527, 1960.

[49] A. Laub. A Schur method for solving algebraic Riccati equations. *IEEE Transactions on Automatic Control*, 24(6):913–921, 1979.

[50] J. Löfberg. YALMIP: A toolbox for modeling and optimization in MATLAB. Proceedings of the CACSD Conference, September 2-4, 2004, Taipei, Taiwan.

[51] A. Loria, T. I. Fossen, and E. Panteley. A separation principle for dynamic positioning of ships: theoretical and experimental results. *IEEE Transactions on Control Systems Technology*, 8(2):332–344, 2000.

[52] P. K. Menon, T. M. Lam, L. S. Crawford, and V. H. L. Cheng. Real time computational methods for SDRE nonlinear control of missiles. Proceedings of the American Control Conference Workshop, May 8-10, 2002, Anchorage, AK, USA.

[53] P. J. Moylan. Implications of passivity in a class of nonlinear systems. *IEEE Transactions on Automatic Control*, AC-19(4):373–381, 1974.

[54] C. P. Mracek and J. R. Cloutier. Control designs for the non-linear benchmark problem via the state dependent Riccati equation method. *International Journal of Robust Nonlinear Control*, 8(4-5):401–433, 1998.

[55] S. Muhammad and A. Dòria-Cerezo. Output feedback passivity based controllers for dynamic positioning of ships. Proceedings of Dynamic Positioning Conference, October 12-13, 2010, Houston, USA.

[56] S. Muhammad and A. Dòria-Cerezo. Passivity-based control applied to the dynamic positioning of ships. *IET Control Theory and Applications*, Accepted for Publication.

[57] S. Muhammad and J. W. van der Woude. The Fourier series interpolation method for the solution of the SDARE. Proceedings of the UKACC International Conference on Control (CONTROL 2010), September 7-10, 2010, Coventry, UK.

[58] S. Muhammad and J. W. van der Woude. A counter example to a recent result on the stability of nonlinear systems. *IMA Journal of Mathematical Control and Information*, 26(3):319–323, 2009.

[59] S. Muhammad and J. W. van der Woude. On stability conditions for systems with periodic state dependent coefficients: a counter example. *IMA Journal of Mathematical Control and Information*, 28(1):97–102, 2011.

[60] G. J. Olsder and J. W. van der Woude. *Mathematical Systems Theory*. VSSD, Third edition, 2005.

[61] R. Ortega, M. Galaz, A. Bazanella, and A. Stankovic. An energy-shaping approach to excitation control of synchronous generators. Proceedings of the American Control Conference, June 25-27, 2001, Arligton, VA, USA.

[62] R. Ortega and E. Garcí-Canseco. Interconnection and damping assignment passivity-based control: A survey. *European Journal of Control*, 10(5):432–450, 2004.

[63] R. Ortega and M. Spong. Adaptive motion control of rigid robots: A tutorial. *Automatica*, 25(6):877–888, 1989.

[64] R. Ortega, M. W. Spong, F. Gómez-Estern, and F. Blankenstein. Interconnection and damping assignment passivity-based control of port-controlled Hamiltonian systems. *IEEE Transactions on Automatic Control*, 47(8):1218–1233, 2002.

[65] R. Ortega, A. van der Schaft, B. Maschke, and G. Escobar. Interconnection and damping assignment passivity-based control of port-controlled Hamiltonian systems. *Automatica*, 38(4):585–596, 2002.

[66] D. K. Parrish and D. B. Ridgely. Altitude control of a satellite using the SDRE method. Proceedings of the American Control Conference, June 4-6, 1997, New Mexico, USA.

[67] J. D. Pearson. Approximation methods in optimal control. *Journal of Electronics and Control*, 13(5):453–465, 1962.

[68] T. Perez. *Ship Motion Control*. Springer, 2005.

[69] H. Rodriguez, R. Ortega, and N. Barabanov. A robustly stable output feedback saturated controller for the boost DC-to-DC converter. *Systems and Control Letters*, 40(1):1–8, 2000.

[70] H. Rodriguez, R. Ortega, and I. Mareels. Nonlinear control of magnetic levitation systems via energy-balancing. Proceedings of the American Control Conference, June 28-30, 2000, Chicago, IL, USA.

[71] C. Scherer and S. Weiland. *Lecture Notes: DISC Course on Linear Matrix Inequalities in Control*. 2006.

[72] D. Simon. *Optimal State Estimation*. John Wiley & Sons, Inc., 2006.

[73] J. J. E. Slotine and W. Li. *Applied Nonlinear Control*. Prentice Hall International Inc., 1991.

[74] J. G. Snijders. Wave filtering and thruster allocation for dynamic positioned ships. Master's thesis, Mathematical Systems Theory Group, DIAM, EWI Faculty, TU Delft, The Netherlands, November 2005.

[75] J. G. Snijders and J. W. van der Woude. Nonlinear observer design for dynamic positioning. Proceedings of Dynamic Positioning Conference, September 27-28, 2005, Houston, USA.

[76] A. J. Sørensen, S. I. Sagatun, and T. I. Fossen. Design of a dynamic positioning system using model-based control. *Control Engineering Practice*, 4(3):359–368, 1996.

[77] J. Spouge. Review of methods for demonstrating redundancy in dynamic positioning systems for the offshore industry. Research Report 15, DNV, Consulting, London, 2004.

[78] J. F. Sturm. Using SeDuMi 1.01, a MATLAB toolbox for optimization over symmetric cones. *Optimization Methods and Software*, 11(1):625–653, 1999.

[79] V. Torre. Existence of limit cycles and control in complete Keynesian system by theory of bifurcations. *Econometrica*, 45(6):1457–1466, 1977.

[80] G. Torsetnes, J. Jouffroy, and T. I. Fossen. Nonlinear dynamic positioning of ships with gain-scheduled wave filtering. Proceedings of the 43rd IEEE Conference on Decision and Control, December 14-17, 2004, Atlantis, The Bahamas.

[81] P. Tsiotras, M. Corless, and M. Rotea. Counter example to a recent result on the stability of nonlinear systems. *IMA Journal of Mathematical Control and Information*, 13(2):129–130, 1996.

[82] J. van Amerongen. *Adaptive Steering of Ships: a model reference approach to improved manoevring and economical course keeping*. PhD thesis, Delft University of Technology, Delft, The Netherlands, 1982.

[83] P. van der Klugt. *Rudder Roll Stabilization*. PhD thesis, Delft University of Technology, Delft, The Netherlands, 1987.

[84] A. J. van der Schaft. L_2-*Gain and Passivity Techniques in Nonlinear Control*. Springer, 2000.

[85] F. Verhulst. *Nonlinear Differential Equations and Dynamical Systems*. Springer, 1996.

[86] V. Vidyasagar. *Nonlinear Systems Analysis*. SIAM, Second edition, 2002.

[87] J. C. Willems. Dissipative dynamical systems, part I: General theory. *Archives for Rational Mechanics and Analysis*, 45(5):321–351, 1972.

[88] A. A. Zaher. Nonlinear control of systems with multiple equilibria and unknown sinusoidal disturbance. *Communications in Nonlinear Science and Numerical Simulation*, 12(8):1518–1533, 2007.

List of Abbreviations and Acronyms

DP	Dynamic Positioning
EKF	Extended Kalman Filter
FPSO	Floating Production, Storage and Offloading
IDA	Interconnection Damping Assignment
LMI	Linear Matrix Inequality
LF	Low Frequency
LQ	Linear Quadratic
LQR	Linear Quadratic Regulation
MATLAB	MATrix LABoratory
OCP	Optimal Control Problem
PBC	Passivity Based Control
PHS	Port Hamiltonian Systems
RSF	Real Schur Form
SDARE	State Dependent Algebraic Riccati Equation
SDC	State Dependent Coefficient
SeDuMi	Self Dual Minimization
SPD	Symmetric Positive Definite
SPSD	Symmetric Positive Semidefinite
WF	Wave Frequency
YALMIP	Yet Another Linear Matrix Inequality Parser

Summary

Dynamic positioning (DP) refers to maintaining the position and heading of a sea vessel under specified limits by exclusively using thrusters and propellers. This was usually achieved by using conventional techniques like anchoring and mooring, until the late sixties. Since then more sophisticated DP systems are being used for dynamic positioning.

A DP system consists of three main units: a power system, a DP control system, and a thruster system. A vessel whose motion is controlled by DP system is called a DP vessel. With the fast growing offshore industry, the demand for more accurate and stable DP systems has increased to ensure safety of the DP operations.

The focus of this research is the control system design for DP vessels. Starting point of the study of the DP control system design is a mathematical model of the sea vessel. Two motion components of the vessel motion in sea are distinguished: a low frequency (LF) motion component and a wave frequency (WF) motion component. The LF motion is due to the slowly varying forces and moments due to the control actions, waves, wind, and sea currents. The WF motion is caused by the first order wave-induced wave loads. The measurement signal from the sensors (GPS and gyro) essentially contains both motion components.

An important consideration in the control system design for many dynamic positioning problems is to compensate only the LF motion of the vessel. This is to avoid unnecessary wear and tear of the propulsion units. As the measurement signal plays an important role in the control design procedures, filtering of the WF component from the measurement signal is essential so that only the LF component is transmitted to the controller. This problem of separating the LF motion component from the WF motion component is called *wave filtering*.

An important aspect of control system design is its stability. In this thesis, we first study the local and the global aspects of the asymptotic stability of the DP vessel. The vessel model, we consider in this thesis, is nonlinear. This nonlinearity is due to a single state variable which represents the heading angle of the vessel. The so-called state dependent coefficient (SDC) parametrization will transform the nonlinear vessel model into a pseudo-linear form with the system matrix being a function of the heading angle.

Some results on the global asymptotic stability studies of similar systems are recapitulated. Then we discuss two counterexamples to analyze the sufficient conditions

for the global asymptotic stability of the pseudo-linear system. In the first counterexample, we consider a system matrix which is a function of a single state component. We show that it is continuous, Hurwitz, and exponentially bounded. We further show that these conditions are not sufficient to establish global asymptotic stability of the corresponding pseudo-linear system. In the second counterexample, in addition to the above mentioned set of conditions for the system matrix, we also assume that the system matrix is periodic in the single state component. We show that this still does not lead to the set of sufficient conditions for global asymptotic stability of the pseudo-linear system.

For the case of a periodic dependence of the system matrix on a single state component, we propose a technique to prove the global asymptotic stability of the pseudo-linear system. This technique is a combination of the linear matrix inequalities (LMIs) and the Lyapunov stability theory. We use this technique to prove the global asymptotic stability of the nominal (all the external disturbances are known or there are no disturbances) vessel model with a naive state feedback controller in Chapter 3 and with the Riccati equation based controller in Chapter 4.

In this thesis, the so-called state dependent algebraic Riccati equation (SDARE) technique is used to address the regulation problem of the DP vessel. We start with a nominal case when there is no WF motion involved and measurements are noise free. The SDARE control design is used to regulate the vessel to the desired equilibrium position. We then proceed with the so-called nonnominal case in which the disturbance vector is unknown and the measurements also contain noise. The disturbance vector is modeled as a first order Markov process. Therefore, the disturbance vector can be concatenated with the state of the vessel model.

The SDARE control design is a state feedback method. Therefore, knowledge of the entire state of the system is required. The output equation in the model of the DP vessel indicates that only the noisy position and heading measurements are available for feedback. Therefore, an observer is required to estimate the complete state of the system. The pseudo-linear SDARE observer is used to get these state estimates. We conclude the SDARE control design concept by taking into account the WF component in the measurement model. In this case, the noisy measurements are contaminated with the WF component as well, which requires wave filtering. We use the SDARE technique to address the estimation and filtering problems. Simulation experiments performed by using the data of a supply vessel have shown good results as far as the performance of the SDARE controller and observer is concerned.

We present the Fourier series interpolation (FSI) method which reduces the computation time of the algebraic Riccati equation. The effectiveness of the FSI method is shown in the SDARE approach for the DP control system design. This is especially useful in situations where the solution of the SDARE is required online. The fast computation of the SDARE may be required in the cases when this technique is used with systems whose dynamic response is fast/high. The idea of the method discussed in this thesis is limited to the special case of the SDARE whose coefficient matrices depend on a single state component in a periodic way. The underlying idea behind the reduction in computation time of the solution of the SDARE is the offline computation of the Fourier coefficients which effectively reduces the online computations.

The regulation problem of the DP vessel is also addressed by using the port-Hamiltonian formulation. In this context, we study only the control design problem.

The estimation and wave filtering are assumed to be addressed separately and we move on from this point to address the control design problem. The interconnection damping assignment passivity based control (IDA-PBC) design technique is used to introduce two control laws: the classical IDA-PBC design and the extended IDA-PBC design. The former controller provides the desired performance in the nominal case but it fails to stabilize the system at the desired location in presence of unknown external disturbances. To address this bottleneck in the design, the extended IDA-PBC design is introduced to yield the desired performance.

There are two notable features in the port-Hamiltonian based study of the DP problem. The first one is that there is an additional degree of freedom in the form of the Hamiltonian (also sometimes referred to as the energy of the system) function which helps in improving the performance and analysis of the controller. The second feature of the port-Hamiltonian formulation is that it offers the freedom to add additional damping through the controller action which helps in improving the performance of the controller and it simplifies the tuning of the gains.

To explain the effects of the Hamiltonian formulation on the performance of the controller, we consider two different formulations of the Hamiltonian function: a quadratic and a trigonometric. Simulation results have revealed that each formulation gives a different heading angle profile of the vessel in cases when the initial heading angle is above π radians. The profile corresponding to the trigonometric formulation gives the optimal heading angle profile. The effect of additional damping is also explained by a simulation result.

In conclusion, the search for the sufficient conditions for global asymptotic stability of the pseudo-linear systems with state dependency of the system matrix on a single state component, is still open for further research. The DP problem has a wide range of issues associated with it. This study is mainly focussed on the regulation of the DP vessel to a desired equilibrium point. The ideas and techniques introduced in this dissertation can be employed also to study various other DP problems like path following, trajectory tracking, etc. The study of the port-Hamiltonian framework for filtering and estimation problems of the DP vessel also remains an interesting and challenging research problem.

Samenvatting

Dynamisch positioneren (DP) is een term uit de scheepvaart die betrekking heeft op het regelen van de positie en behouden van de koers van een vaartuig, binnen voorgeschreven grenzen en uitsluitend door middel van boegschroeven en propellers. Tot in de tweede helft van de zestiger jaren werd dit voornamelijk gedaan door conventionele technieken, zoals verankering en meertrossen. Sindsdien is men gaandeweg overgegaan op complexere DP systemen.

Een DP systeem omvat drie hoofdbestanddelen: een stroomvoorzieningssysteem, een DP regelsysteem, en een boegschroef systeem. Een DP vaartuig is een vaartuig wiens sturing wordt geregeld door een DP systeem. Dankzij de snelle groei van de offshore industrie, stijgt de vraag naar nauwkeurigere en stabielere DP systemen die de veiligheid van DP operaties waarborgen.

In dit onderzoek ligt de nadruk op het regelsysteem voor DP vaartuigen. Hiertoe moet allereerst een mathematisch model van het vaartuig worden gemaakt. De beweging van een vaartuig op zee kan worden opgesplitst in twee componenten: een lage golffrequentie (LF) component en een hogere golffrequentie (GF) component. De LF component wordt veroorzaakt door de traag veranderende krachten en momenten door de regeling, en door golven, wind, en zeestromingen. De WF component wordt veroorzaakt door de impact van eerste orde golven. Deze twee componenten kunnen worden reconstrueerd uit het meetsignaal van de bewegingssensoren (GPS en gyro).

Een belangrijk aspect van het ontwerp van een DP regel systeem is dat men bij voorkeur alleen wil anticiperen op de LF component van de beweging. Dit voorkomt onnodig gebruik (en dus slijtage) van de propellers. Daarom is het van belang om zo nauwkeurig mogelijk de WF component uit het meetsignaal te filteren. Dit probleem wordt *wave filtering* genoemd.

Stabiliteit is een belangrijk aspect van een regelsysteem. In dit proefschrift beschouwen we zowel lokale als de globale asymptotische stabiliteit van een DP vaartuig. Het mathematische model voor een vaartuig is niet-linear. Het niet-linear zijn wordt veroorzaakt door één toestandsvariabele die de koershoek van het vaartuig beschrijft. Door middel van een zogenaamde toestands-afhankelijke coëfficienten parameterizatie (*SDC parametrization*) kan het niet-lineare stelsel worden omgeschreven in een psuedo-lineair stelsel, waarvan de systeem matrix een functie is van de koershoek.

Enkele resultaten betreffende globale asymptotische stabiliteit worden in dit proefschrift kort samengevat. Vervolgens bespreken we een tweetal tegenvoorbeelden die informatie verschaffen over voldoende voorwaarden voor globale asymptotische stabiliteit van het pseudo-lineaire systeem. Het eerste tegenvoorbeeld betreft een systeemmatrix die afhangt van één toestandsvariabele. We laten zien dat deze systeemmatrix continu, Hurwitz, en exponentieel begrensd is. Echter, dit blijkt niet voldoende voor globale stabiliteit van een desbetreffende pseudo-lineair systeem. Ons tweede tegenvoorbeeld toont aan dat, als naast de bovengenoemde eigenschappen van de systeemmatrix ook nog wordt aangenomen dat deze periodiek is, dit nog steeds niet hoeft te leiden globale asymptotische stabiliteit.

Voor het geval dat de systeemmatrix periodiek afhangt van één variabele, wordt een aanpak geponeerd die geschikt zou kunnen zijn om de globale asymptotische stabiliteit van het systeem aan te tonen. Deze aanpak is gebaseerd op een combinatie van lineaire matrix ongelijkheden (LMIs) en de Lyapunov stabiliteits theorie. Wij passen deze aanpak toe om de globale asymptotische stabiliteit aan te tonen van een nominaal vaartuigmodel met twee verschillende regelingen: In hoofdstuk 3 beschouwen we een *naive state feedback* regelsysteem, en in hoofdstuk 5 een regelsysteem gebaseerd op de Riccatti vergelijking. Een nominaal vaartuigmodel is een model waarbij alle eventuele externe verstoringen bekend worden verondersteld.

In dit proefschrift wordt de regeling van het DP vaartuig gerealiseerd met behulp van de zogenaamde toestandsafhankelijke algebraïsche Riccatti vergelijking (SDARE). We beginnen met het eenvoudige geval dat er geen sprake is van een WF bewegingscomponent en het meetsignaal geen ruis bevat. We gebruiken het SDARE regelsysteem dat een vaartuig in de gewenste evenwichts positie brengt. We vervolgen ons onderzoek door het geval te beschouwen dat de verstoringsvector onbekend is en het meetsignaal ruis bevat. De verstoringsvector wordt gemodelleerd door een eersteorde Markov process. Het gevolg daarvan is dat de verstoringsvector ingebracht kan worden in de toestand van het vaartuig.

Het SDARE regelsysteem is een feedback systeem. Daarom is het nodig beschikking te hebben over de toestand (positie, richting) van het systeem. Echter, de vergelijking met behulp waarvan de positie en richting van een DP vaartuig kan worden bepaald, bevat ruis. Daarom moet een *waarnemer* worden ontworpen die de daadwerkelijke toestand en richting schat. De pseudo-lineaire SDARE observer is gebruikt om deze schattingen te maken. Als laatste toevoeging aan het ontwerp van het SDARE regelsysteem wordt het effect van de WF bewegingscomponent meegenomen. In dit geval moet uit de meetsignalen met ruis ook nog de WF component worden gefilterd. We gebruiken de SDARE teckniek om de ruis en de WF component weg te filteren. Simulaties op basis van de data van een bestaand vaartuig laten zien dat de SDARE regelaar en waarnemer goed presteren.

We presenteren de Fourier reeks interpolatie (FSI) methode, die de rekentijd voor het oplossen van de algebraische Riccati vergelijking verkort. Deze methode blijkt effectief voor de SDARE aanpak van het ontwerp van een DP regelsysteem. In het bijzonder is de aanpak nuttig als de oplossing van SDARE online nodig is. De snelheid van SDARE kan nodig zijn in systemen waarvan de dynamische response hoog/snel is. In dit proefschrift bestuderen we deze aanpak slechts voor SDARE waarvan de coëfficient matrices afhangen van één toestandscomponent, en wel op een periodieke wijze. Het achterliggende idee van de reductie in rekentijd van de oplossing van SDARE is dat de Fourier coëfficienten offline bepaald worden, hetgeen de rekentijd van de online berekeningen effectief reduceert.

Naast SDARE beschouwen wij ook de port-Hamiltoniaanse formulering voor het regelsysteem van een DP voertuig. In deze context beschouwen we alleen het ontwerp van de regelaar. Wij presenteren dus geen aanpak voor het filteren van de ruis en de WF component. Voor de regelaar gaan wij uit van de *interconnection damping assignment passivity based control* (IDA-PBC). Hierbij maken we verschil tussen het klassieke IDA-PBC ontwerp en het uitgebreide IDA-PBC ontwerp. Het klassieke ontwerp leidt tot een goed gedrag bij het nominale geval. Echter, indien er onbekende externe verstoringen zijn, is het systeem met een klassieke IDA-PBC niet stabiel. De uitgebreide IDA-PBC heeft dit probleem niet.

De port-Hamiltoniaanse aanpak van het DP probleem heeft twee aantrekkelijke eigenschappen. Ten eerste is er een extra vrijheidsgraad in de vorm van de Hamiltoniaan (ook wel de energie van het systeem genoemd). De tweede aantrekkelijke eigenschap van de port-Hamiltoniaanse aanpak is dat het de mogelijkheid biedt een extra demping aan de acties van de regelaar toe te voegen. Beide eigenschappen verbeteren de prestaties van de regelaar, en de tweede eigenschap vereenvoudigt het afstellen.

Wat betreft de keuze van de Hamiltoniaan beschouwen wij twee verschillende formuleringen: een kwadratische en een trigonometrische Hamiltoniaan. Uit simulaties is gebleken dat de twee methoden ieder een ander koersprofiel geven van het vaartuig als de initiële koers meer dan π radialen is. Het profiel horende bij de trigonometrische formulatie geeft het optimale profiel. Het effect van extra demping wordt geanalyseerd met behulp van een simulatie.

Kort samengevat is de zoektocht nog open betreffende een algemene voldoende voorwaarde voor globale asymptotische stabiliteit van een pseudo-linear systeem waarvan de systeemmatrix middels een enkele parameter van de toestand afhangt. Het ontwikkelen van een DP systeem brengt veel uitdagingen met zich mee. Dit proefschrift beschouwt in eerste instantie of een regelsysteem van een DP voertuig het vaartuig in een gewenst evenwicht kan brengen. De ideeën en technieken die in dit proefschrift zijn ontwikkeld kunnen ook worden gebruikt om andere DP gerelateerde problemen te bestuderen, zoals het volgen en bijhouden van de koers. Een ander interessant en uitdagend onderzoeksprobleem blijft het ontwikkelen van een filter voor ruis en voor de WF component in het port-Hamiltoniaanse framework.

Acknowledgments

I am immensely elated to write the acknowledgments for my thesis. It is the culmination of my PhD research and an end to my formal student life. It all started almost 30 years ago from a far-flung, two-room primary school in my native village Dhurnal. Starting from a school which still doesn't have electricity, I had never thought that one day I would end my student life by completing a PhD from a university like TU Delft. This long journey was not a stroll. There were many ups and downs. Therefore, first of all, I express my utmost gratitude to Almighty Allah who helped me to remain steadfast and made it possible for me to complete a PhD from one of the world's best technical universities, after such a humble start.

I especially thank my supervisor Jacob and promoters Geert Jan (my promoter for first two years of my PhD) and Arnold (my promoter till the end of my PhD). I wish to extend my profound thanks to Jacob and Geert Jan for providing me the opportunity to join TU Delft as a PhD student in the mathematical system theory group. I thank Arnold, Geert Jan, and Jacob for their persistent confidence and trust in me. They always motivated and encouraged me in times of doldrums and stagnation during my PhD research. They provided me with many opportunities to improve my scientific and professional skills by sending me to many scientific events during my tenure as a PhD student. I thank Arnold and Jacob for several reviews of my thesis draft and giving useful feedback which helped me to improve its contents and presentation.

My primary interaction was with Jacob. He has been very supportive, candid, helpful and patient throughout my stay in Delft. We had numerous productive and useful discussions. I learnt a lot of professionalism from him, of which this thesis is just a subset. He provided me annual breaks to visit my family which really helped me and my family. Thank you Jacob for all these favors and your help.

This part of acknowledgment is not complete without mentioning the warm hospitality and honor that Geert Jan, Elke, Jacob and Yvon have given to my wife and children when they came to the Netherlands. Especially, I admire the amiable and friendly nature of Elke and Yvon: amazingly my kids became their intimate friends in one meeting.

I would like to express my gratitude to Dori, Evelyn, Dorothee, and Cindy for their kind support in various office matters and related documentation at the department during my PhD tenure. Most of my contact was with Dori. She is a wonderful person. Her interaction with colleagues is very passionate, like a mother I would say. She made me feel at home! Many thanks to Dori and Dorothee for arranging wonderful days out with DIAM.

Special thanks to Carl and Kees for their support in Windows- and Linux- related issues. They were always around when I needed them. They were always kind to answer my silliest questions! Thank you for making my computers function smoothly.

I would like to appreciate the assistance provided by Nuffic and CICAT. I would like to thank Mrs. Minkman (and her colleagues) for the smooth dispersal of the monthly stipend which made my stay in the Netherlands free from any financial issues. Franca Post from CICAT deserves special thanks from me, my wife, and my children for her contribution in our family reunion in Delft. Those were the best days during my stay in the Netherlands and Franca deserves the credit for providing us with those joyous moments. Besides this extraordinary occasion, she helped a lot in various office matters and related documentation. Thank you Franca!

I shared an office with many people. I thank Kateřina, Diana, Adolfo, Arnau, Evans, Jeroen, Jonas, Yusef, and Saeeda for being supportive, accommodating, and cheerful officemates. Kateřina was my first colleague in TU Delft. She deserves my exclusive acknowledgment for providing me a lot of help in difficult times in the early phase of my PhD life. Kateřina, I still fondly remember your frequently used amusing phrases:“I am disappearing slowly”, “Was somebody looking for me?”, “Am I disturbing you!”, “Sorry, talking to myself!”. Arnau also deserves special recognition. He helped me a lot with putting my PhD on track. His arrival at DIAM was a blessing for me. He provided the catalyst for my PhD process. I wish both Kateřina and Arnau the very best in their lives!

I would like to express appreciation for all people from the probability and risk analysis group, analysis group, and optimization and system theory group for providing a wonderful working environment. It was a pleasure to be a part of this friendly milieu. Thank you for all the smiles and greetings!

My special thanks goes to Eddie Kim for reading my thesis and English propositions. Thank you Eddie for helping me in improving the text and presentation. He also deserves special appreciation for being a lively and wonderful person.

I would like to thank Prof. Jan van Schuppen for his time and interest in reading my thesis. Thank you Jan for many useful discussions and remarks about my research.

I thank Sonja Cox for sparing her precious time and helping me with the Dutch summary of my thesis and the Dutch translation of my thesis propositions. I appreciate her friendly and very supportive disposition.

I would like to thank the Dutch Society in general. I really enjoyed my stay in the free and open environment. People really respect each other irrespective of race, religion, and appearance. People are very friendly and supportive although they are very reserved in general. It was a pleasure and a great learning experience for me during my stay in the Netherlands. I really like the way people greet each other.

I appreciate the Ima’ms and the committee of Masjid Sultan Ahmet for their hospitality and care during the months of Ramadhan. The iftar arrangements were a great facility and comfort for students in Delft. The presence of a sizable Muslim community in Delft was a great source of convenience in many aspects.

Hisham, Mehfooz, and Zubair deserve special mention for their help on my initial arrival in Delft. They really ensured that I would not face any trouble being new in Delft. I had a long stay in Delft spanning over 5 years. I lived with many persons during my stay in Delft. I appreciate and commend Haleem, Hamayun, Raghu, Sidharth, Iftikhar Faraz, Asim, Khaled, Ibrahim, and Hanan for their support, patience, and versatile and pragmatic company. You all made my stay in Delft cozy and comfortable.

My heartiest thanks go to Hanan for many delicious and generous dinners and food. Hanan, you really saved me from starving! I never met such a jolly and generous Sheikh and would not meet again. Keep it like that and try being a bit more responsible! I would like to thank Iftikhar Faraz for his kind hospitality and help on numerous occasions! I would like to extend my gratitude to Ibrahim for his kind scoldings and for motivating me to memorize the recitation of surah Al-Rehman. Words of thanks go to Faisal Nadeem for being a frank and a dependable friend, helping me on various occasions, sharing gossip, and numerous discussions on cricket! I would like to thank Tariq Abdullah for being a supportive and caring neighbor during my stay in the Vrijenban region of Delft.

Nadeem deserves a special mention for arranging weekly study circle gatherings of compatriots in Delft. I always enjoyed those meetings. I learned many new things. All those who used to take part in those meetings deserve special thanks for making them useful and productive.

I was lucky to have so many Pakistanis around during my stay in Delft. This was a great blessing! Life became very easy due to useful information sharing and giving one another small favors. Generally, people were friendly, social, and supportive. We had many memorable social events and get togethers. I would like to extend my thanks to all those who provided opportunities to enjoy Pakistani food from time to time. We had a good cricket team and we enjoyed playing together.

I would also like to mention my Indian friends here. It was here in the Netherlands that I met an Indian national for the first time. I am really amazed by their modesty and friendly nature in general. We enjoyed good times playing cricket and had a lot of fun! Special thanks to Navin and Amol for their time and useful discussions about my research.

A word of thanks goes to Dr. Ata ur Rehman for his brainchild which revolutionized the higher education sector in Pakistan. I would also like to thank the Higher Education Commission of Pakistan, the government, and the people of Pakistan who all made it possible for me to come and stay in the Netherlands to pursue PhD studies.

There are many people in Pakistan who helped and encouraged me in difficult times during my stay in the Netherlands. They made it possible so that I wouldn't have any problems back home in Pakistan which allowed me to be focussed with my job in Delft. My mother, brothers and sisters, and in-laws of my sisters have all supported me well in their capacity. Especially, my youngest brother Rizwan and my bhabhi Rehmat deserve very special recognition for being very supportive. The family of my wife deserves special acknowledgments for being caring and supportive to my family in my absence. My special thanks goes to my cousins Khalda and Abdul Khaliq, my aunts Mehr Bibi and Saeeda, Uncles Abdul Latif, Said Ahmad, and Yasin (and his family), friends, and relatives who supported me from time to time. Some of them really deserve more recognition but I am sorry for being brief here.

My late father, Dil Kabeer, who is unfortunately not with us today deserves very special recognition. It was his dream to see his children becoming successful in their lives. He sacrificed his leisures to provide a good education to his children. I have no doubt that he would have been the happiest person in the world at the successful completion of my PhD. Abbu! This work is a small token for your struggle and sacrifices!

Now I come to the most difficult and important part of this acknowledgment! It's hard for me to describe in words the role of my wife and kids during my PhD studies. They deserve very special appreciation for their patience and endurance during my long and protracted PhD stint. I always received a lot of motivation and inspiration from my wife whenever I got tired from research. The gleaming eyes and smiling faces of my kids always provided me great vigor in listless moments. On one hand it was a tough time for all of us but on the other hand it was a great learning experience as well. We realized the value and importance of many things which will help us in future life. I applaud my wife for her pristine love, good work in running the family affairs and raising the children excellently in my absence. I am happy that the testing time is going to end soon with a fruitful outcome. It's carnival time for all of us. I am raring to see you all and to spend more time with you! I wish and pray for a happy and peaceful future with you all!

A word of thanks goes to myself for enduring all stress and fatigue. There were hardly any serendipitous moments in the last 5 years. But on a positive note, I should not forget the experiences gained and promises made to myself during these years. Now it's time to pay attention to things which I put off due to PhD priorities.

To the readers of this acknowledgment page, I want to share a personal experience. When you decide to do anything in life, you will do it for sure, sooner or later. It depends upon your determination and focus. Never give up!

Finally, I thank the members of my promotion committee for devoting some of their precious time to scrutinize my thesis, and I acknowledge those committee members who traveled to Delft for the public defense of this dissertation. Thank you all very much for your time and interest. Thank you for reading my work with interest and all the insightful feedback!

–The End –

- تمّت با الخیر -

Shah Muhammad
March 22, 2012

شاہ محمد
٢٢ مارچ ٢٠١٢

Publications

SHAH MUHAMMAD AND JACOB VAN DER WOUDE
A counter example to a recent result on the stability of nonlinear systems, IMA Journal of Mathematical Control and Information. Vol. 26, No. 3, August 2009, pp 319-323.

SHAH MUHAMMAD AND JACOB VAN DER WOUDE
The Fourier Series Interpolation (FSI) Method for the Solution of the SDARE. In proceedings of the UKACC International Conference on Control (CONTROL 2010), September 7-10, 2010, Coventry, UK.

SHAH MUHAMMAD AND ARNAU DÒRIA-CEREZO
Output Feedback Passivity-based Controllers for Dynamic Positioning of Ships. In Proceedings of the 14th Edition of the Dynamic Positioning Conference (DP CONFERENCE 2010), October 12-13, 2010, Houston, USA.

SHAH MUHAMMAD AND JACOB VAN DER WOUDE
On stability conditions for systems with periodic state dependent coefficients, IMA Journal of Mathematical Control and Information. Vol. 28, No. 1, March 2011, pp 97-102.

SHAH MUHAMMAD AND ARNAU DÒRIA-CEREZO
Passivity Based Control Applied to the Dynamical Positioning of Ships. To appear in IET Journal of Control Theory and Applications.

Curriculum Vitae

Shah Muhammad was born on the 6^{th} of January, 1977 in Talagang, Pakistan. He got his primary and secondary education mainly from government schools and colleges in his native town. He completed his B.Sc. in 1997 from the University of the Punjab and subsequently he earned an M.Sc. in Mathematics from Islamia University Bahawalpur in 1999 with distinction. Later on he worked as a Scientific Officer for four years in Ghulam Ishaq Khan (GIK) Institute of Engineering Sciences and Technology, Topi, Pakistan. This stint ended on June 30, 2005. Since September 2006, he has been in the Netherlands, pursuing his PhD in the Mathematical System Theory and Optimization group at the Delft Institute of Applied Mathematics, Delft University of Technology.

He has presented several papers during his PhD studies in various seminars and conferences related to dynamical systems and control theory. Prominent activities include his participation and presentation in the 1st Elgersburg School on Mathematical Systems Theory, organized by Technische Universität Ilmenau on March 30-April 3, 2009 in Elgersburg, Germany, the Benelux meetings on systems and control (2009 and 2010 editions), the UKACC Conference on Control held in Coventry, UK in 2010, and the 2010 DP Conference held in Houston, USA. He has also reviewed scientific articles in his field. He has two published and one accepted journal article.

Sports and reading formed Shah's extra-academic activities during his student life. At Islamia University Bahawalpur, he won first prize in the 5 Km long distance race and ended up third in the 1500 m race. He is a good player of cricket. He is a fluent top order batsman who likes to play aggressively. He is also a very agile fielder and has a very safe pair of hands anywhere in the outfield and in the slip cordon. Shah is a strong believer that sports are an indispensable part of an individual's life and he intends to promote sporting culture among the masses and society as a whole.

Shah's post PhD plans are to join a dynamic and growing organization or institute where he can use the knowledge and expertise acquired during his academic and research career. He likes to share and transfer his experience to prospective colleagues and students. He believes that research culture is a key to solve the problems of daily life and to overcome the challenges of the modern era. Shah intends to work for the promotion of research culture, especially in the developing and third world countries.